

Theoretical perspective on the glass transition and amorphous materials

Ludovic Berthier

*Laboratoire Charles Coulomb, UMR 5221 CNRS and Université Montpellier 2,
Montpellier, France*

Giulio Biroli

*Institut de Physique Théorique, CEA, IPhT, 91191 Gif sur Yvette,
France and CNRS URA 2306*

(Received 13 April 2010; published 20 June 2011)

A theoretical perspective is provided on the glass transition in molecular liquids at thermal equilibrium, on the spatially heterogeneous and aging dynamics of disordered materials, and on the rheology of soft glassy materials. We start with a broad introduction to the field and emphasize its connections with other subjects and its relevance. The important role played by computer simulations in studying and understanding the dynamics of systems close to the glass transition at the molecular level is given. The recent progress on the subject of the spatially heterogeneous dynamics that characterizes structural relaxation in materials with slow dynamics is reviewed. The main theoretical approaches are presented describing the glass transition in supercooled liquids, focusing on theories that have a microscopic, statistical mechanics basis. We describe both successes and failures and critically assess the current status of each of these approaches. The physics of aging dynamics in disordered materials and the rheology of soft glassy materials are then discussed, and recent theoretical progress is described. For each section, an extensive overview is given of the most recent advances, but we also describe in some detail the important open problems that will occupy a central place in this field in the coming years.

DOI: [10.1103/RevModPhys.83.587](https://doi.org/10.1103/RevModPhys.83.587)

PACS numbers: 05.20.Jj, 64.70.kj

CONTENTS

I. Incipit	588	4. Current status of MCT	610
II. A Broad Introduction About Glasses	589	5. Quantitative computations using replica	611
A. Some phenomenology	589	6. Scaling arguments beyond mean-field theory and point-to-set length scale	613
1. The basic phenomenon	589	7. Current status of RFOT theory	614
2. Kinetic fragility	589	C. Kinetically constrained models and dynamic facilitation	615
3. Thermodynamic aspects	590	1. The physical picture	615
4. Static and dynamic correlation functions	591	2. Kinetically constrained models	616
B. Other glasses in science	592	3. Diffusing defects, excitation lines, and space-time bubbles	617
1. The jamming transition of colloids and grains	592	4. Main predictions and results	619
2. More glasses in physics and beyond	593	5. Current status of the facilitation approach	620
C. Computer simulations of molecular glass formers	593	D. Geometric frustration, avoided criticality, and Coulomb frustrated theories	621
III. Dynamic Heterogeneity	596	1. Physical picture and simple models	621
A. Existence of spatiotemporal dynamic fluctuations	596	2. Current status of the frustration-limited domains theory	623
B. Multipoint correlation functions	598	V. Off-Equilibrium Dynamics: Aging and Rheology	624
1. Why four-point correlators? The spin glass case	598	A. Why aging? Phenomenology and simple models	624
2. Four-point functions in supercooled liquids	598	B. Mean-field aging and effective temperatures	626
3. Three-point correlation and response functions	600	C. Beyond the mean field: Experiments, critical points, and kinetically constrained models	629
4. Inequalities on χ_4 and experimental measurements	602	D. Driven dynamics of glassy materials	632
C. Current status of dynamic heterogeneity studies	603	E. Current status of nonequilibrium studies	635
IV. Some Models and Theoretical Approaches	604	VI. Some General and Concluding Remarks	636
A. A few key questions	604	A. Growing length scale(s)	636
B. Mean-field free-energy landscapes and random first-order transition theory	604	B. Glass and jamming transitions	637
1. Mean-field glass theory and complex free-energy landscapes	604	C. Metastability and the role of the crystal	638
2. Mode-coupling theory	608	D. The ideal glass transition	638
3. Dynamical correlations within mode-coupling theory	610	E. Concluding remarks	639

I. INCIPIT

Glasses belong to a well-known state of matter (Tabor, 1991): glasses are easily designed with desired mechanical or optical properties on an industrial scale, and they are widely present in our daily life. Yet, a deep microscopic understanding of the glassy state of matter remains a challenge for condensed matter physicists (Angell, 1995; Debenedetti and Stillinger, 2001).

Glasses share similarities with crystalline solids since they are both mechanically rigid, but also with liquids because they both have similar disordered structures at the molecular level. It is mainly this mixed character that makes them fascinating even to nonscientists (Zanotto, 1998). Given that glasses are neither normal liquids nor standard solids, they are quite often not described in any detail by standard textbooks. For instance, glasses are not described in textbooks on condensed matter (Chaikin and Lubensky, 2000), or solid state physics (Ashcroft and Mermin, 1976); they made it into only the latest edition of the reference textbook on liquids (Hansen and McDonald, 2006), while statistical mechanics textbooks usually culminate with a presentation of our current understanding of phase transitions in pure materials using renormalization group concepts (Chandler, 1987; Sethna, 2006), leaving out disordered systems.

As described in detail in this review, modern statistical mechanics approaches to the glass transition involve good knowledge of advanced liquid state theory, field theory, the renormalization group, solution of lattice models, percolation, replica calculations, and concepts developed for far-from-equilibrium, driven systems (Young, 1998; Barrat *et al.*, 2003; Binder and Kob, 2005). These developments are all posterior to the mid-1970s important breakthroughs on phase transitions: the canonical spin glass Hamiltonian was introduced in 1975 (Edwards and Anderson, 1975) to be solved in infinite dimension only several years later (Parisi, 1980; Mézard *et al.*, 1988). Mode-coupling theory was developed in the mid-1980s (Götze, 1999), just before kinetic lattice glass models were introduced (Fredrickson and Andersen, 1984). The aging and rheology of disordered systems such as spin glasses or soft materials emerged as broad research fields during the 1990s. In this paper we review the fruits that have grown out of these important seeds. Given that none of these advances has allowed the derivation of a complete, well-accepted theory of amorphous media, we present a large number of different approaches. We discuss both successes and failures, explain similarities and differences between them, and present the current status of each approach. Thus, the article takes at times a somewhat subjective tone.

A glass can be obtained by cooling the temperature of a liquid below its glass temperature T_g . The quench must be fast enough that the more standard first-order phase transition toward the crystalline phase is avoided. The glass “transition” is not a thermodynamic transition at all, since T_g is only empirically defined as the temperature below which the material has become too viscous to flow on a “reasonable” time scale (and it is hard to define the word reasonable in any reasonable manner). Therefore, T_g does not play a fundamental role, as a phase transition temperature would. It is simply

the temperature below which the material looks solid. When quenched in the glass phase below T_g , liquids slowly evolve toward an equilibrium state they cannot reach on experimental time scales. Physical properties are then found to evolve slowly with time in far-from-equilibrium states, a process known as “aging” (Struik, 1978).

The subject of the glass transition has quite broad implications. A material is said to be “glassy” when its typical relaxation time scale becomes of the order of, and often much larger than, the typical duration of an experiment or a numerical simulation. With this generic definition, a large number of systems can be considered as glassy materials (Young, 1998). One can be interested in the physics of liquids (window glasses are then the archetype), in “hard” condensed matter (for instance, type-II superconductors in the presence of disorder, such as high- T_c superconducting materials), in charge density waves or spin glasses, in “soft” condensed matter with numerous complex fluids such as colloidal assemblies, emulsions, foams, but also granular materials, proteins, etc. Glass physics thus covers a remarkably broad range of time scales and length scales, as illustrated in Fig. 1. All these materials exhibit, in some part of their phase diagrams, some sort of glassy dynamics characterized by a rich phenomenology with effects such as aging, hysteresis, creep, memory, effective temperatures, rejuvenation, dynamic heterogeneity, nonlinear response, etc.

These long enumerations explain why this research field has received increasing attention from physicists in the last two decades. Glassy topics now go much beyond the physics of simple liquids (glass transition physics) and models and

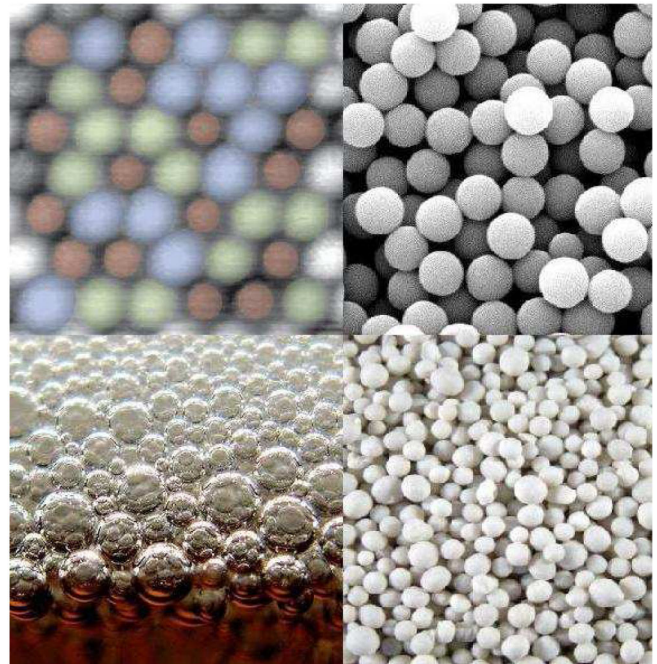


FIG. 1 (color online). Glassy phases occur at low temperature or large density in many different systems spanning a broad range of length scales, such as atomic [top left, atomic force spectroscopy image of an alloy of linear size 4.3 nm (Sugimoto *et al.*, 2007)], colloidal (top right) systems, foams (bottom left, a beer foam with bubbles of submillimeter size), and granular materials (bottom right, a fertilizer made of millimeter size grains).

concepts developed for one system often find applications elsewhere in physics, from algorithmics to biophysics (Mézard *et al.*, 2007). Motivations to study glassy materials are numerous. Glassy materials are everywhere around us and therefore obviously attract interest beyond academic research. At the same time, the glass conundrum provides theoretical physicists with deep fundamental questions since standard statistical mechanics tools are sometimes not sufficient to properly account for the glass state. Additionally, simulation in the computer of the dynamics of microscopically realistic material on time scales that are experimentally relevant is not an easy task, even with modern computers. Finally, the field is constantly stimulated by new, and sometimes quite beautiful, experimental developments to produce new types of disordered materials, or to obtain more microscopic information on the structure and dynamics of glassy systems.

The outline of the article is as follows. Section II provides a broad introduction to glassy materials. The issue of dynamic heterogeneity is tackled in Sec. III, while the main theoretical perspectives, characterized by a microscopic, statistical mechanics basis, are summarized in Sec. IV. Aging and non-equilibrium phenomena occupy Sec. V. Finally, we present a set of general and concluding remarks in Sec. VI.

II. A BROAD INTRODUCTION ABOUT GLASSES

A. Some phenomenology

1. The basic phenomenon

A vast majority of liquids (molecular liquids, polymeric liquids, etc.) form a glass if cooled fast enough to avoid the crystallization transition (Angell, 1995). Typical values of cooling rate in laboratory experiments are 0.1–100 K/min. The metastable phase reached in this way is called the “supercooled phase.” In this regime the typical time scales increase in a dramatic way, and they end up being many orders of magnitude larger than microscopic time scales at T_g , the glass transition temperature.

For example, around the melting temperature T_m , the typical time scale τ_α on which density fluctuations relax, is of the order of $\sqrt{ma^2/k_B T}$, which corresponds to a few picoseconds (m is the molecular mass, T is the temperature, k_B is the Boltzmann constant, which will often be set to unity in the later theoretical sections, and a is a typical distance between molecules). At T_g the typical time scale has become of the order of 100 s, i.e., 14 orders of magnitude larger. This increase is even more remarkable because the corresponding temperature decrease is, as a rule of thumb, about $\frac{1}{3}T_m$, not a large value if one considers $k_B T_m$ as the typical energy scale. The increasing of τ_α is accompanied by a concomitant increase of the shear viscosity η . This can be understood by a simple Maxwell model in which η and τ_α are related by $\eta = G_\infty \tau_\alpha$, where G_∞ is the instantaneous (elastic) shear modulus which does not vary considerably in the supercooled regime. In fact, viscosities at the glass transition temperature are of the order of 10^{12} Pa s. In order to grasp how viscous this is, recall that the typical viscosity of water at ambient temperature is of the order of 10^{-2} Pa s. How long would one have to wait to drink a glass of water with a viscosity 10^{14}

times larger, or how long would it take for cathedral glasses to flow (Zanotto, 1998)?

As a matter of fact, the temperature at which the liquid does not flow anymore and becomes an amorphous solid, called a “glass,” is protocol dependent. It depends on the cooling rate and on the patience of the people carrying out the experiment: solidity is a time-scale-dependent notion (Sausset *et al.*, 2010). Pragmatically, T_g is defined as the temperature at which the shear viscosity is equal to 10^{13} Poise (also 10^{12} Pa s).

2. Kinetic fragility

The increase of the relaxation time scale of supercooled liquids is remarkable not only because of the large number of decades involved but also because of its temperature dependence. This is vividly demonstrated by plotting the logarithm of the viscosity (or the relaxation time) as a function of T_g/T , as in Fig. 2. This is called the Angell plot (Angell, 1995) and is helpful in classifying supercooled liquids. A liquid is called strong or fragile depending on its position in the Angell plot. Straight lines correspond to “strong” glass formers and to an Arrhenius behavior,

$$\tau_\alpha = \tau_0 \exp\left(\frac{E}{k_B T}\right). \quad (1)$$

In this case, one can extract from the plot an effective activation energy E , suggesting quite a simple mechanism for relaxation by locally “breaking,” for instance, a chemical bond. The typical relaxation time is then dominated by the energy barrier to activate this process and, hence, has an Arrhenius behavior. Window glasses generically fall in this category. The terminology strong and “fragile” is not related to the mechanical properties of the glass but was introduced in relation to the evolution of the short-range order close to T_g . Strong liquids, such as SiO_2 , typically have a locally

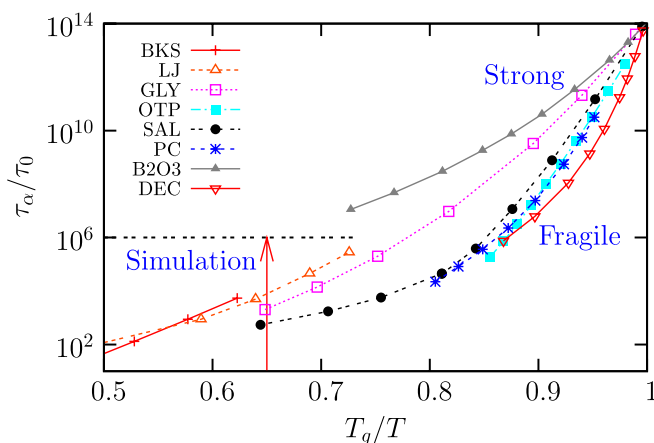


FIG. 2 (color online). Arrhenius plot of the relaxation time of several glass-forming liquids approaching the glass temperature T_g . For “strong” glasses, τ_α increases in an Arrhenius manner as temperature is decreased, $\log \tau_\alpha \sim E/(k_B T)$, where E is an activation energy and the plot is a straight line. For “fragile” liquids, the plot is bent and the effective activation energy increases when T is decreased toward T_g . Time scales accessible to numerical simulations are indicated. BKS, numerical model of silica; LJ, numerical model of a binary Lennard-Jones mixture; GLY, glycerol; OTP, *ortho*-terphenyl; SAL, salol; PC, propylene carbonate; DEC, decaline.

tetrahedric structure which persists both below and above the glass transition, in contrast to fragile liquids. Nowadays, the notion of fragility appears in connection with the temperature evolution of transport properties.

If one tries to define an effective activation energy for fragile glass formers using the slope of the curve in Fig. 2, then one finds that this energy scale increases when the temperature decreases, a “super-Arrhenius” behavior. This increase of energy barriers immediately suggests that the glass formation is a collective phenomenon for fragile supercooled liquids. Support for this interpretation is provided by the fact that a good fit of the relaxation time or the viscosity is given by the Vogel-Fulcher-Tamman law (VFT):

$$\tau_\alpha = \tau_0 \exp\left[\frac{DT_0}{(T - T_0)}\right], \quad (2)$$

which suggests a divergence of the relaxation time, and therefore perhaps a phase transition of some kind, at a finite temperature T_0 . A smaller D in the VFT law corresponds to a more fragile glass. Note that there are other comparably good fits of these curves, such as the Bässler law (Bässler, 1987),

$$\tau_\alpha = \tau_0 \exp\left[K\left(\frac{T}{T_*}\right)^2\right], \quad (3)$$

that only lead to a divergence at zero temperature. Another fit proposed and tested recently consists of replacing $1/T$ by $1/T - 1/T_{\text{on}}$ in the Bässler law. This form, where T_{on} represents some onset temperature for slow dynamics, is motivated in part by dynamical facilitation models (Elmatad *et al.*, 2009); see Sec. IV.C.2. Actually, although the relaxation time increases by 14 orders of magnitude, the increase of its logarithm, and therefore of the effective activation energy is modest, and experimental data do not allow one to unambiguously determine the true underlying functional law without any reasonable doubt (Hecksher *et al.*, 2008). Several comparisons between fits aimed at determining the best one can be found in the literature; see, e.g., the recent work of Elmatad *et al.* (2010). Although these works are certainly useful, one should not forget that since the increase of the effective activation energy is modest, preasymptotic effects to the “true” limiting behavior can play an important role. Hence, comparisons of simple fits with a small number of parameters could be misleading. For this and other reasons, physical interpretations in terms of a finite-temperature phase transition must always be taken with a grain of salt. It is recommended to use the same grain of salt to deal with fits supposedly demonstrating the absence of finite-temperature singularities (Hecksher *et al.*, 2008; Elmatad *et al.*, 2009).

3. Thermodynamic aspects

There are additional experimental facts that shed some light and might reinforce the interpretation of data in terms of a finite-temperature singularity. Among them is an empirical connection found between kinetic and thermodynamic behaviors. Consider the part of the entropy of the liquids, S_{exc} , which is in excess compared to the entropy of the corresponding crystal. Once this quantity, normalized by its value at the melting temperature, is plotted as a function of T , a remarkable connection with the dynamics, in particular, the VFT law, emerges [see Martinez and Angell (2001) for a compilation of

TABLE I. Values of glass transition temperature, VFT singularity, and Kauzmann temperatures for five supercooled liquids (Richert and Angell, 1998). OTP, o-terphenyl; 2-MTH, 2-methyltetrahydrofuran; N-PROP, *n*-propanol; 3-BP, 3-bromopentane. 12PD, 1–2 prop-diol.

Substance	OTP	2-MTH	N-PROP	3-BP	12PD
T_g	246.0	91.0	97.0	108.0	172.0
T_0	202.4	69.6	70.2	82.9	114.0
T_K	204.2	69.3	72.2	82.5	127.0
T_K/T_0	1.009	0.996	1.028	0.995	1.11

experimental data and Debenedetti and Stillinger (2001) for a discussion]. As for the relaxation time, one cannot follow this curve below T_g in thermal equilibrium. However, extrapolating the curve below T_g apparently indicates that the excess entropy vanishes linearly at some finite temperature, called T_K , which is close to zero for strong glasses and, generically, close to T_0 , the temperature at which a VFT fit diverges. This coincidence is quite remarkable: For materials with glass transition temperatures that vary from 50 to 1000 K the ratio T_K/T_0 remains close to 1. Some examples are provided in Table I; see Richert and Angell (1998) for a more extensive list. For the majority of liquids the ratio is close to 1 up to a few percent. Note, however, that there are some liquids for which T_K and T_0 differ by as much as 20%, and so a perfect correlation between the two temperatures is not established experimentally (Tanaka, 2003).

The chosen subscript for T_K stands for Kauzmann (1948) who recognized T_K as an important temperature for the physics of glasses. Kauzmann further suggested that some change of behavior (phase transition, crystal nucleation, etc.) must take place above T_K , because below T_K the entropy of the liquid, a disordered state of matter, becomes less than the entropy of the crystal, an ordered state of matter. This situation, which seemed perhaps paradoxical at that time, is, in fact, not a serious problem. There is no general principle that would constrain the entropy of the liquid to be larger than that of the crystal. As a matter of fact, the crystallization transition for hard spheres takes place precisely because the crystal becomes the state with the largest entropy at sufficiently high density (Alder and Wainwright, 1962).

On the other hand, the importance of T_K stands, partially because it is experimentally close to T_0 . Additionally, the quantity S_{exc} , which vanishes at T_K , is thought to be a proxy for the so-called configurational entropy S_c , which quantifies the number of metastable states (actually, its logarithm, see below). A popular physical picture due to Goldstein (1969) is that close to T_g the system explores a part of the energy landscape (or configuration space) which is full of minima separated by barriers that increase when temperature decreases. The dynamic evolution in the energy landscape would then consist of a rather short equilibration inside the minima followed by “jumps” between different minima that are well separated in time. At T_g the barriers have become so large that the system remains trapped in one minimum, identified as one of the possible microscopic amorphous configurations of a glass. Following this interpretation, one can split the entropy into two parts. The first contribution is due to the fast relaxation inside one minimum, and the

second one, counting the number of metastable states, $S_c = \log N_{\text{metastable}}$, is called the “configurational” entropy. Assuming that the contribution to the entropy due to the “vibrations” around an amorphous glass configuration is not much different from the entropy of the crystal, one finds that $S_{\text{exc}} \approx S_c$. Within this approximation T_K corresponds to the temperature at which the configurational entropy vanishes. Since the configurational contribution to the specific heat is given by TdS_{exc}/dT , a linear vanishing of S_{exc} near T_K (suggested by both experimental observations and theoretical arguments, see Sec. IV) would lead to a discontinuity (a downward jump) of the specific heat and thus to a thermodynamic phase transition. Note, however, that the above assumptions should not be taken for granted; see, for instance, the recent discussions by [Angell and Borick \(2002\)](#), [Dyre \(2006\)](#), and [Wyart \(2010\)](#). Furthermore, locating the transition temperature requires an extrapolation that is not well controlled, as is also required for the relaxation time.

4. Static and dynamic correlation functions

At this point the reader might have reached, despite our numerous warnings, the conclusion that the glass transition may not be such a difficult problem: There are experimental indications of a diverging time scale and a concomitant singularity in the thermodynamics. It simply remains to find static correlation functions displaying a diverging correlation length related to the emergence of “amorphous order,” which would indeed classify the glass transition as a standard second-order phase transition. Remarkably, this remains an open and debated question despite several decades of research. Simple static correlation functions are quite featureless in the supercooled regime, notwithstanding the dramatic changes in the dynamics. A simple static quantity is the structure factor defined by

$$S(q) = \left\langle \frac{1}{N} \rho_{\mathbf{q}} \rho_{-\mathbf{q}} \right\rangle, \quad (4)$$

where the Fourier component of the density reads

$$\rho_{\mathbf{q}} = \sum_{j=1}^N e^{i\mathbf{q} \cdot \mathbf{r}_j}, \quad (5)$$

with N the number of particles, V the volume, and \mathbf{r}_j the position of particle j . The structure factor measures the spatial correlations of particle positions, but it does not show any diverging peak, in contrast to what happens, for example, at the liquid-gas critical point where there is a divergence at small \mathbf{q} . A snapshot of a supercooled liquid configuration, in fact, just looks like a glass configuration, despite their widely different dynamic properties. More complicated static correlation functions have been studied ([Debenedetti, 1996](#)), especially in numerical work, but until now there are no strong indications of a diverging static length scale, although this issue is constantly debated ([Menon and Nagel, 1995](#); [Nelson, 2002](#); [Fernandez et al., 2006](#); [Cavagna, 2009](#); [Tanaka et al., 2010](#)). Recent results suggest that it is possible to identify some growing static length scales. We come back to this point in Sec. VI and in other sections.

The difficulty in finding a signature of the glass transition disappears if one focuses on dynamic correlations or response functions. For instance, a dynamic observable studied in light

and neutron scattering experiments is the intermediate scattering function,

$$F(\mathbf{q}, t) = \left\langle \frac{1}{N} \rho_{\mathbf{q}}(t) \rho_{-\mathbf{q}}(0) \right\rangle. \quad (6)$$

Different $F(\mathbf{q}, t)$ measured by neutron scattering in supercooled glycerol ([Wuttke et al., 1996](#)) are shown for different temperatures in Fig. 3. These curves suggest a first, rather fast (and hence not accessible in this experiment), relaxation to a plateau followed by a second, much slower, relaxation. The plateau is due to the fraction of density fluctuations that are frozen on intermediate time scales, but eventually relax during the second relaxation. The latter is called “ α relaxation” and corresponds to the structural relaxation of the liquid. This plateau is akin to the Edwards-Anderson order parameter q_{EA} defined for spin glasses which measure the fraction of frozen spin fluctuations ([Mézard et al., 1988](#); [Binder and Kob, 2005](#)). Note that q_{EA} continuously increases from zero below the spin glass transition. Instead, for structural glasses, a finite plateau already appears above any putative transition. Figures 4, 6, and 13 contain illustrations of the different time regimes observed in time correlators.

The intermediate scattering function can be probed only on a relatively small regime of temperatures. In order to track the dynamic slowing down from microscopic to macroscopic time scales, other correlators have been studied. A popular one is obtained from the dielectric susceptibility, which is related by the fluctuation-dissipation theorem to the time correlation of polarization fluctuations. It is generally admitted that different dynamic probes reveal similar temperature dependencies for the relaxation time ([Jakobsen et al., 2005](#)). The temperature evolution of the imaginary part of the dielectric susceptibility, $\epsilon''(\omega)$, is shown in Fig. 4 for the glass-former benzophenone, where a wide temperature window is covered ([Pardo et al., 2007](#)). At high temperature, a good representation of the data is given by a Debye law $\epsilon(\omega) = \epsilon(\infty) + \Delta\epsilon/(1 + i\omega\tau_\alpha)$, which corresponds to an exponential relaxation in the time domain. When temperature is

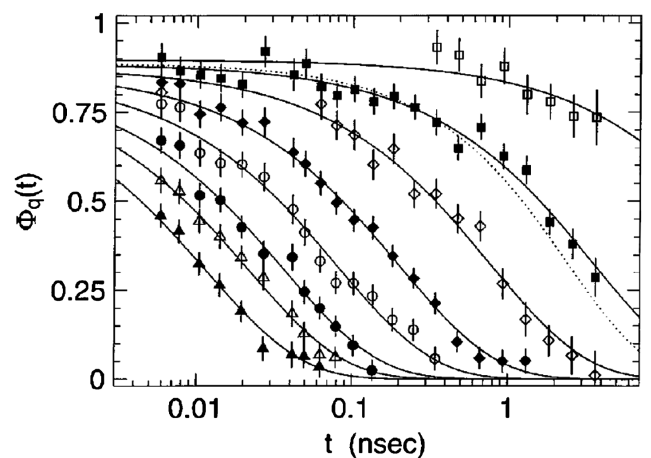


FIG. 3. Temperature evolution of the intermediate scattering function normalized by its value at time equal to 0 for supercooled glycerol ([Wuttke et al., 1996](#)). Temperatures decrease from 413 to 270 K from left to right. The solid lines are fit with a stretched exponential with exponent $\beta = 0.7$. The dotted line represents another fit with $\beta = 0.82$.

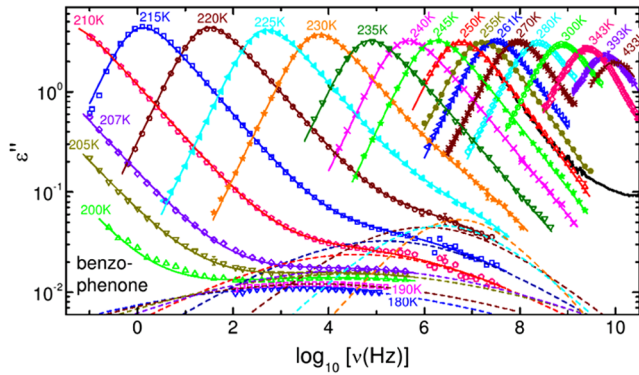


FIG. 4 (color online). Temperature evolution of the dielectric susceptibility of the glass-former benzophenone measured over more than 10 decades of relaxation times (Pardo *et al.*, 2007). Dynamics slows down dramatically as temperature is decreased and relaxation spectra become broad at low temperature and reveal the existence of additional “secondary” relaxation processes.

decreased, however, the relaxation spectra become broad and strongly non-Debye, which is the frequency analog of the stretching of the relaxation observed in the time domain. Indeed, one particularly well-known feature of the spectra is that they are well fitted, in the time domain, for times corresponding to the α relaxation with a stretched exponential $\exp[-(t/\tau_\alpha)^\beta]$. In the Fourier domain, forms such as the Havriliak-Negami law are used, $\epsilon(\omega) = \epsilon(\infty) + \Delta\epsilon/[1 + (i\omega\tau_\alpha)^\alpha]^\gamma$, which generalizes the Debye law. The exponents β , α , and γ depend, in general, on temperature and on the particular dynamic probe chosen, but they capture the fact that relaxation is increasingly nonexponential when T decreases toward T_g . A connection was empirically established between fragility and degree of nonexponentiality, more fragile liquids being characterized by broader relaxation spectra (Debenedetti and Stillinger, 2001), although the correlation is, again, not very solid (Heuer, 2008). Figure 4 also makes it clear that the relaxation spectra are actually quite complex and characterized by one or several secondary processes that have been quite extensively studied experimentally (Johari and Goldstein, 1970; Dixon *et al.*, 1990; Blochowicz *et al.*, 2006).

To sum up, there are many remarkable phenomena that take place when a supercooled liquid approaches the glass transition. Striking ones have been presented, but many others have been left out for lack of space (Angell, 1995; Debenedetti, 1996; Debenedetti and Stillinger, 2001; Binder and Kob, 2005). We discussed physical behaviors, relationships, or empirical correlations observed in a broad class of materials. These are quite remarkable and suggest that there is some interesting physics to be studied in the problem of the glass transition, which we see as a collective (critical?) phenomenon which is relatively independent of microscopic details.

B. Other glasses in science

We now introduce some other systems whose phenomenological behavior is close or, at least, related, to that of glass-forming liquids, showing that glassiness is truly ubiquitous. It appears not only in many different physical situations but also in more abstract contexts, such as computer science.

1. The jamming transition of colloids and grains

Colloidal suspensions consist of big particles suspended in a solvent (Larson, 1999). The typical radii of the particles are in the range $R = 1\text{--}500$ nm. The solvent, which is at equilibrium at temperature T , acts as a source of noise on the particles whose short-time dynamics is better described as being Brownian rather than Newtonian. The microscopic time scale for this diffusion is given by $\tau = R^2/D$, where D is the short-time self-diffusion coefficient. Typical values are of the order of $\tau \sim 1$ ms, and thus are much larger than the ones for molecular liquids (in the picosecond regime). The interaction potential between particles depends on the systems, and this large tunability makes colloids attractive objects for technical applications.

A particularly relevant case, on which we will focus in the following, is the purely hard-sphere potential, which is zero when particles do not overlap and infinite otherwise. In this case the temperature becomes irrelevant, apart from a trivial rescaling of the microscopic time scale. Colloidal hard-sphere systems have been intensively studied (Larson, 1999) in experiments, simulations, and theory, with varying density ρ or volume fraction $\phi = \frac{4}{3}\pi R^3\rho$. Hard spheres display a fluid phase from $\phi = 0$ to intermediate volume fractions, a freezing-crystallization transition at $\phi \simeq 0.494$, and a melting transition at $\phi \simeq 0.545$. Above this latter value the system can be compressed until the close packing point $\phi \simeq 0.74$, which corresponds to the fcc crystal. Interestingly for our purposes, a small amount of polydispersity (particles with slightly different sizes) efficiently prevents crystallization. In this case, the system can be more easily “supercompressed” above the freezing transition without nucleating the crystal, at least on experimental time scales. In this regime the relaxation time scale increases rapidly with ϕ (Pusey and van Meegen, 1986). At a packing fraction $\phi_g \simeq 0.57\text{--}0.59$ it becomes so large compared to typical experimental time scales that the system does not relax anymore: It is “jammed.” This jamming transition is obviously reminiscent of the glass transition of molecular systems. In particular, the location ϕ_g of the colloidal glass transition is as ill defined as the glass temperature T_g .

Actually, the phenomena that take place increasing the volume fraction are analogous to the ones seen in molecular supercooled liquid (Pusey and van Meegen, 1986): The viscosity increases rapidly and can be fitted (Cheng *et al.*, 2002) by a VFT law in density as in Eq. (2). Dynamical correlation functions display a broad spectrum of time scales and develop a plateau (Pusey and van Meegen, 1987); no static growing correlation length has been found, etc. Also the phenomenon of dynamic heterogeneity addressed in Sec. III seems similar in colloids and atomic systems (Kegel and van Blaaderen, 2000; Weeks *et al.*, 2000). However, it is important to underline a major difference: Because the microscopic time scale for colloids is so large, experiments can only track at best the first 5–6 decades of slowing down (Brambilla *et al.*, 2009). A major consequence is that the comparison between the glass and colloidal transitions must be performed by focusing in both cases on the first five decades of the slowing down, which corresponds to relatively high temperatures in molecular liquids. Understanding how much and to what extent the glassiness of colloidal suspensions is related to

the one of molecular liquids remains an active domain of research.

The glassiness of driven granular media has recently been thoroughly analyzed. Grains are macroscopic objects and, as a consequence, do not have any thermal motion. A granular material is therefore frozen in a given configuration if no energy is injected into the system (Jaeger *et al.*, 1996). However, it can be forced into a steady state by an external drive, such as shearing or tapping. The dynamics in this steady state shows remarkable similarities (and differences) with simple fluids. The physics of granular materials is a broad subject (Jaeger *et al.*, 1996). In the following we address only briefly what happens to a polydisperse granular fluid at high packing fractions. As for colloids, the time scales for relaxation or diffusion increase rapidly when density is increased, without any noticeable change in structural properties. Again, it is now established (D’Anna and Gremaud, 2001; Marty and Dauchot, 2005; Chaudhuri *et al.*, 2007; Keys *et al.*, 2007; Candelier *et al.*, 2010) that many phenomenological properties of the granular glass transition also occur in granular assemblies. As for colloids, going beyond the mere analogy and understanding how much these different physical systems are related is an active domain of research (Liu and Nagel, 2001).

This very question has been asked in a visual manner by Liu and Nagel (1998) who rephrased it in a single picture, now known as a “jamming phase diagram.” By building a common phase diagram for glasses, colloids, and grains, they asked whether the glass and jamming transitions of molecular liquids, colloids, and granular media are different facets of the same jammed phase. In this unifying phase diagram, a jammed phase (or jammed phases) can be reached either by lowering the temperature, as in molecular liquids, or increasing the packing fraction or decreasing the external drive in colloids and granular media.

2. More glasses in physics and beyond

There are many other physical contexts in which glassiness plays an important role (Young, 1998). One of the most famous examples is the field of spin glasses. Experimentally, spin glasses are composed of magnetic impurities interacting by quenched random couplings. At low temperatures, their dynamics become extremely slow and they freeze in an amorphous spin configuration dubbed a “spin glass” by P. W. Anderson. Experiments on spin glasses, in particular, aging studies, have played an important role in the context of amorphous materials. There are many other physical systems, often characterized by quenched disorder, that show glassy behavior, such as Coulomb glasses, Bose glasses, frustrated magnets, etc. In many cases, however, one finds quite different physics from structural glasses: The similarity between these systems is therefore only superficial from the phenomenological point of view, but the theoretical techniques and ideas developed, in particular, in the field of spin glasses are highly relevant in theoretical studies of the glass transition.

Finally, and quite remarkably, glassiness emerges even in other branches of science (Mézard *et al.*, 2007). In particular, it was discovered recently that concepts and techniques developed for glassy systems turn out to apply and be useful tools in the field of neural networks and computer science.

Problems such as combinatorial optimization display phenomena completely analogous to phase transitions, actually, to glassy phase transitions. *A posteriori*, this is quite natural, because a typical optimization problem consists of finding a solution in the presence of a large number of constraints. This can be defined, for instance, as a set of N Boolean variables that satisfies M constraints. For N and M large at fixed $\alpha = M/N$, this problem resembles that of finding a ground state in statistical mechanics with quenched disorder. Indeed one can define an energy function (a Hamiltonian) as the number of unsatisfied constraints, that has to be minimized, as in a $T = 0$ statistical mechanics problem. The connection with glassy systems lies in the fact that in both cases the energy landscape is extremely complicated, full of minima and saddles. The fraction of constraints per degree of freedom α plays a role similar to the density in a hard-sphere system. A detailed presentation of the relationship between optimization problems and glassy systems is clearly out of the scope of this review. We simply illustrate it, pointing out that a central problem in optimization, random k satisfiability, has been shown to undergo a glass transition when α increases that is reminiscent of the one of structural glasses and can be treated analytically using similar tools (Krzakala *et al.*, 2007).

C. Computer simulations of molecular glass formers

Studying the glass transition of molecular liquids at a microscopic level is in principle straightforward since one has to answer a simple question: How do particles move in a liquid close to T_g ? It is, of course, a daunting task to attempt answering this question experimentally, because one should then resolve the dynamics of single molecules to be able to follow the trajectories of objects that are a few angstroms large on time scales of tens or hundreds of seconds, which sounds like eternity when compared to typical molecular dynamics usually lying in the picosecond regime. In recent years, such direct experimental investigations have been attempted using time- and space-resolved techniques such as atomic force microscopy (Vidal Russell and Israeloff, 2000) or single molecule spectroscopy (Adhikari *et al.*, 2007; Mackowiak *et al.*, 2009), but this remains a difficult task.

In numerical simulations, by contrast, the trajectory of each particle in the system can, by construction, be followed at all times. This allows one to easily quantify single-particle dynamics, as proved in Fig. 5, where the averaged mean-squared displacement $\Delta(t)$ measured in a simple Lennard-Jones glass former is shown. The mean-squared displacement is defined by

$$\Delta(t) = \left\langle \frac{1}{N} \sum_{i=1}^N |\mathbf{r}_i(t) - \mathbf{r}_i(0)|^2 \right\rangle, \quad (7)$$

where $\mathbf{r}_i(t)$ represents the position of particle i at time t in a system composed of N particles; the angular brackets indicate an ensemble average over initial conditions weighted with the Boltzmann distribution. The main observation from the data shown in Fig. 5 is that single-particle displacements considerably slow down when T is decreased. This can be quantified by measuring the self-diffusion constant D_s , formally defined as $D_s = \lim_{t \rightarrow \infty} \Delta(t)/(6t)$. The data in Fig. 5 show that D_s decreases by orders of magnitude when temperature

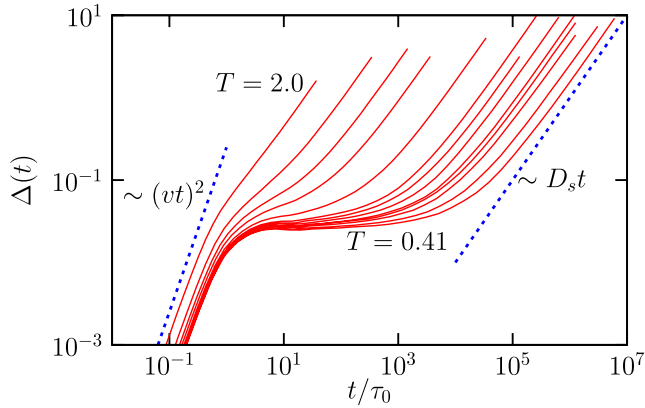


FIG. 5 (color online). Mean-squared displacements of individual particles in a simple model of a glass-forming liquid composed of Lennard-Jones particles observed on a wide time window. When temperature decreases (from left to right), the particle displacements become increasingly slow with several distinct time regimes corresponding, in this order, to ballistic, localized, and diffusive regimes.

decreases, and thus mirrors the behavior of the (inverse of the) viscosity shown in Fig. 2 for real systems. Therefore, to explain the phenomenon of the glass transition, one must equivalently explain why molecular motions become so slow at low temperatures.

Additionally, a rich dynamics is observed in Fig. 5, with a plateau regime at intermediate time scales, corresponding to an extended time window during which particles vibrate around their initial positions, as in a crystalline solid. The difference with a crystal is, of course, that this transient localization does not correspond to a well-defined position in an ordered structure, and it is only transient so that all particles eventually escape and, concomitantly, the structure relaxes at long times. Describing the molecular motions responsible for this broad spectrum of relaxation time scales is a challenge.

In recent years, computer experiments played an increasingly important role in glass transition studies (Andersen, 2005). It could almost be said that particle trajectories in numerical work have been studied under so many different angles that probably little remains to be learned from such studies in the regime that is currently accessible using present day computers. Unfortunately, this does not imply complete knowledge of the physics of supercooled liquids. As shown in Fig. 5, it is presently possible to follow the dynamics of a simple glass-forming liquid over more than eight decades of time, and over a temperature window in which average relaxation time scales increase by more than five decades. This might sound impressive, but a quick look at Fig. 2 shows, however, that at the lowest temperatures studied in the computer, the relaxation time scales are still orders of magnitude faster than in experiments performed close to the glass transition temperature. Simulations can be directly compared to experiments performed in this high-temperature regime, but this also implies that simulations focus on a relaxation regime that is about eight to ten decades of times faster than in experiments performed close to T_g . Whether numerical works are useful in understanding the glass transition itself at all is therefore an open, widely debated question. We believe that it

is now possible to numerically access temperatures which are low enough that many features associated with the glass transition physics can be observed: strong decoupling phenomena (see Sec. III), clear deviations from fits to the mode-coupling theory (which are experimentally known to hold only at high temperatures, see Sec. IV.B.2), and crossovers toward truly activated dynamics.

Classical computer simulations of supercooled liquids usually proceed by solving a cleverly discretized version of Hamilton's equations for the particles' positions and momenta and a given potential interaction between particles (Allen and Tildesley, 1987):

$$\frac{\partial \mathbf{r}_i}{\partial t} = \frac{\partial H}{\partial \mathbf{p}_i}, \quad \frac{\partial \mathbf{p}_i}{\partial t} = -\frac{\partial H}{\partial \mathbf{r}_i}, \quad (8)$$

where

$$H(\{\mathbf{p}_i, \mathbf{r}_i\}) = \sum_{i=1}^N \frac{\mathbf{p}_i^2}{2m_i} + V(\{\mathbf{r}_i\}) \quad (9)$$

is the system's Hamiltonian composed of a kinetic part and an interaction term $V(\{\mathbf{r}_i\})$. We have written Eqs. (8) and (9) in terms of the center of mass trajectories, as is appropriate for atoms although, of course, numerical simulations can deal with molecular degrees of freedom as well (Allen and Tildesley, 1987). Since the equations of motion are energy conserving, they describe the dynamics of atomistic systems in the microcanonical ensemble. Constant temperature or constant pressure schemes have been developed, allowing simulations to be performed in any desired statistical ensemble (Allen and Tildesley, 1987). Similarly, nonequilibrium simulation techniques exist that allow, for instance, computer studies of the aging dynamics or the nonlinear rheology of supercooled fluids (Evans and Morris, 2008); see also Sec. V.

If quantitative agreement with experimental data on an existing specific material is sought, the interaction must be carefully chosen in order to reproduce reality, for instance, by combining classical to *ab initio* simulations. From the more fundamental perspective adopted here, one rather seeks the simplest model that is still able to qualitatively reproduce the phenomenology of real glass formers, while being considerably simpler to study. The implicit, but quite strong, hypothesis is that molecular details are not needed to explain the behavior of supercooled liquids, so that the glass transition is indeed a topic for statistical mechanics, with little influence from chemical details. A considerable amount of work has therefore been dedicated to studying models where point particles interact via a simple pair potential such as Lennard-Jones interactions:

$$V(\{\mathbf{r}_i\}) = \sum_{i=1}^N \sum_{j=i}^N \epsilon \left[\left(\frac{\sigma}{r_{ij}} \right)^{12} - \left(\frac{\sigma}{r_{ij}} \right)^6 \right], \quad (10)$$

where $r_{ij} = |\mathbf{r}_i - \mathbf{r}_j|$, and ϵ and σ represent an energy scale and the particle diameter, respectively. Other popular models are soft spheres, where only the steep short-range repulsion in Eq. (10) is considered, or even hard spheres where the repulsion is made infinitely steep. If the system is too simple, such as the one defined in (10), the glass transition cannot be studied because crystallization takes place when temperature is lowered. Some frustration must be introduced to devise

numerical models with good glass-forming abilities. A common solution, inspired by experimental studies of metallic glasses, is to use mixtures of different atoms, as in the popular model devised by Kob and Andersen (1994, 1995a, 1995b) which uses a nonadditive binary mixture of Lennard-Jones particles.

More realistic materials are also studied focusing, for instance, on the physics of network forming materials (such as silica, SiO_2 , the main component of window glasses), multicomponent ones, anisotropic particles, or molecules with internal degrees of freedom. Connections to experimental work can be made by computing quantities that are experimentally accessible such as the intermediate scattering function, Eq. (6), static structure factors, $S(\mathbf{q})$, Eq. (4), or thermodynamic quantities such as specific heat or configurational entropy, which are directly obtained from particle trajectories and can be measured in experiments as well. As an example we show in Fig. 6 the intermediate scattering function $F(\mathbf{q}, t)$ obtained from a molecular dynamics simulation of a classical model for SiO_2 as a function of time for different temperatures (Horbach and Kob, 2001). The numerical data compare favorably with the experimental results obtained from neutron scattering shown in Fig. 3. Note that they actually access the dynamics over a broader range of time scales and temperatures.

An important role is played by simulations, also because a large variety of dynamic and static quantities can be simultaneously measured in a single model system. As we shall discuss later, there exist scores of different theoretical approaches to describe the physics of glass formers, and they sometimes have their own set of predictions that can be readily tested by numerical work. For instance, quite a large number of numerical papers have been dedicated to testing in detail the predictions formulated by the mode-coupling theory of the glass transition, as reviewed recently by Götze (1999, 2008). Here computer simulations are particularly well suited as the theory specifically addresses the relatively high-temperature window that is studied in computer simulations.

While Newtonian dynamics is mainly used in numerical work on supercooled liquids, a most appropriate choice for atomistic materials, it can be interesting to consider alternative dynamics that are not deterministic or that do not conserve the

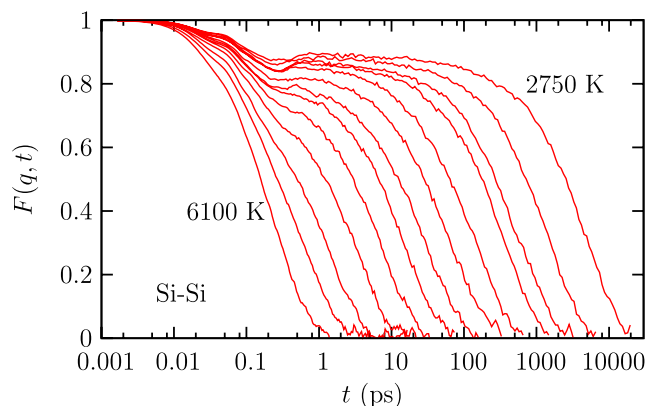


FIG. 6 (color online). Intermediate scattering function at wave vector $q = 1.7 \text{ \AA}^{-1}$ for the Si atoms from $T = 6100$ to $T = 2750$ K, obtained from molecular dynamics simulations of silica. From Horbach and Kob, 2001.

energy. In colloidal glasses and physical gels, for instance, particles undergo Brownian motion arising from collisions with molecules in the solvent, and a stochastic dynamics is more appropriate. Theoretical considerations might also suggest the study of different sorts of dynamics for a given interaction between particles, for instance, to assess the role of conservation laws and structural information. Of course, if a given dynamics satisfies detailed balance with respect to the Boltzmann distribution, all structural quantities remain unchanged, but the resulting dynamical behavior might be different. More generally one can ask the question: How universal is the glass transition phenomenon? Does it depend upon the specific microscopic dynamics?

Several papers studied in detail the influence of the dynamics on the resulting dynamical behavior in glass formers using different types of microscopic dynamics. Gleim *et al.* (1998) studied “stochastic dynamics” which generalizes Newton’s equations to include nondeterministic forces:

$$m_i \frac{d^2 \mathbf{r}_i}{dt^2} = - \frac{\partial V(\{\mathbf{r}_i\})}{\partial \mathbf{r}_i} - \zeta \frac{\partial \mathbf{r}_i}{\partial t} + \eta_i. \quad (11)$$

Specifically, a friction term proportional to the velocity with a damping constant ζ is added to the right-hand side, as well as a Gaussian distributed white noise η_i , whose correlations are related to the damping via the fluctuation-dissipation theorem $\langle \eta_i(t) \eta_j(t') \rangle = 6k_B T \zeta \delta_{ij} \delta(t - t')$, so that the equilibrium distribution at temperature T is indeed recovered. When ζ gets large the dynamics becomes similar to a purely Brownian dynamics, as recently studied, for instance, by Szamel and Flenner (2004):

$$\zeta \frac{\partial \mathbf{r}_i}{\partial t} = - \frac{\partial V(\{\mathbf{r}_i\})}{\partial \mathbf{r}_i} + \eta_i. \quad (12)$$

In that case, particles are described by their positions only, and, therefore, momenta play no role. A similar type of description, although numerically more efficient (Berthier, 2007a; Berthier and Kob, 2007), is obtained using a standard Monte Carlo approach where the change in potential energy between two configurations is used to accept or reject a trial move. In both cases of Brownian and Monte Carlo dynamics, particles have diffusive (rather than ballistic) behavior at short times where differences between the different types of dynamics can therefore be expected.

Quite surprisingly, however, the equivalence between these three types of stochastic dynamics and the originally studied Newtonian dynamics was quantitatively established at the level of the averaged dynamical correlators for all three types of dynamics mentioned above, except at short times where obvious differences are indeed expected. This equivalence can probably be traced back to the existence of fast and slow degrees of freedom. It is reasonable to think that the former act as an effective thermal bath for the latter, thus making the three types of dynamics equivalent on long time scales. However, this interpretation has to be taken with a grain of salt since important differences were found when fluctuations of dynamical correlators were considered (Berthier *et al.*, 2007a), even in the long-time regime corresponding to the structural relaxation.

Another crucial advantage of molecular simulations is illustrated in Fig. 7. Figure 7 shows a spatial map of

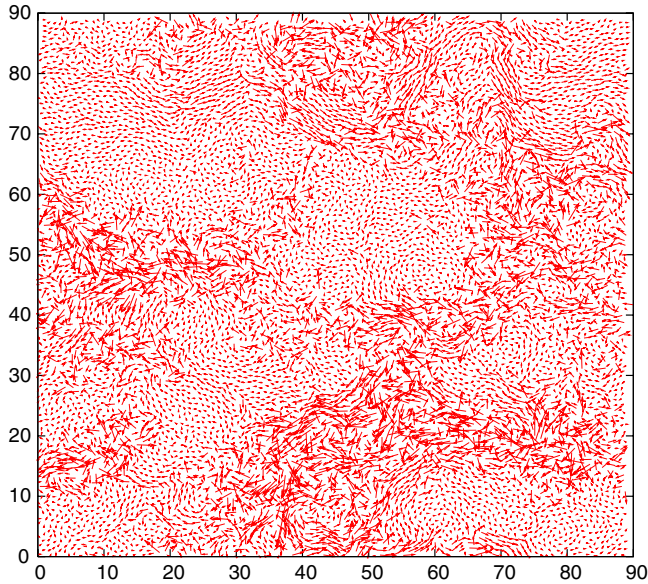


FIG. 7 (color online). Spatial map of single-particle displacements in the simulation of a binary mixture of Lennard-Jones mixture in two dimensions. Arrows show the displacement of each particle in a trajectory of length comparable to the structural relaxation time. The map reveals the existence of particles with different mobilities during relaxation, but also the existence of spatial correlations between these dynamic fluctuations.

single-particle displacements recorded during the simulation of a binary Lennard-Jones mixture in two dimensions. This type of measurement, out of reach of most experimental techniques that study the liquid state, reveals that dynamics might be different from one particle to another (transiently). More importantly, Fig. 7 also unambiguously reveals the existence of spatial correlations between these dynamic fluctuations. The presence of nontrivial spatiotemporal fluctuations in supercooled liquids is called “dynamic heterogeneity” (Ediger, 2000; Berthier *et al.*, 2011). The phenomenon has become a substantial component of the field of the glass transition, and computer simulations have naturally played an important role since they reveal the heterogeneous nature of the relaxation much more directly than experiments. We discuss the phenomenon of dynamic heterogeneity in more detail in the next section.

III. DYNAMIC HETEROGENEITY

A. Existence of spatiotemporal dynamic fluctuations

A new facet of the relaxational behavior of supercooled liquids has emerged in the last decade thanks to a considerable experimental and theoretical effort. It is called dynamic heterogeneity and now plays a central role in modern descriptions of glassy liquids (Ediger, 2000). As anticipated in the discussion of Fig. 7 in the previous section, the phenomenon of dynamic heterogeneity is related to the spatiotemporal fluctuations of the dynamics. Initial motivations stemmed from the search for an explanation of the nonexponentiality of relaxation processes in supercooled liquids, related to the existence of a broad relaxation spectrum. Two natural, but fundamentally different, explanations can be put forward.

(1) The relaxation is locally exponential, but the typical relaxation time scale varies spatially. Hence, global correlation or response functions become nonexponential upon spatial averaging over this spatial distribution of relaxation times. (2) The relaxation is complicated and inherently non-exponential, even locally. Experimental and theoretical works (Ediger, 2000) suggest that both mechanisms are likely at play, but definitely conclude that relaxation is spatially heterogeneous, with regions that are faster and slower than the average. Since supercooled liquids are ergodic systems, a slow region will eventually become fast, and vice versa. A physical characterization of dynamic heterogeneity entails the determination of the typical lifetime of the heterogeneities, as well as their typical length scale.

A clearer and more direct confirmation of the heterogeneous character of the dynamics also stems from simulation studies. For example, whereas the simulated average mean-squared displacements are smooth functions of time (see Fig. 5), time signals for individual particles clearly exhibit specific features that are not observed unless dynamics is resolved in both space and time. These features are displayed in Fig. 8. What do we see? We mainly observe that particle trajectories are not smooth but rather composed of a succession of long periods of time where particles simply vibrate around well-defined locations, separated by rapid jumps. Vibrations were previously inferred from the plateau observed at intermediate times in the mean-squared displacements of Fig. 5, but the existence of jumps that are clearly statistically widely distributed in time cannot be guessed from averaged quantities only. The fluctuations in Fig. 8 suggest, and direct measurements confirm, the importance played by fluctuations around the averaged dynamical behavior.

A simple type of such fluctuations has been studied in much detail. When looking at Fig. 8, it is indeed natural to ask, for any given time, what is the distribution of particle displacements? This is quantified by the self-part of the van Hove function defined as

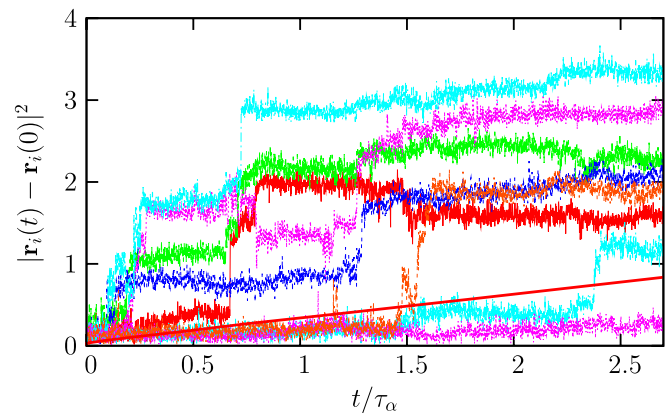


FIG. 8 (color online). Time-resolved squared displacements of individual particles in a simple model of a glass-forming liquid composed of Lennard-Jones particles near the fitted mode-coupling critical temperature. The average is shown as a smooth full line. Trajectories are composed of long periods of time during which particles vibrate around well-defined positions, separated by rapid jumps that are widely distributed in time, underlying the importance of dynamic fluctuations.

$$G_s(\mathbf{r}, t) = \left\langle \frac{1}{N} \sum_{i=1}^N \delta(\mathbf{r} - [\mathbf{r}_i(t) - \mathbf{r}_i(0)]) \right\rangle. \quad (13)$$

For an isotropic Gaussian diffusive process, one gets $G_s(\mathbf{r}, t) = \exp[-|\mathbf{r}|^2/(4D_s t)]/(4\pi D_s t)^{3/2}$. Simulations reveal instead strong deviations from Gaussian behavior on the time scales relevant for structural relaxation (Kob *et al.*, 1997). In particular, they reveal tails in the distributions that are “fat,” in the sense that they are much wider than expected from the Gaussian approximation. These tails are, in fact, well described by an exponential, rather than Gaussian, decay in a wide time window comprising the structural relaxation, such that $G_s(\mathbf{r}, t) \sim \exp[-|\mathbf{r}|/\lambda(t)]$ (Chaudhuri *et al.*, 2007). Thus, they reflect the existence of a population of particles that distinctively moves farther than the rest and appears therefore to be much more mobile. The exponential form of the tail originates from the intermittent nature of the particle trajectories exposed in Fig. 8, made of a succession of jumps separated by vibrations (Chaudhuri *et al.*, 2007). Actually, such a tail would be present in simple jump models for diffusion (Hansen and McDonald, 2006). This observation implies that relaxation in a viscous liquid differs qualitatively from that of a normal liquid where diffusion is close to Gaussian, and that a nontrivial statistics of single-particle displacements exists.

A long series of questions immediately follows this seemingly simple observation. Answering them has been the main occupation of many workers in this field over the last decade. What are the particles corresponding to the tails effectively doing? Why are they faster than the rest? Are they located randomly in space or do they cluster? What is the geometry, time, and temperature evolution of the clusters? Are these spatial fluctuations correlated to geometric or thermodynamic properties of the liquids? Do similar correlations occur in all glassy materials? Can one predict these fluctuations theoretically? Can one understand glassy phenomenology using fluctuation-based arguments? How can these fluctuations be detected experimentally?

Another influential phenomenon that was early related on to the existence of dynamic heterogeneity is the decoupling of self-diffusion (D_s) and viscosity (η). In the high-temperature liquid self-diffusion and viscosity are related by the Stokes-Einstein relation (Hansen and McDonald, 2006), $D_s \eta/T = \text{const}$. For a large particle moving in a fluid the constant is equal to $1/(6\pi R)$, where R is the particle radius. Physically, the Stokes-Einstein relation means that two different measures of the relaxation times R^2/D_s and $\eta R^3/T$ lead to the same time scale up to a constant factor. In supercooled liquids this phenomenological law breaks down, as shown in Fig. 9 for *ortho*-terphenyl (Mapes *et al.*, 2006). It is commonly found that D_s^{-1} does not increase as fast as η/T so that, at T_g , the product $D_s \eta/T$ has increased by 2–3 orders of magnitude as compared to its Stokes-Einstein value. This phenomenon, although less spectacular than the overall change of viscosity, is a significant indication that different ways to measure relaxation times lead to different answers and, thus, is a strong hint of the existence of broad “distributions” of relaxation time scales.

Indeed, a natural explanation of this effect is that different observables probe differently the underlying distribution of relaxation times (Ediger, 2000). For example, the self-diffusion coefficient of tracer particles is dominated by the

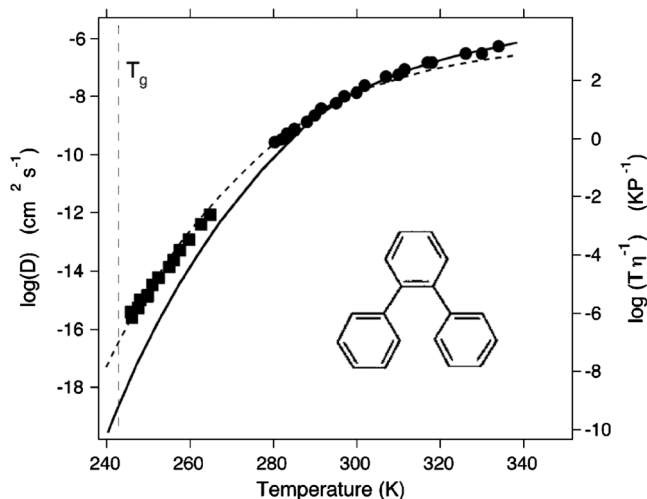


FIG. 9. Decoupling between viscosity (full line) and self-diffusion coefficient (symbols) in supercooled *ortho*-terphenyl (Mapes *et al.*, 2006). The dashed line shows a fit with a “fractional” Stokes-Einstein relation $D_s \sim (T/\eta)^\zeta$ with $\zeta \sim 0.82$ instead of the “normal” value $\zeta = 1$ which holds only at high temperatures.

more mobile particles, whereas the viscosity or other measures of structural relaxation probe the time scale needed for every particle to move. An unrealistic but instructive example is a model where there is a small, nonpercolative subset of particles that are blocked forever, coexisting with a majority of mobile particles. In this case, the structure never relaxes but the self-diffusion coefficient is nonzero because of the mobile particles. Of course, in reality all particles move, eventually, but this shows how different observables are likely to probe different moments of the distribution of time scales, as explicitly shown within several theoretical frameworks (Stillinger and Hodgdon, 1994; Tarjus and Kivelson, 1995; Jung *et al.*, 2004).

The phenomena described above clearly show that the dynamics is spatially heterogeneous. However, they are in principle not able to probe whether this is related to *purely local* fluctuations or if there are instead increasingly *spatially correlated* fluctuations. This is, however, a fundamental issue from both the experimental and theoretical points of view. How large are the regions that are faster or slower than the average? How does their size depend on temperature? Are these regions compact or fractal? These important questions were first addressed in pioneering works using four-dimensional NMR (Tracht *et al.*, 1998; Reinsberg *et al.*, 2001), or by directly probing fluctuations at the nanoscopic scale using microscopy techniques. In particular, Vidal Russell and Israeloff (2000), using atomic force microscopy techniques, measured the polarization fluctuations in a volume of size of a few tens of nanometers in a supercooled polymeric liquid (PVAc) close to T_g . In this spatially resolved measurement, the hope is to probe a small enough number of dynamically correlated regions and detect their dynamics. Indeed, the signals shown by Vidal Russell and Israeloff (2000) reveal that the dynamics is intermittent in time: It switches between moments with intense activity and moments with no dynamics at all, suggesting that extended regions of space indeed transiently behave as fast and slow regions. A much smoother signal would have been measured

if such dynamically correlated “domains” were not present. Spatially resolved studies such as NMR experiments or atomic force microscopy are quite difficult to perform. They give undisputed information about the typical lifetime of the dynamic heterogeneity, but their determination of a dynamic correlation length scale is rather indirect and performed on a small number of liquids in a small temperature window. Nevertheless, the outcome is that a nontrivial dynamic correlation length emerges at the glass transition, where it reaches a value of the order of about ~ 10 molecule diameters (Ediger, 2000).

B. Multipoint correlation functions

Recently, substantial progress in characterizing spatiotemporal dynamical fluctuations was performed. In particular, it is now understood that dynamical fluctuations can be measured and characterized through the use of high-order correlation and response functions. These multipoint functions can be seen as generalizations of the spin glass susceptibility measuring the extent of amorphous long-range order in spin glasses. We now introduce these dynamical functions and summarize the main results obtained from their study.

1. Why four-point correlators? The spin glass case

No simple static correlation has yet been found to reveal any notable feature upon approaching the glass transition (see Sec. VI for recent theoretical progress). As a consequence, it is quite natural to investigate whether a growing length scale associated with the slowing down of the system is hidden in some dynamic correlation function.

Spin glass theory faced a similar conundrum, whose solution we briefly recall because it has been instrumental in the developments for glass-forming liquids. We know that some hidden long-range order develops at the spin glass transition (Binder and Young, 1986). However, also for spin glasses, conventional two-point functions are useless. Even if spins $s_{\mathbf{x}}$ and $s_{\mathbf{x}+\mathbf{y}}$ have nonzero static correlations $\langle s_{\mathbf{x}}s_{\mathbf{x}+\mathbf{y}} \rangle$ in the spin glass phase, the average over space, $[\cdot \cdot \cdot]_{\mathbf{x}} = V^{-1} \int d\mathbf{x} \cdot \cdot \cdot$, for a given distance $|\mathbf{y}|$ vanishes because the pairwise correlations randomly change sign whenever \mathbf{x} changes. The insight of Edwards and Anderson (1975) is that one should first square $\langle s_{\mathbf{x}}s_{\mathbf{x}+\mathbf{y}} \rangle$ before averaging over space. In this case, the resulting *four-spin* correlation function indeed develops long-range tails in the spin glass phase. This correlation, in fact, decays so slowly that its volume integral, related to the nonlinear magnetic susceptibility of the material, diverges in the whole spin glass phase (Binder and Young, 1986).

Edwards and Anderson’s idea can, in fact, be understood from a dynamical point of view, which is important for understanding both the physics of the spin glass just above the transition and its generalization to structural glasses. Consider, in the language of spins, the following four-point correlation function:

$$G_4(\mathbf{y}, t) = [\langle s_{\mathbf{x}}(t=0)s_{\mathbf{x}+\mathbf{y}}(t=0)s_{\mathbf{x}}(t)s_{\mathbf{x}+\mathbf{y}}(t) \rangle]_{\mathbf{x}}. \quad (14)$$

Suppose that spins $s_{\mathbf{x}}$ and $s_{\mathbf{x}+\mathbf{y}}$ develop static correlations $\langle s_{\mathbf{x}}s_{\mathbf{x}+\mathbf{y}} \rangle$ within the glass phase. In this case, $G_4(\mathbf{y}, t \rightarrow \infty)$ will clearly converge to the spin glass correlation $[\langle s_{\mathbf{x}}s_{\mathbf{x}+\mathbf{y}} \rangle^2]_{\mathbf{x}}$. More generally, $G_4(\mathbf{y}, t)$ for finite t is able to

detect *transient* tendencies to spin glass order, for example, slightly above the spin glass transition temperature T_c . Close to the spin glass transition, both the persistence time and the dynamic length diverge in a critical way:

$$G_4(\mathbf{y}, t) \approx y^{2-d-\eta} \hat{G}\left(\frac{y}{\xi}, \frac{t}{\tau}\right), \quad (15)$$

where $\xi \sim (T - T_c)^{-\nu}$ and $\tau \sim (T - T_c)^{-z\nu}$. As mentioned above, the static nonlinear susceptibility diverges as $\int d\mathbf{y} G_4(\mathbf{y}, t \rightarrow \infty) \sim \xi^{2-\eta}$. More generally, one can define a time-dependent dynamic susceptibility as

$$\chi_4(t) \equiv \int d\mathbf{y} G_4(\mathbf{y}, t), \quad (16)$$

which defines, provided $G_4(\mathbf{0}, t)$ is a number of order 1, a correlation volume, i.e., the typical number of spins correlated in dynamic events taking place over the time scale t . As we shall discuss, $\chi_4(t)$ can also be interpreted as a quantitative measure of the dynamic fluctuations. Note, however, that the precise relation between χ_4 and ξ depends on the value of the exponent η , which is physically controlled by the detailed spatial structure of dynamically correlated regions encoded in G_4 :

$$\chi_4(t = \tau) \propto \xi^{2-\eta}. \quad (17)$$

Therefore, spin glasses offer a precise example of a system which gets slower and slower upon approaching T_c but without any detectable long-range order appearing in two-point correlation functions. Only more complicated four-point functions are sensitive to the genuine amorphous long-range order that sets in at T_c and give nontrivial information even above T_c . In the case of spin glasses it is well established that the transition is related to the emergence of a low-temperature spin glass phase.

In the case of the glass transition of viscous liquids the situation is much less clear. First, unlike spin glasses where the disorder is quenched, glass formers tend to freeze in an amorphous state where disorder is instead self-induced. Second, there might be no true phase transition toward a low-temperature amorphous phase. It is nevertheless still reasonable to expect that the dramatic increase of the relaxation time is due to a transient amorphous order that sets in and whose range grows approaching the glass transition. Growing time scales should be somehow related to growing length scales (Montanari and Semerjian, 2006b). A good candidate to unveil the existence of this phenomenon is the function $G_4(\mathbf{y}, t)$ introduced previously, since nothing in the above arguments was specific to systems with quenched disorder. The only difference is that although transient order is detected in $G_4(\mathbf{y}, t)$ or its volume integral $\chi_4(t)$ for times of the order of the relaxation time, in the long-time limit these two functions may not, and indeed do not in the case of supercooled liquids, show long-range amorphous order. This is rooted back in the different natures of the glass and spin glass transitions.

2. Four-point functions in supercooled liquids

In the case of liquids, we consider a certain space-dependent observable $o(\mathbf{x}, t)$, such as, for example, the local excess density $\delta\rho(\mathbf{x}, t) = \rho(\mathbf{x}, t) - \rho_0$, where ρ_0 is the average density of the liquid, or the local dipole moment, the excess energy, etc. We will assume in the following that

the average of $o(\mathbf{x}, t)$ is equal to 0, and the variance of $o(\mathbf{x}, t)$ is normalized to unity. The dynamic two-point correlation is defined as

$$C_o(\mathbf{r}, t) = [o(\mathbf{x}, t = 0)o(\mathbf{x} + \mathbf{r}, t)]_{\mathbf{x}}, \quad (18)$$

where the normalization ensures that $C_o(\mathbf{r} = \mathbf{0}, t = 0) = 1$. The Fourier transform of $C_o(\mathbf{r}, t)$ defines a generalized dynamic structure factor $S_o(\mathbf{k}, t)$ (Hansen and McDonald, 2006). All experimental and numerical results known to date suggest that as the glass transition is approached, no spatial anomaly of any kind appears in $C_o(\mathbf{r}, t)$ [or in $S_o(\mathbf{k}, t)$], although, of course, there could still be some signal which is perhaps too small to be measurable. The only remarkable feature is that the slowing down of the two-point correlation functions often obeys, to a good approximation, “time-temperature superposition” in the α -relaxation regime $t \sim \tau_\alpha$, i.e.,

$$C_o(\mathbf{r}, t) \approx q_o(\mathbf{r})f\left(\frac{t}{\tau_\alpha(T)}\right), \quad (19)$$

where q_o is often called the nonergodicity (or Edwards-Anderson) parameter, and the scaling function $f(x)$ depends only weakly on temperature. This property will be used to simplify the following discussions, but it is not a needed ingredient.

The spatial correlations of the relaxation process can be probed studying the distribution (over dynamical histories) of the correlation $C_o(\mathbf{r}, t)$, in particular, its covariance. Quite generally, one expects that since $C_o(\mathbf{r}, t)$ is defined as an average over some large volume V , its variance Σ_C^2 is of order $\xi^{2-\eta}/V$, where ξ is the length scale over which $C_o(\mathbf{r}, t)$ is significantly correlated. More precisely we define

$$G_4(\mathbf{y}, t) = [o(\mathbf{x}, 0)o(\mathbf{x} + \mathbf{r}, t)o(\mathbf{x} + \mathbf{y}, 0)o(\mathbf{x} + \mathbf{y} + \mathbf{r}, t)]_{\mathbf{x}} - [o(\mathbf{x}, t = 0)o(\mathbf{x} + \mathbf{r}, t)]_{\mathbf{x}}^2, \quad (20)$$

and its space integral,

$$\Sigma_C^2 = \frac{1}{V} \int d\mathbf{y} G_4(\mathbf{y}, t), \quad (21)$$

which is nothing but the variance of the spontaneous fluctuations of $C_o(\mathbf{r}, t)$ averaged over a volume V . This variance can thus be expressed as an integral over space of a four-point correlation function, which measures the spatial correlation of the temporal correlation. This integral over space is also the Fourier transform of $G_4(\mathbf{y}, t)$ with respect to \mathbf{y} at the wave vector \mathbf{q} equal to 0. We want to insist at this stage that \mathbf{r} and \mathbf{y} in the above equations play different roles: The former enters the definition of the correlator we are interested in, Eq. (18), whereas the latter is associated with the scale over which the dynamics is potentially correlated. Correspondingly, great care should be devoted to distinguish the wave vector \mathbf{k} , conjugate to \mathbf{r} , and \mathbf{q} conjugate to \mathbf{y} .

Specializing to the case $\mathbf{r} = \mathbf{0}$ (local dynamics), one finally obtains

$$\chi_4(t) \equiv N \Sigma_C^2. \quad (22)$$

The analogy with spin glasses developed above suggests that this quantity reveals the emergence of transient amorphous

long-range order. Although, as we discuss, the situation is more complicated than was originally surmised; this analogy was indeed the main motivation for the first numerical investigation of $\chi_4(t)$ in a supercooled liquid (Dasgupta *et al.*, 1991). It was later realized that $\chi_4(t)$ is, in fact, the natural diverging susceptibility in the context of p -spin descriptions of supercooled liquids, where a true dynamical phase transition occurs at a certain critical temperature (Kirkpatrick and Thirumalai, 1988; Franz and Parisi, 2000). However, since in real systems no true phase transition can be observed, one expects $\chi_4(t)$ to grow until $t \approx \tau_\alpha$ and decay back to zero thereafter. Until τ_α , there cannot be strong differences between a system with quenched disorder and a system where disorder is dynamically self-induced.

Measuring the “local” relaxation suggests following the displacement of single particles over distances typically corresponding to the interparticle distance. Therefore, $\chi_4(t)$ can be accessed either by measuring the fluctuations of the Fourier transform of $C_o(\mathbf{r}, t)$ evaluated at a wave vector k_0 , of the order of the first peak in the structure factor (Berthier, 2004), or by performing a spatial average $\int d\mathbf{r} C_o(\mathbf{r}, t)w(\mathbf{r})$, where $w(\mathbf{r})$ is an overlap function equal to one for lengths of the order of $2\pi/k_0$ and zero otherwise (Lacevic *et al.*, 2003) or a Gaussian function with a suitable width (Dauchot *et al.*, 2005). The dependence of dynamical correlations on the coarse-graining length has been thoroughly studied, in both simulations (Chandler *et al.*, 2006) and experiments (Dauchot *et al.*, 2005; Duri and Cipelletti, 2006; Abate and Durian, 2007), showing that the dynamics becomes homogeneous when the coarse graining is made too small (where dynamics is dominated by trivial thermal vibrations), or too large (because dynamics results in this limit from a succession of several uncorrelated rearrangements).

For supercooled liquids, the function $\chi_4(t)$ has been measured by molecular dynamics, Brownian, and Monte Carlo simulations in different liquids (Bennemann *et al.*, 1999; Franz *et al.*, 1999; Parisi, 1999; Glotzer, 2000; Lacevic *et al.*, 2003; Berthier, 2004; Vogel and Glotzer, 2004; Berthier, 2007a; Parsaeian and Castillo, 2008; El Masri *et al.*, 2010). Moreover, its behavior has been theoretically investigated using various perspectives, as described in Sec. IV.

As suggested by its definition in Eq. (22), the four-point dynamic susceptibility is measured in practice through the repeated measurement of a chosen local time-correlation function, $\chi_4(t)$ being nothing but the variance of the statistical fluctuations between different measurements.

A typical example of such a measurement is shown in Fig. 10, taken from Monte Carlo simulations of a simple Lennard-Jones supercooled liquid. A similar qualitative behavior is found in nearly all cases, as detailed by Toninelli *et al.* (2005). At a given temperature, $\chi_4(t)$ is an increasing function of time at short times reflecting the fact that dynamic heterogeneities slowly build up with time. It then has a peak on a time scale that tracks the structural relaxation time scale τ_α , and finally it decreases back to zero when $t \rightarrow \infty$. When temperature is decreased the observed time evolution becomes slower, mimicking the overall slowing down of the dynamics also seen in averaged two-time correlators; see Fig. 10. The decrease at long times constitutes the above mentioned major difference with spin glasses. In a spin glass,

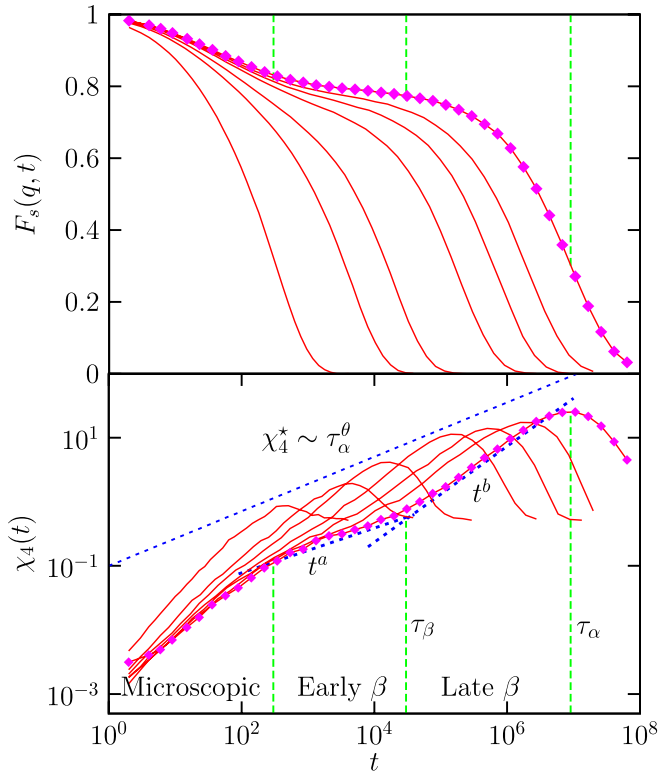


FIG. 10 (color online). Time dependence of the self-intermediate scattering function (top panel), and its spontaneous fluctuations (bottom panel), for different temperatures decreasing from left to right in a Lennard-Jones supercooled liquid in Monte Carlo simulations. The lowest temperature is highlighted with symbols. For each temperature, $\chi_4(t)$ has a maximum near the relaxation time τ_α , which shifts to larger times and has a larger value when T is decreased, revealing the increasing length scale of dynamic heterogeneity in supercooled liquids approaching the glass transition. Moreover, the time dependence of $\chi_4(t)$ is characterized by several distinct time regimes, corresponding to microscopic, early, and late β regimes, and structural relaxation, as indicated by the vertical lines.

$\chi_4(t)$ would be a monotonically increasing function of time whose long-time limit coincides with the static spin glass susceptibility.

The most important information extracted from the temperature evolution of $\chi_4(t)$ is that, at least in the range available to numerical simulations, the value of the peak at τ_α increases typically from a high-temperature value of order 1, and increases by at most 2 orders of magnitude down to the lowest temperature at which the system can be equilibrated, suggesting that dynamics becomes spatially increasingly correlated when T decreases.

As shown in Fig. 10, the time and temperature behavior of $\chi_4(t)$ is rich. The growth of $\chi_4(t)$ toward its peak value is composed of several time regimes, closely reflecting the broad spectrum of relaxation processes characterizing time-correlation functions; see Fig. 10. The short-time dynamics corresponding to the approach and departure from the plateau in time-correlation functions is also reflected in the time dependence of $\chi_4(t)$, which grows with distinct temporal power laws in the early and late β regimes. Additionally, the temperature evolution of $\chi_4(t)$, and, in particular, the peak height, can be quantitatively studied. This peak value χ_4^* measures the

volume on which the dynamical processes relevant to structural relaxation at $t \approx \tau_\alpha$ are correlated. It is found to increase when the temperature decreases and the dynamics slows down. In the temperature regime above the mode-coupling temperature, the growth is well described by an algebraic relation between the peak amplitude χ_4^* and the relaxation time τ_α , as shown in Fig. 10. The different exponents introduced in Fig. 10 are discussed by Toninelli *et al.* (2005).

More direct evidences of a growing dynamical correlation length can be obtained by directly measuring $G_4(\mathbf{y}, t)$. It has been checked that the increase of the peak of $\chi_4(t)$ corresponds, as expected, to a growing dynamic length scale ξ (Yamamoto and Onuki, 1998a; Bennemann *et al.*, 1999; Donati *et al.*, 1999; Doliwa and Heuer, 2000; Lacevic *et al.*, 2002, 2003; Whitelam *et al.*, 2004; Berthier *et al.*, 2007a). However, these measurements are much harder than the ones of χ_4 , because large systems need to be simulated to determine ξ unambiguously (Stein and Andersen, 2008; Karmakara *et al.*, 2009; Flenner and Szamel, 2010). Note that if the dynamically correlated regions were compact, the peak of χ_4 would be proportional to ξ^3 in three dimensions, directly relating χ_4 measurements to that of the relevant length scale of dynamic heterogeneity.

The study of the growth laws of $\chi_4(t)$, ξ , and the evolution of $G_4(\mathbf{y}, t)$ contains useful information to unveil the complexity of the relaxation processes and to contrast theoretical approaches (Toninelli *et al.*, 2005). In fact, many theories of the glass transition assume or predict, in one way or another, that the dynamics slows down because there are increasingly larger regions over which particles have to relax in a correlated or cooperative way; see Sec. IV.

Furthermore, the growth of ξ suggests that the glass transition is indeed a collective phenomenon characterized by growing time scales and length scales, reminiscent of critical phenomena. A clear and conclusive understanding of the relationship between the length scale obtained from $G_4(\mathbf{y}, t)$ and the relaxation time scale is still the focus of an intense research activity.

3. Three-point correlation and response functions

Although readily accessible in numerical simulations, $\chi_4(t)$ is in general small and difficult to measure directly in experiments, except when the range of the dynamic correlation is macroscopic, as in granular materials (Dauchot *et al.*, 2005; Marty and Dauchot, 2005; Keys *et al.*, 2007) or in soft glassy materials (Weeks *et al.*, 2007), where it can reach in some cases the micrometer and even millimeter range (Mayer *et al.*, 2004; Duri and Cipelletti, 2006; Maccarrone *et al.*, 2010). To access $\chi_4(t)$ in molecular liquids, one should perform time-resolved dynamic measurements probing small volumes, with a linear size of the order of a few nanometers. Although doable, such experiments remain to be performed with the needed accuracy.

It was recently realized that simpler alternative procedures exist (Berthier *et al.*, 2005). The central idea underpinning these results is that induced dynamic fluctuations are in general more easily accessible than spontaneous ones, and both types of fluctuations can be related to one another by fluctuation-dissipation theorems. The physical motivation is that while four-point correlations offer a direct probe of the

dynamic heterogeneities, other multipoint correlation functions give useful and direct information about the microscopic mechanisms leading to these heterogeneities. For example, one might expect that the slow part of a local enthalpy (or energy, density, etc.) fluctuation per unit volume δh at position \mathbf{x} and time $t = 0$ triggers or eases the dynamics in its surroundings, leading to a systematic correlation between $\delta h(\mathbf{x}, t = 0)$ and $o(\mathbf{x} + \mathbf{y}, t = 0)o(\mathbf{x} + \mathbf{y} + \mathbf{r}, \tau_\alpha)$. This physical intuition suggests the definition of a family of three-point correlation functions that relate thermodynamic or structural fluctuations to dynamical ones. Interestingly, and crucially, some of these three-point correlations are both experimentally accessible and give bounds or approximations to the four-point dynamic correlations, as we now detail.

In the same way that the space integral of the four-point correlation function is the variance of the two-point correlation, the space integral of the above three-point correlation is the covariance of the dynamic correlation with enthalpy fluctuations:

$$\begin{aligned}\Sigma_{CH} &= \frac{1}{VN} \int d\mathbf{x} d\mathbf{x}' o(\mathbf{x}' + \mathbf{r}, t) o(\mathbf{x}', 0) \delta h(\mathbf{x}, 0) \\ &\equiv \frac{1}{N} \int d\mathbf{y} [o(\mathbf{x} + \mathbf{y} + \mathbf{r}, t) o(\mathbf{x} + \mathbf{y}, 0) \delta h(\mathbf{x}, 0)]_{\mathbf{x}}.\end{aligned}\quad (23)$$

Note that for the enthalpy we use the notation $H(t = 0) = (1/N) \int d\mathbf{x} h(\mathbf{x}, t = 0)$, so that h is an enthalpy per unit volume. Hence, using the fact that the enthalpy fluctuations per particle are of order $\sqrt{c_P k_B T}$ (where c_P is the specific heat in k_B units), the quantity $N \Sigma_{CH} / \sqrt{c_P k_B T}$ defines the number of particles over which enthalpy and dynamics are correlated. Of course, analogous identities can be derived for the covariance with, say, energy or density fluctuations.

Although interesting in itself, the covariance Σ_{CH} is just as hard (or even harder) to measure experimentally as χ_4 . However, Σ_{CH} can be related, using linear response theory, to a response function which is much easier to access in experiments. We now prove this by considering a system in the grand-canonical NPT ensemble. The probability of a given configuration \mathcal{C} is given by the Boltzmann weight $\exp(-\beta H[\mathcal{C}])/Z$, where $\beta = 1/k_B T$ and Z is the grand-partition function. Suppose one studies a static observable O with the following properties: (i) O depends only on the current microscopic configuration \mathcal{C} of the system and (ii) O can be written as a sum of local contributions:

$$O = \frac{1}{V} \int d\mathbf{y} o(\mathbf{y}).\quad (24)$$

In this case, a well-known static fluctuation-dissipation theorem holds (Hansen and McDonald, 2006):

$$\frac{\partial \langle O \rangle}{\partial \beta} = - \int d\mathbf{y} \langle o(\mathbf{y}) \delta h(\mathbf{0}) \rangle \equiv -N \Sigma_{OH},\quad (25)$$

where we decomposed the enthalpy in a sum of local contributions as well (Hansen and McDonald, 2006).

Interestingly, in the case of *deterministic* Hamiltonian dynamics, the value of any local observable $o(\mathbf{x}, t)$ can be seen as a highly complicated function of the initial configuration at time $t = 0$. Therefore, a two-time correlation function, now averaged over both space and initial conditions, can be rewritten as a thermodynamical average:

$$\begin{aligned}C_o(\mathbf{r}, t; T) &= \frac{1}{Z(\beta)V} \int d\mathbf{x} o(\mathbf{x} + \mathbf{r}, t) o(\mathbf{x}, t = 0) \\ &\quad \times \exp\left[-\beta \int d\mathbf{x} h(\mathbf{x}, t = 0)\right].\end{aligned}\quad (26)$$

Hence, the derivative of the correlation with respect to temperature (at fixed pressure) directly leads, in the case of purely conservative Hamiltonian dynamics, to the covariance between initial energy fluctuations and the dynamical correlation, in direct analogy with Eq. (25). Defining

$$G_T(\mathbf{y}, t) = \langle o(\mathbf{y} + \mathbf{r}, t) o(\mathbf{y}, 0) \delta h(\mathbf{0}, 0) \rangle,\quad (27)$$

one finds

$$\chi_T(\mathbf{r}, t) \equiv \frac{\partial C_o(\mathbf{r}, t; T)}{\partial T} \Big|_P = \frac{1}{k_B T^2} \int d\mathbf{y} G_T(\mathbf{y}, t).\quad (28)$$

Hence, the sensitivity of a two-time dynamical function to temperature χ_T is directly related to a three-point spatial correlation function. The result in Eq. (28) is extremely general and applies to many different situations. However, it does not apply when the dynamics is not Newtonian, as, for instance, for Brownian particles or in Monte Carlo numerical simulations (Doliwa and Heuer, 2000; Berthier and Kob, 2007). The reason is that in these cases, not only the initial probability but also the transition probability from the initial to the final configuration itself explicitly depends on temperature. In Brownian dynamics, for example, the noise in the Langevin equation depends on temperature. Hence, $\partial C_o(\mathbf{r}, t; T) / \partial T$ receives extra contributions from the whole trajectory that depend on the explicit choice of dynamics.

The equality (28), although in a sense a trivial result obtained from linear response theory, has a deep physical consequence, which is the growth of a dynamical length upon cooling in glassy systems, as we show. Define $\tau_\alpha(T)$ such that $C_o(\mathbf{0}, t = \tau_\alpha; T) = e^{-1}$ (say). Differentiating this definition with respect to T gives

$$0 = \frac{\partial \tau_\alpha}{\partial T} \frac{\partial C_o(\mathbf{0}, t = \tau_\alpha; T)}{\partial t} + \frac{\partial C_o(\mathbf{0}, t = \tau_\alpha; T)}{\partial T}.\quad (29)$$

Since $C_o(\mathbf{0}, t; T)$ decays from 1 to zero over a time scale τ_α , one finds that generically, using Eq. (28),

$$\int d\mathbf{y} \frac{\langle o(\mathbf{y}, t = \tau_\alpha) o(\mathbf{y}, 0) \delta h(\mathbf{0}, 0) \rangle}{\rho_0 \sqrt{c_P k_B T}} \sim \frac{T}{\rho_0 \sqrt{c_P}} \frac{\partial \ln \tau_\alpha}{\partial T}.\quad (30)$$

Now, since δh is of order $\rho_0 \sqrt{c_P k_B T}$ and $\langle o^2 \rangle$ is normalized to unity, the quantity $\chi_0 \equiv G_T(\mathbf{0}, \tau_\alpha) / \rho_0 \sqrt{c_P k_B T}$ is not expected to appreciably exceed unity. The above integral can be written as $\chi_0 v_T$, which defines a volume v_T over which enthalpy fluctuations and dynamics are appreciably correlated. Note that the interpretation of v_T as a true correlation volume requires that χ_0 be of the order of 1, and its increase is only significant if χ_0 is essentially temperature independent. If this is not the case, then the integral defined in Eq. (30) could grow due to a growing χ_0 and not a growing length, which would obviate the notion that v_T is a correlation volume.

Assuming $\chi_0 \leq 1$, a divergence of the right-hand side of the equality (28) necessarily requires the growth of v_T . More precisely, as soon as τ_α increases faster than an inverse power of temperature, the slowing down of a Hamiltonian system

must necessarily be accompanied by the growth of a dynamic correlation length, which is therefore a general, powerful consequence of the use of linear response theory. This result is thus directly relevant to supercooled liquids, where τ_α typically increases in an activated manner, with, possibly, a finite-temperature dynamic singularity. From a theoretical perspective, it also implies that any theory predicting a dynamic singularity necessarily contains a prediction for diverging dynamic length scales accompanying the glass transition.¹

The study of these three-point correlation and response functions is therefore a useful path to characterize dynamical heterogeneity and dynamical correlations. Quantitative results can be obtained experimentally studying χ_T . This has been done in connection with an inequality on χ_4 that we shall describe in the following section. Another interesting development that will be discussed later on consists of focusing on response functions, such as χ_T , but where the perturbing field is spatially dependent, e.g., with an oscillatory shape (Biroli *et al.*, 2006). This allows one to directly probe the size and the shape of the dynamically correlated regions.

Before concluding, we stress that we have considered the response of time correlations to a temperature change, but other perturbing fields may also be relevant, such as density, pressure, concentration of species in the case of mixtures, etc. For example, for hard-sphere colloids, temperature plays little role, whereas small changes of density can lead to enormous changes in relaxation times (Pusey and van Meegen, 1986). The derivation of this section can be straightforwardly extended to these cases (Berthier *et al.*, 2007a).

4. Inequalities on χ_4 and experimental measurements

In previous sections, we argued that understanding of $\chi_4(t)$ is fundamental in order to understand dynamic heterogeneities in supercooled liquids, but we then proceeded to describe a series of alternative multipoint susceptibilities, in particular, $\chi_T(t)$, which contain alternative information on heterogeneities. We now close the loop and show that both types of susceptibilities are, in fact, not independent from one another, but closely related.

This can be done using the general formalism developed long ago by Lebowitz *et al.* (1967), which gives expressions for the strength of fluctuations of physical observables measured in distinct statistical ensembles. Applied to the spontaneous fluctuations of global two-time correlation functions, and considering transformation from *NPH* (where enthalpy is fixed and temperature fluctuates) to *NPT* (where temperature is fixed but enthalpy fluctuates), one obtains

$$\chi_4^{NPT}(t) = \chi_4^{NPH}(t) + \frac{T^2}{c_p} \left(\frac{\partial C_o(\mathbf{0}, t; T)}{\partial T} \Big|_p \right)^2, \quad (31)$$

¹An intriguing case, which is not fully understood, is the example of systems with an Arrhenius behavior at low temperature. The general considerations laid out in the text suggest that these systems are characterized by a dynamical correlation length diverging at zero temperature, which contrasts with the idea that relaxation in Arrhenius systems is a simple, locally activated process. However, the present results hold only for energy-conserving systems for which thermal activation may be more collective than usually surmised (Tarzia *et al.*).

where $\chi_4^{NPH}(t)$ is the variance of the correlation function in the *NPH* ensemble where enthalpy does not fluctuate, a manifestly non-negative quantity. This allows us to obtain the following inequality:

$$\chi_4(t) \geq \frac{T^2 \chi_T^2(t)}{c_p} = \frac{T^2}{c_p} \left(\frac{\partial C_o(\mathbf{0}, t; T)}{\partial T} \Big|_p \right)^2. \quad (32)$$

Note that there is a simpler way to obtain the above inequality. In the previous section, $\chi_T(t)$ was shown to be related to the covariance of enthalpy and dynamic fluctuations, Σ_{CH} . Since χ_4 is related to the covariance of dynamic fluctuations Σ_{CC} , one can easily check that Eq. (32) is just a rewriting of the Cauchy-Schwarz bound: $\Sigma_{CH}^2 \leq \Sigma_C^2 \Sigma_H^2$, where Σ_H^2 is the variance of the enthalpy fluctuations, equal to $c_p(k_B T)^2/N$ in the *NPT* ensemble.

The inequality (32) is interesting because the right-hand side is an experimentally measurable quantity which therefore provides a *direct lower bound* on χ_4 . Thus, if $T^2 \chi_T^2(t)/c_p$ increases substantially above 1, χ_4 has to increase as least as much if not more. In particular, as soon as χ_T increases faster than T^{-1} at low temperatures, χ_4 will eventually exceed unity; since χ_4 is the space integral of a quantity bounded from above, this again means that the length scale over which the four-point correlation $G_4(\mathbf{y}, t)$ extends *has to grow* as the system gets slower and slower. Again, more quantitative statements require information on the amplitude and shape of $G_4(\mathbf{y}, t)$, which has to be provided from theoretical or numerical calculations.

Equation (31) makes precise the intuition that dynamic fluctuations are partly induced by the fluctuations of quantities that physically affect the dynamic behavior (Ediger, 1998; Donth, 2001), in that case the enthalpy. The inequality (32) provides a correct estimate of χ_4 if there are no “hidden” variables which also contribute to the dynamic fluctuations. However, it is quite difficult to determine whether such additional contributions exist. Theoretical investigations in the context of approximate models for the glass transition described in Sec. IV, and detailed numerical calculations where all terms in Eq. (31) can be separately evaluated, greatly clarified this issue. The main conclusion is that the experimentally accessible response functions which quantify the sensitivity of average correlation functions to an infinitesimal change in control parameters can be used in Eq. (32) not only to yield lower bounds to $\chi_4(t)$, but, in fact, to provide useful quantitative approximations to four-point functions. Although the relative precision on $\chi_4(t)$ provided by the bound at a given temperature is modest, the rate of growth is accurately reproduced.

The results discussed above have opened the way to experimental characterization of the growth of χ_4 in molecular glass formers close to T_g . In order to make use of the inequality (32) one must be able to detect time-correlation functions at constant temperature $C_0(t; T)$ with sufficient precision that dynamics at nearby temperatures T and $T + \Delta T$ can be resolved, when ΔT is small enough that linear response holds:

$$\frac{\partial C_0(t; T)}{\partial T} \approx \frac{C_0(t; T) - C_0(t; T + \Delta T)}{\Delta T}. \quad (33)$$

A simpler alternative, critically discussed by Dalle-Ferrier *et al.* (2007), is to fit $C_0(t; T)$ with an empirical form

containing a few numbers of parameters, and then take the temperature derivative of these parameters to indirectly estimate $\chi_T(t)$. Combining these different methods, the lower bound (32) to χ_4 has been computed for many molecular glass-forming liquids. It is easy to convince oneself that the lower bound has also the correct time dependence, with a peak developing for times of the order of the relaxation time scale. The value of this peak is therefore a lower bound to the peak of χ_4 and, hence, to the number of dynamically correlated molecules, denoted $N_{\text{corr},4}$. Figure 11 shows the evolution of $N_{\text{corr},4}$ for many different glass formers in the entire supercooled regime (Dalle-Ferrier *et al.*, 2007) as a function of the relaxation time scale τ_α . Note that, actually, $N_{\text{corr},4}$ is expected to be equal to the number of dynamically correlated molecules up to a proportionality constant which is not known from experiments, probably explaining why the high-temperature values of $N_{\text{corr},4}$ are smaller than 1. Figure 11 also indicates that $N_{\text{corr},4}$ grows faster when τ_α is not large, close to the onset of slow dynamics, and a power-law relationship $N_{\text{corr},4} \sim \tau_\alpha^\theta$ (see Fig. 10) is a good description in this regime ($\tau_\alpha/\tau_0 < 10^4$). The growth of $N_{\text{corr},4}$ becomes much slower closer to T_g . A change of six decades in time corresponds to a mere increase of a factor of about 4 of $N_{\text{corr},4}$, suggesting logarithmic rather than power-law growth of dynamic correlations. This is in agreement with several theories of the glass transition which are based on activated dynamic scaling; see Sec. IV.

Note that all the results above can be generalized to cases where the order parameter inducing the glass transition is the density. This happens for colloids and granular media (Berthier *et al.*, 2005; Lechenault *et al.*, 2008a; Brambilla *et al.*, 2009). One can obtain a new inequality where density

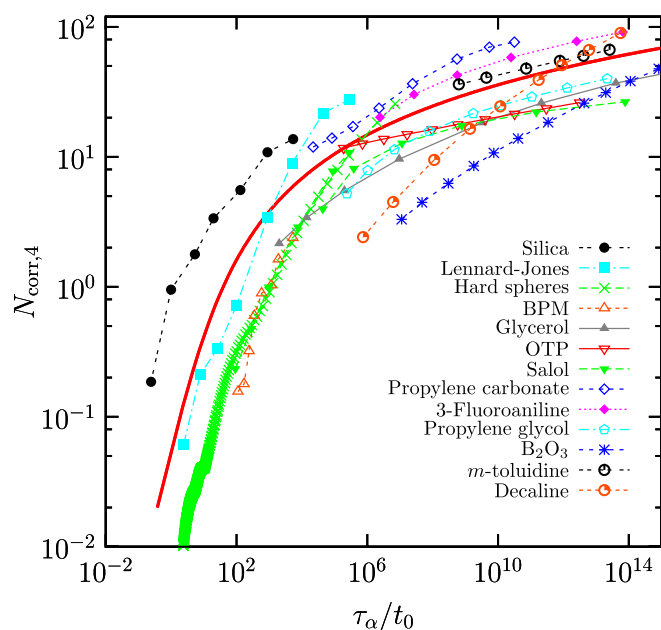


FIG. 11 (color online). Dynamic scaling relation between the number of dynamically correlated particles $N_{\text{corr},4}$ and relaxation time scale τ_α for a number of glass formers, determined using Eq. (32). For all materials, a similar trend is found, with a rapid initial increase of $N_{\text{corr},4}$ near the onset of slow dynamics, followed by a slower, presumably logarithmic behavior, closer to the laboratory glass temperature. Adapted from Dalle-Ferrier *et al.*, 2007.

fluctuations play the same role of enthalpy fluctuations and that provide a lower bound to χ_4 in terms of the derivative of the correlation function with respect to the density. These different inequalities yielding experimentally accessible ways to quantify the strength of dynamic heterogeneity certainly have the appeal of simplicity and are by now routinely used in many different systems (Stevenson and Wolynes, 2006; Capaccioli *et al.*, 2008; Dalle-Ferrier *et al.*, 2008; Chen *et al.*, 2009; Gainaru *et al.*, 2010; Koppensteiner *et al.*, 2010; Maggi *et al.*, 2010; Roland *et al.*, 2010).

C. Current status of dynamic heterogeneity studies

The present section on dynamic heterogeneity is a brief summary of a collective research effort of large amplitude that lasted about 20 years and which already forms the core of several recent reviews (Silleescu, 1999; Ediger, 2000; Richert, 2002), and a book (Berthier *et al.*, 2011). Progress to characterize, visualize, and quantify dynamic heterogeneity as well as an exploration of its detailed physical consequences has been truly dramatic in recent years. The impact of this research is such that tools developed to study dynamic heterogeneity in liquids are now routinely used in scores of different systems, and dynamic heterogeneity is a concept that is commonly employed in a broad range of situations, much beyond the physics of the glass transition (Berthier *et al.*, 2011).

Despite this progress, several key questions are still unanswered. Our discussion has focused on the issue of the characterization of the spatial fluctuations involved in the phenomenon of dynamic heterogeneity. This is justified because direct measurements of growing dynamic length scales have provided the long-sought evidence in favor of the collective nature of the glass transition itself. This fact being now established, it remains to understand more precisely and quantify the connection between these growing length scales and the increasing viscosity of liquids approaching the glass transition, which appears as a topic for research in the coming years.

We have described in some detail the physical content of multipoint dynamic susceptibility such as $\chi_4(t)$. These functions played a major role in the above story, but we now understand that they contain also a number of embarrassing features. For instance, we mentioned how $\chi_4(t)$ retains a dependence on the statistical ensemble where it is measured, as in Eq. (31), and that it also depends on the microscopic equations of motion for the system (Newtonian versus Brownian). These subtle issues make the analysis of four-point susceptibilities somewhat ambiguous, especially when estimates for length scales are sought. We shall describe, for instance, in Sec. IV.B.3, that alternative dynamic functions now exist that should be easier to analyze, but these have not all been measured in simulations or experiments yet. Thus, more detailed studies of a larger family of dynamic susceptibilities are certainly most wanted in the future. A promising avenue of research consists of studying nonlinear responses (Bouchaud and Biroli, 2005). The first pioneering experimental measurement of nonlinear dielectric susceptibility for glass formers appeared recently (Crauste-Thibierge *et al.*, 2010).

Additionally, direct experimental measurements of dynamic length scales are still not available for molecular glass

formers and are scarce even for colloidal materials. Thus, it would be useful to develop new experimental tools to resolve the dynamics of molecular glass formers on small length scales and longer time scales to obtain this much needed information. It is not yet clear whether molecular dynamics simulations of model systems covered a broad enough range of time scales and are thus relevant in understanding the physics of real glass formers near the experimental glass transition temperature. We also believe that further work should be devoted to a better characterization of the geometry (and not only a typical length scale) of the dynamically heterogeneous regions, since contradicting results are available in the literature (Donati *et al.*, 1998; Appignanesi *et al.*, 2006).

IV. SOME MODELS AND THEORETICAL APPROACHES

A. A few key questions

We now present some theoretical approaches to the glass transition. It is impossible to cover all of them in this review, simply because there are too many of them. This is perhaps the clearest indication that the glass transition remains an open theoretical problem.

We have chosen to present in some detail those approaches that, we believe, contain keystone ideas and at the same time have a solid statistical mechanics basis. Loosely speaking, they have a Hamiltonian, they can be simulated numerically, or studied analytically with tools from statistical mechanics. Of course, the choice of Hamiltonian is crucial and contains important assumptions about the nature of the glass transition. All the approaches we present have given rise to unexpected results. One finds more in them than what was supposed at the beginning, and this leads to new, testable predictions. Furthermore, with models that are precise enough, one can test (and hopefully falsify) these approaches by working out all their predictions in great detail and comparing the outcome to experimental data. Such detailed analysis is often not possible with “physical pictures,” or simpler phenomenological modeling of the problem. Our drastic choice of theories leaves behind many other approaches that, although interesting, could not be covered without increasing the length of this review beyond reasonable limits. Recent reviews are available on these and we refer the interested reader to [Debenedetti \(1996\)](#), [Donth \(2001\)](#), [Sciortino \(2005\)](#), [Dyre \(2006\)](#), and [Chen *et al.* \(2010\)](#).

Before going into models and theories, we formulate a few important questions that theoreticians seek to address and that will guide our presentation of theories:

- (1) Why do the relaxation time and the viscosity increase when T_g is approached? Why is this dramatic growth different from an Arrhenius law?
- (2) Can one understand and describe quantitatively the broad relaxation spectra characterizing the dynamical behavior of supercooled liquids, in particular, nonexponential relaxations, and their evolution with fragility?
- (3) Is there a deep relation between kinetics and thermodynamics (such as $T_0 \approx T_K$) and why?
- (4) Can one understand and describe quantitatively the spatiotemporal fluctuations of the dynamics? How and why are these fluctuations related to the dynamic slowing down?
- (5) Is the glass transition a collective phenomenon? If yes, of which kind? What is the correct “order parameter” and the nature of the associated transition?
- (6) Is the experimental glass transition at T_g the manifestation of a finite- or zero-temperature phase transition, sometimes called the “ideal glass transition”? Or is there instead an avoided, hidden, or inaccessible transition?
- (7) Is there a geometric, real space explanation for the dynamic slowing down that takes into account molecular degrees of freedom?
- (8) Are there simplified (e.g., lattice) glass models which essentially capture the physics of the glass transition of molecular liquids?

Before embarking on detailed theoretical explanations, it is important to stress that the glass transition appears as a kind of “intermediate coupling” problem, since, for instance, typical correlation length scales are found to be at most a few tens of particles long close to T_g . As a consequence, recognizing and validating the correct theory is extremely difficult since key signatures could be buried (and probably are) under preasymptotic, microscopic details. Because of these incorrect theories may appear reasonable. To obtain quantitative, testable predictions, one must therefore be able to work out also these preasymptotic effects. This is a particularly difficult task, especially in cases where the asymptotic theory itself has not satisfactorily been worked out yet. Therefore, at this time, theories are mainly judged by their overall predictive power and theoretical consistency.

B. Mean-field free-energy landscapes and random first-order transition theory

1. Mean-field glass theory and complex free-energy landscapes

In the last two decades, three independent lines of research, the Adam-Gibbs theory ([Adam and Gibbs, 1965](#)), the mode-coupling theory ([Götze, 2008](#)), and the spin glass theory ([Mézarid *et al.*, 1988](#)), have been merged in a common framework to produce a theoretical ensemble that now goes under the name of random first-order transition theory (RFOT), a terminology introduced by Kirkpatrick, Thirumalai, and Wolynes ([Kirkpatrick and Thirumalai, 1987](#); [Kirkpatrick and Wolynes, 1987](#)) who played, among many other researchers, a key role in its development. Here we did not follow the rambling developments as they took place, but summarized the RFOT theory in a more modern and unified way. Note that our use of the name RFOT is much broader than the more common, but much narrower meaning often implied in the literature. Reviews dedicated to different aspects of the RFOT theory have appeared recently ([Lubchenko and Wolynes, 2007](#); [Götze, 2008](#); [Biroli and Bouchaud, 2009](#); [Cavagna, 2009](#); [Mézarid and Parisi, 2010](#)).

As discussed previously, two hallmarks of the dynamics of glass formers are that (i) close to T_g a liquid remains stuck for a long time in amorphous configurations and (ii) the number of these configurations is exponentially large in the system

size. RFOT theory starts as a mean-field approach to these phenomena. As such it has to be able to capture the right kind of symmetry breaking and deal with an exponential number of states.

Broadly speaking, mean-field theory is based on the study of the free-energy landscape as a function of the order parameter. For example, for ferromagnets, in the Curie-Weiss approach, one computes the free energy as a function of the global magnetization by a mean-field approximation. This yields direct access to the nature and properties of the ferromagnetic phase transition and a simple description of the low-temperature phase since the two minima of the free energy correspond to the two ferromagnetic states. However, computing the free energy as a function of the global energy or density is not enough for the glass transition, because one must deal with the existence of many different amorphous configurations. As a consequence one is forced to compute the free energy F as a function of the entire density field (instead of a single variable as in the ferromagnetic transition) F being defined through the Legendre transform.

Consider for simplicity an interacting particle lattice model (the generalization to continuum systems is straightforward). A given configuration is determined by the number of particles n_i on each site i . In order to define F , one first introduces the thermodynamic “potential”

$$W(\{\mu_i\}) = -\frac{1}{\beta} \log \sum_{\{n_i\}} \exp\left(-\beta H(\{n_i\}) + \sum_i \beta \mu_i n_i\right),$$

where $H(\{n_i\})$ is the Hamiltonian. The free energy function $F(\{\rho_i\})$ is defined as

$$F(\{\rho_i\}) = W(\{\mu_i^*\}) + \sum_i \mu_i^* \rho_i, \quad (34)$$

where the μ_i^* s satisfy the equations $\partial W / \partial \mu_i + \rho_i = 0$ and, hence, are functions of $\{\rho_i\}$, which specifies an averaged density profile. Note that this construction can be generalized to spin systems replacing the positive integer n_i by ± 1 variables s_i . In this context F is called the “TAP” free energy since its introduction by Thouless, Anderson, and Palmer in the context of mean-field spin glasses (Thouless *et al.*, 1977). The generalization to a continuum system can be performed by replacing the discrete variable n_i by a continuum density field $\rho(\mathbf{x})$. In this case F is called the “density functional” (Oxtoby, 1990).

The free energy landscape is the hypersurface generated by scanning F over all possible values of $\{\rho_i\}$. Its critical points, in particular, the minima, play a crucial role. In fact, by deriving Eq. (34) with respect to ρ_i one finds

$$\frac{\partial F}{\partial \rho_i} = \mu_i^*. \quad (35)$$

Thus, when there are no external fields (or local chemical potentials) the solutions of these equations are all the stationary points of the free energy landscape.²

²For particle systems there is always a global chemical potential μ fixing the number of particles. In this case, one includes the global term $\mu \sum_i n_i$ in the definition of F so that all μ_i^* are zero.

What are the main features of F for a system approaching the glass transition? Unfortunately, this question cannot be answered exactly for a realistic three-dimensional system. One has to either make use of approximations (as in the Curie-Weiss description of ferromagnets) or focus on simplified geometries, such as mean-field Bethe lattices, which, hopefully, provide a good approximation to finite-dimensional ones.

Quite a large number of such studies have led to similar results and thus to a consistent mean-field picture. The free energy landscape becomes “rugged” at low temperature and characterized by many minima and saddle points. Actually, the number of minima is exponentially large in the system size, which suggests the definition of an entropy, called “configurational entropy” or “complexity”:

$$s_c = \frac{1}{N} \log \mathcal{N}(f), \quad (36)$$

where $\mathcal{N}(f)$ is the number of free-energy minima with a given free-energy density f (per unit of free-energy density). The density profile corresponding to one given minimum is amorphous and lacks any type of periodic long-range order, and different minima are different. This is a welcome theoretical result, as real glasses can be found in a large number of different amorphous configurations, which can be interpreted as mean-field free-energy minima.

Assuming that all minima are mutually accessible, one can compute the thermodynamic properties, i.e., the partition function by summing over all states with their Boltzmann weights:

$$Z = e^{-\beta W} = \sum_{\alpha} e^{-\beta f_{\alpha} N}, \quad (37)$$

where the sum runs over the minima. Formally, one can introduce a free-energy-dependent complexity $s_c(f, T)$ that counts the number of free-energy minima with free-energy density f at temperature T . The partition function of the system then reads

$$Z(T) = \int df \exp\left[-\frac{Nf}{T} + N s_c(f, T)\right]. \quad (38)$$

For large N , one can as usual perform a saddle-point estimate of this integral that fixes the dominant value of f , denoted $f^*(T)$:

$$\left. \frac{\partial s_c(f, T)}{\partial f} \right|_{f=f^*(T)} = \frac{1}{T}. \quad (39)$$

The temperature-dependent complexity is therefore $s_c(T) \equiv s_c(f^*(T), T)$. The total free energy of the system is $f_p(T) = f^* - T s_c(T)$. A typical shape of the configurational entropy as a function of f and a graphic solution of Eq. (38) are plotted in Fig. 12. The analysis of the configurational entropy, or complexity $s_c(T)$, reveals that $s_c(T)$ decreases when temperature decreases, as long as T is above a critical temperature T_K , below which $s_c(T)$ vanishes. There exists also a second, higher temperature $T_{\text{MCT}} > T_K$, above which $s_c(T)$ drops discontinuously to zero again. We use the symbol T_{MCT} (as in mode-coupling theory) on purpose, and justify our choice below. Although the complexity vanishes in both regimes, the situations below T_K and above T_{MCT} are

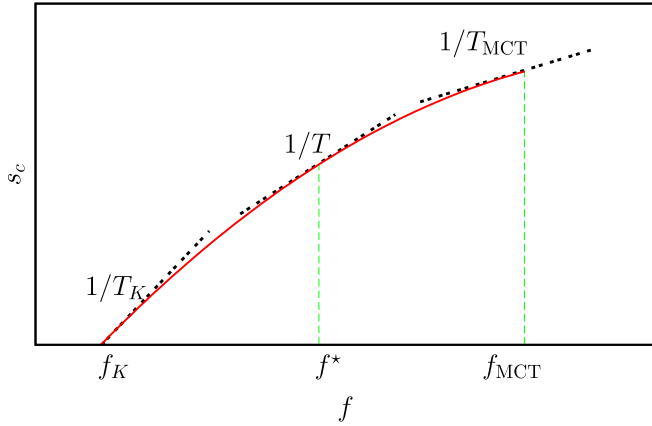


FIG. 12 (color online). Typical shape of the configurational entropy s_c as a function of free-energy density f in the range $T_K < T < T_{MCT}$ for random first-order landscapes. A graphic solution of Eq. (39) is obtained by finding the value of f at which the slope of the curve is β . Note that s_c is also a function of temperature, so this curve, in fact, changes with T .

different. At these two temperatures the part of the free-energy landscape relevant for the thermodynamics changes drastically in two different ways. Above T_{MCT} , there is just one minimum dominating the equilibrium measure corresponding to the homogeneous density profile of the high-temperature liquid. At T_{MCT} the homogeneous liquid state becomes fragmented in an exponential number of states, or minima. At T_K the number of minima becomes subexponential in the system size, such that $s_c(T < T_K) = 0$.

Surprisingly the total free energy $f_p(T)$ is not singular at T_{MCT} . This is one of the most unexpected results consistently emerging from analytical solutions. This suggests that at T_{MCT} the liquid state fractures into an exponential number of amorphous states, but that this transition has no thermodynamical counterpart and is therefore a purely dynamical phenomenon. At T_K instead, a thermodynamic phase transition takes place since the contribution to the entropy coming from the configurational entropy disappears, typically linearly, $s_c(T) \sim (T - T_K)$. Therefore, the specific heat is found to make a sharp downward jump at T_K , thus providing an exact realization of the “entropy vanishing” mechanism conjectured by Kauzmann (1948). This is a second welcome result: The thermodynamic signature of this mean-field transition mirrors the basic experimental finding that the specific heat is nearly discontinuous at the experimental glass temperature T_g .

This rich physical behavior can be derived from a number of perspectives. A first concrete example is given by “lattice glass models” (Biroli and Mézard, 2001) solved by the Bethe approximation or on Bethe lattices (Pica Ciamarra *et al.*, 2003; Rivoire *et al.*, 2004; Hansen-Goos and Weigt, 2005). Lattice glass models contain hard particles sitting on the sites of a lattice. The Hamiltonian is infinite if there is more than one particle on a site and, more crucially, if the number of occupied neighbors of an occupied site is larger than a fixed parameter m . The Hamiltonian is zero otherwise. Tuning the parameter m , changing the type of lattice, in particular, its connectivity, can yield different models. Lattice glasses are

simple statistical mechanical models mimicking the physics of hard-sphere systems. Numerical simulations on cubic lattices have shown that they seem to behave as *bona fide* glass formers (Pica Ciamarra *et al.*, 2003; Darst *et al.*, 2010).

Alternatively, a density functional theory analysis of the free-energy landscape yields similar results (Singh *et al.*, 1985; Dasgupta and Valls, 2000). This is a more realistic microscopic starting point, but it inevitably contains some approximations, in particular, related to the specific form of the free-energy functional (Singh *et al.*, 1985; Dasgupta *et al.*, 1991). The adopted form is the Ramakrishnan-Youssouf density functional and most studies focused on hard-sphere systems. In the first of these investigations (Singh *et al.*, 1985), a particular amorphous profile, whose only free parameter was the cage radius over which particles are free to vibrate, was plugged in the density functional. Minimization with respect to the cage radius revealed that amorphous structures become stable, in a variational sense, at high enough density. More recent investigations performed a full minimization and reached qualitatively similar, but much more detailed conclusions (Dasgupta *et al.*, 1991; Chaudhuri, Karmakar, and Dasgupta, 2008).

Finally, other popular models are the ones introduced in the spin glass literature. Probably the most studied example of such spin glasses is the p -spin model, defined by the Hamiltonian (Gross and Mézard, 1984)

$$H = - \sum_{i_1, \dots, i_p} J_{i_1, \dots, i_p} S_{i_1} \cdots S_{i_p}, \quad (40)$$

where the S_i 's are Ising or spherical spins, $p > 2$, and J_{i_1, \dots, i_p} are quenched random couplings with zero mean and variance $p!/(2N^{p-1})$.

These models are certainly not realistic in terms of modeling microscopic degrees of freedom in a fluid, but they are representative of the class of systems with a random first-order transition. They have the advantage that a variety of computations can be performed without any approximation, and both their dynamic and static properties can be investigated analytically in full detail, again yielding results as described above. Their dynamics can be studied in full detail, including various nonequilibrium conditions as described in Sec. V. Another result concerns the interpretation of the nature of the low-temperature phase in terms of replica symmetry breaking, so that connections with the field of disordered systems can be made (Mézard *et al.*, 1988; Parisi, 2003). Technically, the thermodynamics of the p spin can be solved, for $p > 2$, using a one-step replica symmetry breaking ansatz; see Castellani and Cavagna (2005) for a review. This means that the probability distribution function of the overlap between states, the Parisi function $P(q)$, has two peaks below T_K , one at $q(T) > 0$ which quantifies the self-overlap within the states, and another one at $q = 0$, implying that different states are totally uncorrelated (Mézard *et al.*, 1988).

We now discuss the dynamical behavior which results from the above analysis of the free-energy landscape. Below T_{MCT} , the system is in a metastable state from which it cannot escape, because free-energy barriers diverge with system size (Barrat *et al.*, 1996). This divergence is a direct consequence of the mean-field nature of the present set of

approximations. Therefore, the relaxation time diverges, within the mean field, at T_{MCT} . The stability of these states can be analyzed by computing the free-energy Hessian in the minima. One finds that states become more fragile when $T \rightarrow T_{\text{MCT}}^-$, are marginally stable at $T = T_{\text{MCT}}$, and unstable for $T > T_{\text{MCT}}$. As a consequence, one expects that the dynamics slows down approaching T_{MCT} from above as the free-energy landscape becomes more and more “flat” (Kurchan and Laloux, 1996).

Indeed the dynamics of many of these models can be analyzed exactly (Cugliandolo, 2003). In particular, mean-field p -spin models have been analyzed in great detail and provide a paradigm for mean-field glassy dynamics. The equations of motion considered in the literature are Langevin equations,

$$\frac{\partial s_i(t)}{\partial t} = -\mu(t)s_i(t) - \frac{\partial H}{\partial s_i(t)} + \eta_i(t), \quad (41)$$

where $\eta_i(t)$ is a Gaussian thermal noise of zero mean and variance $2T$ given by the fluctuation-dissipation theorem.

We focus on the spherical version of the model, and on the time autocorrelation function $C(t) = (1/N)\sum_i \langle s_i(t)s_i(0) \rangle$. Note that $\mu(t)$ is the Lagrange multiplier enforcing the constraint $C(0) = 1$. The equation of motion for $C(t)$ at thermal equilibrium reads

$$\frac{dC(t)}{dt} = -TC(t) - \frac{p}{2T} \int_0^t dt' C^{p-1}(t-t') \frac{dC(t')}{dt'}. \quad (42)$$

We meet this equation again in the next section about mode-coupling theory. We shall then postpone a detailed study and just anticipate some results that will be derived later. At high temperature, the correlation function decays quickly to 0. Decreasing the temperature, the relaxation time scale increases and a two-step relaxation emerges; see Fig. 13 where we have plotted the numerical solution of the previous equation. At T_{MCT} the time scale τ_α corresponding to the slow relaxation diverges algebraically,

$$\tau_\alpha \sim \frac{1}{(T - T_{\text{MCT}})^\gamma}, \quad (43)$$

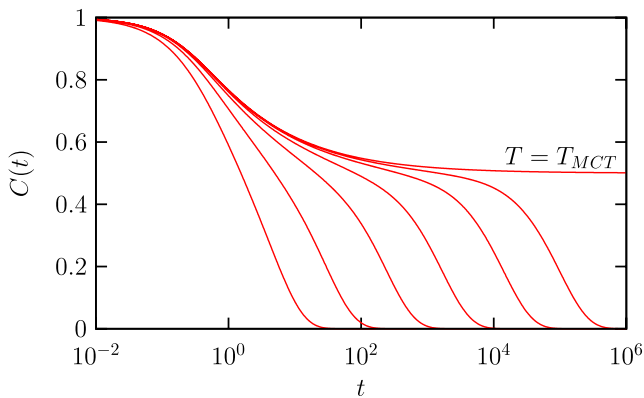


FIG. 13 (color online). Correlation $C(t)$ as a function of time for the p -spin model with $p = 3$ for several temperatures approaching T_{MCT} , obtained from numerical solution of Eq. (42). The curves show the appearance of a two-step decay characterized by several scaling laws discussed in the text.

where γ is a critical exponent. The value of the plateau $q = \lim_{t \rightarrow \infty} C(t)$, called the Edwards-Anderson parameter in the spin glass literature, satisfies a simple equation that can be obtained taking the infinite-time limit of Eq. (42):

$$\frac{q}{1-q} = \frac{p}{2T^2} q^{p-1}. \quad (44)$$

A graphical solution of this equation is presented in Fig. 14, where we plot

$$V(q)/T = \int_0^q dq' \left[\frac{q'}{1-q'} - \frac{p}{2T^2} q'^{p-1} \right].$$

The minima of V are the solutions of Eq. (44). Clearly the minimum at $q = 0$ is always present. Another solution q_{EA} appears at $T_{\text{MCT}} = \sqrt{p(p-2)^{p-2}(p-1)^{1-p}/2}$ and it can be interpreted as the long-time limit of the correlation function inside one typical state. Since the states have an infinite lifetime (in mean-field theory) the system remains trapped forever into the one it started from. It is important that q_{EA} is discontinuous at transition, which leads to the two-step behavior shown in Fig. 13. By contrast in spin glasses, q_{EA} is continuously growing from 0 at the transition.

Note from Fig. 14 that at T_{MCT}^+ the Edwards-Anderson parameter is zero and, concomitantly, $V(q)$ has a vanishing second derivative at q_{EA} . It is possible to show (Franz and Parisi, 1998), that this is indeed related to the fact that the free-energy Hessian of the states below T_{MCT} develops zero modes at T_{MCT} . This behavior resembles the one of a spinodal transition. In fact, this analogy has been fruitfully explored, for instance, to describe real space features of dynamic heterogeneity near T_{MCT} (Kirkpatrick *et al.*, 1989; Stevenson *et al.*, 2006; Cavagna, 2009; Zdeborova and F. Krzakala, 2011).

We now recap the overall picture arising from a mean-field analysis of the properties of the free-energy landscape of glasses. At high temperature the dynamics is fast and the system is in the liquid state. Approaching T_{MCT} the dynamics slows down because of the appearance of incipient stable states. By decreasing the temperature to T_{MCT} , it takes a longer time to find an unstable direction, and thus to relax. Below T_{MCT} there is an exponential (in the system size) number of states. The partition function and the thermody-

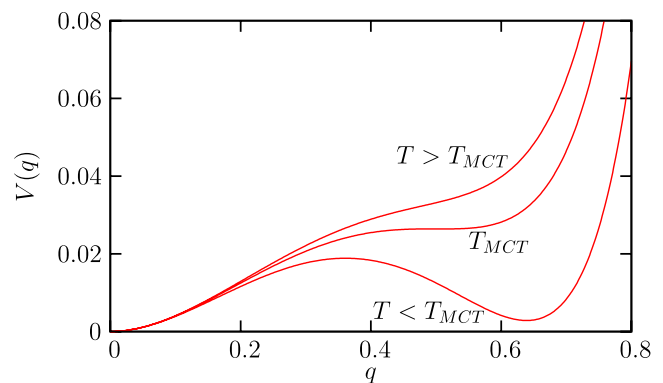


FIG. 14 (color online). Evolution of $V(q)/T = -(1/2T^2)q^p - \log(1-q) - q$ as a function of q for different temperatures across the dynamical transition. The solution with $q > 0$ appears discontinuously at T_{MCT} .

namics are obtained by summing over all of them their corresponding Boltzmann weight. This procedure is justified by the fact that, in a real finite-dimensional system, the barriers between states should actually become finite. In the regime below T_{MCT} , there is competition between single state free energies that would favor the lowest free-energy states, and configurational entropy that would favor the highest ones that are more numerous. Lowering the temperature disfavors the entropy term and at T_K the system undergoes a phase transition where the sum in Eq. (37) is again dominated by only a few terms corresponding to states with free-energy density f_K given by $s_c(f_K, T) = 0$. This transition corresponds to a *bona fide* “entropy crisis” mechanism.

2. Mode-coupling theory

The dynamical transition appearing upon approaching T_{MCT} in RFOT landscapes is mathematically analogous to the one predicted to occur in supercooled liquids by the mode-coupling theory (MCT) of the glass transition, although the latter has *a priori* no direct interpretation in terms of a free-energy landscape. This theory was introduced separately by Leutheusser (1984) and Bengtzelius, Götze, Sjölander, and coworkers (Bengtzelius *et al.*, 1984). It was used to describe and predict the average dynamics, in particular, the dynamical structure factor and the self-diffusion, for moderately supercooled liquids and colloids. Recently, it was generalized to describe dynamical correlations and some aspects of dynamic heterogeneity, as described in Sec. IV.B.3. In Sec. IV.B.4, we discuss successes and limitations of MCT.

Originally, MCT was developed using the projection operator formalism (Bengtzelius *et al.*, 1984; Leutheusser, 1984). An introduction to this method can be found in the book by Zwanzig (2001). The starting point of the method is the derivation of the following equation for the dynamical structure factor $F(k, t)$ of a single-component atomic liquid:

$$\frac{d^2 F(k, t)}{dt^2} + \frac{k^2 k_B T}{mS(k)} F(k, t) + \int_0^t d\tau M(k, \tau) \frac{d}{dt} F(k, t - \tau) = 0. \quad (45)$$

Generalizations to mixtures and nonatomic liquid are also available. This is an exact equation whose inputs are the static structure factor $S(k) = F(k, 0)$ and the memory kernel $M(k, \tau)$ for a given particle mass m and temperature T . In a second, crucial step MCT suggests a self-consistent approximation for the memory kernel $M(k, \tau)$. It is possible to show that the memory kernel corresponds to the variance of the random force acting on the density field; see the review by Reichman and Charbonneau (2005). Thus, $M(k, \tau)$ captures the effect of all degrees of freedom other than the density field on the density field itself. The physical idea motivating MCT is to focus on the slow part of the random force. Technically, the path is in principle straightforward: One should identify the dominant slow modes, project the random force onto them, and derive the dynamical equations for their correlation functions. Of course, in practice this remains difficult because the number of slow modes is infinite.

Within MCT, only the bilinear density products contribute to the slow part of M . After projection, the memory kernel is expressed in terms of a four-point function. In a final

approximation, this function is factorized as the product of two-point density functions $F(k, t)$. This leads to the MCT self-consistent equations:

$$0 = \frac{d^2 F(k, t)}{dt^2} + \nu(k) \frac{dF(k, t)}{dt} + \frac{k^2 k_B T}{mS(k)} F(k, t) + \int_0^t d\tau M_{\text{MCT}}(k, t - \tau) \frac{\partial F(k, \tau)}{\partial \tau}, \quad (46)$$

$$M_{\text{MCT}}(k, t) = \frac{\rho k_B T}{16\pi^3 m} \int d\mathbf{k}' |\tilde{V}_{\mathbf{k}-\mathbf{k}', \mathbf{k}'}|^2 F(k', t) F(|\mathbf{k}' - \mathbf{k}|, t),$$

$$\tilde{V}_{\mathbf{k}-\mathbf{k}', \mathbf{k}'} \equiv \{(\hat{\mathbf{k}} \cdot \mathbf{k}') c(k') + \hat{\mathbf{k}} \cdot (\mathbf{k} - \mathbf{k}') c(|\mathbf{k} - \mathbf{k}'|)\}, \quad (47)$$

where we have rewritten the result using the direct correlation function $c(k) \equiv [1 - 1/S(k)]/\rho$. The effective friction term represents the effect of the fast degrees of freedom.

This final expression clearly shows that MCT is a particular closure of the equations on dynamical correlation functions. It is similar in spirit to several other closure schemes used in physics, such as Kraichnan’s “direct interaction approximation” for turbulence, or various large- N field-theoretical methods (Bouchaud *et al.*, 1996). Indeed, field-theoretical derivations of MCT have long been sought, but this is, in fact, still an active area. The first pioneering works were published shortly after the original MCT derivation (Das *et al.*, 1985; Das, 1990). They started from stochastic equations for the slow degrees of freedom of a liquid, the so-called nonlinear fluctuating hydrodynamics, and rederived the MCT equations as a self-consistent, one-loop approximation. Motivations for the field-theoretical approach are that it provides a complementary way to derive MCT which is, in principle, more suitable to nonequilibrium generalizations, and perhaps to systematic improvement. Unfortunately this approach is plagued by difficulties related to the preservation of time-reversal symmetry in self-consistent loop expansions (Miyazaki and Reichman, 2005; Andreev *et al.*, 2006). Recent work aimed at getting fully consistent field-theoretical derivations of MCT equations (Kim and Kawasaki, 2008; Nishino and Hayakawa, 2008), but this is technically more involved than could be anticipated.

Within MCT, dynamical correlation functions are obtained by numerical integration, once the static structure factor of the liquid is known. This kind of analysis was performed on a large number of different glassy liquids such as Lennard-Jones (Bengtzelius, 1986; Nauroth and Kob, 1997) hard spheres systems (Barrat *et al.*, 1989; Barrat and Latz, 1990; Foffi *et al.*, 2003), or silica melts (Sciortino and Kob, 2001), and it revealed a common behavior. It was found that small changes in $S(k)$ lead, at high density or low temperature, to a great variation in $F(k, t)$ that resembles the one shown in Fig. 13 for the correlation function of the p -spin model. The MCT equations display a dynamical glass transition to a phase where the average density of the liquid remains frozen in an amorphous profile.

The similarity with the p -spin model is not casual, and there is indeed a deep connection between the two. A first, somewhat technical, way to unveil it consists of simplifying

the wave-vector dependence of the equations assuming that the integral over k is dominated by values close to k_0 , where the structure factor has a strong peak. This so-called “schematic” approximation (Bengtzelius *et al.*, 1984; Leutheusser, 1984; Götze, 1999) yields a simplified equation of motion for $F(k_0, t)$ that reads

$$\nu(k_0) \frac{dF(k_0, t)}{dt} = -\frac{k_0^2 k_B T}{mS(k_0)} F(k_0, t) - \frac{k_0 A^2}{8\pi^2 \rho} \times \int_0^t dt' F^2(k_0, t-t') \frac{dF(k_0, t')}{dt'}, \quad (48)$$

where A is the area under the peak of $S(k)$ at k_0 . A simple change of variables maps this equation to that of the 3-spin model, Eq. (42). This relation with fully connected models suggests that MCT should be interpreted as a mean-field approximation. Note that this does not imply that MCT becomes exact in the limit of large spatial dimensionality, as shown by recent calculations (Ikeda and Miyazaki, 2010; Schmid and Schilling, 2010).

The solution of MCT equations displays a rich phenomenology as seen in Fig. 13. There are three time regimes: A fast relaxation toward a plateau, whose value depends on k , a slow relaxation close to the plateau, called β regime, and finally the structural relaxation on the time scale of the α regime; see Kob (2003) and Das (2004) for more details. In the following we shall denote ϵ as the relative distance from the transition. For molecular liquids the control parameter is the temperature and, hence, $\epsilon = (T - T_c)/T_c$; for colloids the control parameter is the density and so $\epsilon = (\phi_c - \phi)/\phi_c$.

Keeping track of the wave-vector dependence, the detailed properties of the dynamics in the three regimes are as follows:

- (1) Fast relaxation—Some degrees of freedom relax on time scales of the order of τ_0 , even close to the transition. This regime is identified taking the limit $\epsilon \rightarrow 0$ and keeping t finite. In this case $F(k, t)$ approaches a plateau at long times whose value is denoted $f_k S(k)$. The nonergodic parameter f_k is the fraction of density fluctuations that becomes frozen at the transition. At large times the behavior of $F(k, t)$ is

$$F(k, t) \approx f_k + \frac{h(k)}{t^a}, \quad t \gg \tau_0. \quad (49)$$

The exponent a satisfies the equation

$$\frac{\Gamma^2(1-a)}{\Gamma(1-2a)} = \lambda, \quad (50)$$

where λ is a number that can be computed using the structure factor only. Its expression is complicated; see Götze (1985). The previous equation implies $0 \leq a < 1/2$.

- (2) β regime—In this sector, the time scale diverges as $\tau_\beta \sim \epsilon^{-1/2a}$ and the dynamical structure factor scales as

$$F(k, t) \approx f_k + \sqrt{\epsilon} h(k) g(t/\tau_\beta), \quad (51)$$

where $g(x) \propto x^{-a}$ for $x \ll 1$ and $g(x) \propto x^b$ for $x \gg 1$. Note that the previous expression implies that all the k dependence factorizes and is contained in $h(k)$ only, the so-called “factorization property.” The exponent b satisfies the equation

$$\frac{\Gamma^2(1+b)}{\Gamma(1+2b)} = \lambda, \quad (52)$$

which implies that $0 \leq b \leq 1$.

- (3) α regime—In this sector the time scale diverges as $\tau_\alpha \sim \epsilon^{-\gamma}$, where $\gamma = 1/2a + 1/2b$. The factorization property does not hold anymore except for small t/τ_α because the solution has to match the one found in the β regime.

We refer the reader again to Fig. 13 for a visual illustration of the different time regimes predicted by MCT for dynamic structure factors in supercooled liquids.

Mode-coupling theory provides predictions also for other correlators such as the self-intermediate scattering function from which the mean-squared displacements and thus the self-diffusion coefficient can be obtained. The previous properties remain essentially unaltered and all correlators display quite similar scalings.

All these predictions have been tested in great detail in numerical simulations and in experiments both on molecular liquids and in colloids. It has also been shown that adding corrections to MCT does not spoil the main predictions and the universality of MCT has been established (Andreanov *et al.*, 2009). Different reviews (Götze, 1999; Kob, 2003; Das, 2004) have already appeared on these tests. When fitting data using MCT, a central difficulty arises from the fact that the actual transition is not present, as expected from its mean-field nature. The absence of a genuine mode-coupling singularity is undisputed for molecular liquids in both simulations and experiments (Götze, 2008). Recent numerical and experimental works suggest that the same situation holds in hard-sphere systems (Santen and Krauth, 2000; Brambilla *et al.*, 2009; Flenner and Szamel, 2010). This is illustrated in Fig. 15, where the predicted MCT algebraic divergence of the structural relaxation time for a Lennard-Jones liquid and a hard-sphere fluid are superimposed on numerical data. While

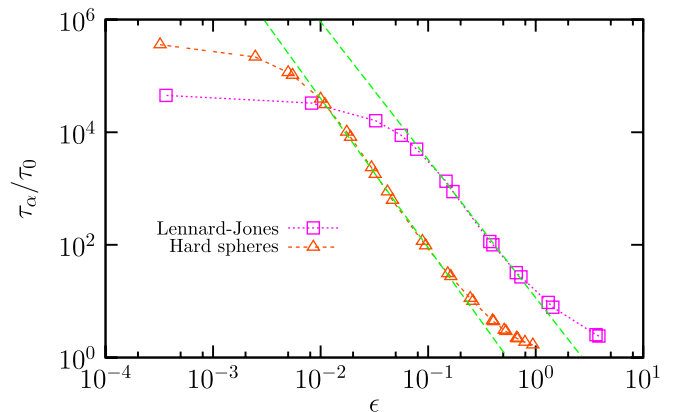


FIG. 15 (color online). Fit of the evolution of the equilibrium structural relaxation time of a Lennard-Jones liquid (temperature is varied) and a hard-sphere fluid (density is varied) with the predicted MCT algebraic divergence $\tau_\alpha \sim \epsilon^{-\gamma}$, where ϵ is the reduced distance to the transition. The plateau at low ϵ shows that τ_α remains finite at $\epsilon = 0$, and the data directly indicate that the transition can actually be crossed at thermal equilibrium and is thus avoided.

the fit is accurate over a window of two to three decades, it clearly fails to capture the low temperature or large density regimes of these systems. Clearly, therefore, mean-field concepts cannot directly be applied to understand the glass transition, and a more refined analysis is needed.

In conclusion, MCT predicts a transition, where the system has a dynamical arrest, particles stop to diffuse, and the density becomes frozen around an amorphous profile. Additionally, MCT yields nontrivial predictions for the behavior of dynamical correlators that serve as a guideline in the study of moderately supercooled liquids.

3. Dynamical correlations within mode-coupling theory

We introduced MCT as a dynamical theory for two-time correlation functions. However, the recent surge of interest in high-order correlation functions as a probe of dynamic correlations and dynamic heterogeneity suggests that it could be interesting to develop an MCT approach also for multipoint correlation functions.

The MCT transition was originally described as a local phenomenon, the self-consistent blocking of the particles in their “cages” (Götze, 1999). On general grounds, a diverging relaxation time is expected to arise from processes involving an infinite number of particles (leaving aside the case of quenched obstacles), as discussed in Sec. III.B and established by rigorous results (Montanari and Semerjian, 2006b). Actually, even the cage mechanism requires some kind of collective behavior: In order to be blocked by one’s neighbors, the neighbors themselves must be blocked by their neighbors and so on until a certain scale that, intuitively, should set the relaxation time scale of the system. So one expects that even within MCT, cages should, in fact, be described as spatially correlated objects (Biroli *et al.*, 2006). It has indeed been shown that all susceptibilities and correlations defined in Sec. III.B, such as χ_4 and χ_T , diverge at the MCT dynamic singularity.

Historically, the “local-cage” point of view was challenged in the context of mean-field disordered systems by Franz and Parisi (2000) [see Kirkpatrick and Thirumalai (1988) and Kirkpatrick *et al.* (1989) for early results], since these models are analogous to schematic MCT equations. Franz and Parisi argued that a dynamical susceptibility similar to $\chi_4(t)$ diverges at the dynamical mode-coupling transition. The first full MCT analysis was developed by Biroli and Bouchaud (2004), using a field-theoretical approach. This clearly showed the existence of a diverging length scale within MCT. Later, a different susceptibility $\chi_{q_0}(\mathbf{q}_1, t)$ was introduced (Biroli *et al.*, 2006) that quantifies the response of the dynamical structure factor to a static oscillatory external perturbation with wave vector \mathbf{q}_0 . For a perturbation localized at the origin $U(\mathbf{x}) = U_0 \delta(\mathbf{x})$, one finds $\delta F(\mathbf{q}_1, \mathbf{y}, t) = U_0 \int d\mathbf{q}_0 e^{i\mathbf{q}_0 \cdot \mathbf{y}} \chi_{q_0}(\mathbf{q}_1, t)$. This susceptibility is akin (although not exactly related) to a three-point density correlation function in the absence of the perturbation. Although quite different from the four-point functions considered previously in the literature, $\chi_{q_0}(\mathbf{q}_1, t)$ is expected to reveal the existence of a dynamical correlation length of the homogeneous liquid as well. Physically, $\chi_{q_0}(\mathbf{q}_1, t)$ indeed measures the influence of a density fluctuation at a given point in space on the dynamics

elsewhere. Additionally its scaling form is not affected by complications due to conservation laws, as is the case for four-point correlators; see Sec. III.C. Recent work on Kac glassy models also found a similar diverging length at the MCT transition (Franz and Montanari, 2007) using replica techniques.

We now summarize the critical properties found for $\chi_{q_0}(\mathbf{q}_1, t)$ by Biroli *et al.* (2006). As for the dynamical structure factor there is a different critical behavior in the β and α regimes, although there is a unique diverging correlation length scale $\xi \propto \epsilon^{-1/4}$.

(1) In the β regime, one has

$$\chi_{q_0}(\mathbf{q}_1, t) = \frac{1}{\sqrt{\epsilon} + \Gamma q_0^2} S(q_1) h(q_1) g_\beta \left(\frac{q_0^2}{\sqrt{\epsilon}}, \frac{t}{\tau_\beta} \right), \quad (53)$$

where g_β is a scaling function, and Γ is a positive constant that are both obtained quantitatively (Biroli *et al.*, 2006). In particular, g_β behaves as a $\sim t^a$ for small t/τ_β , and as $\sim t^b$ for large t/τ_β .

(2) In the α regime the critical behavior of $\chi_{q_0}(\mathbf{q}_1, t)$ is

$$\chi_{q_0}(\mathbf{q}_1, t) = \frac{\Xi(\Gamma q_0^2/\sqrt{\epsilon})}{\sqrt{\epsilon}(\sqrt{\epsilon} + \Gamma q_0^2)} g_{\alpha, q_1} \left(\frac{t}{\tau_\alpha} \right), \quad (54)$$

with Ξ a certain regular function with $\Xi(0) \neq 0$ and $\Xi(v \gg 1) \sim 1/v$ such that χ_{q_0} behaves as q_0^{-4} for large q_0 , independently of ϵ . Also, $g_{\alpha, q_1}(u \ll 1) = S(q_1) h(q_1) u^b$, to match the β regime, and $g_\alpha(u \gg 1, q_1) \rightarrow 0$.

The behavior of four-point quantities, such as G_4 and χ_4 , is more complicated because of ensemble dependencies and the influence of conservation laws; see Berthier *et al.* (2007a) for a detailed discussion. It was found that G_4 and χ_4 should have a similar critical behavior, but not too close to the MCT transition, crossing over to a distinct behavior in its vicinity, due to conservation laws. Therefore, for decisive tests of MCT predictions regarding multipoint functions, the quantity $\chi_{q_0}(\mathbf{q}_1, t)$ should be preferred, but no such study has been reported yet.

The study of critical properties of dynamical correlations for glassy liquids and, hence, the comparison with MCT predictions is still in its infancy (Toninelli *et al.*, 2005; Szamel and Flenner, 2006; Berthier *et al.*, 2007a, 2007b; Stein and Andersen, 2008; Flenner and Szamel, 2010). At the time of this writing many questions remain open and deserve further studies. The determination of the dynamic correlation length is subtle, and because of the complication brought about by the existence of conserved quantities, G_4 could be difficult to analyze. Certainly a numerical study of $\chi_{q_0}(\mathbf{q}_1, t)$ would be important. Furthermore, the role of finite size effects (Berthier, 2003b; Karmakara *et al.*, 2009), the dependence of the results on the observable used to probe dynamical correlations, the universality of the results, the possible anisotropic character of dynamic heterogeneity (Flenner and Szamel, 2007) are all open questions needing further investigation.

4. Current status of MCT

The first and most important drawback of mean-field dynamics and MCT is that the MCT transition it describes

is not observed in real materials. Additionally, a comparison between Eqs. (2) and (43) makes it clear that MCT cannot be used to describe viscosity data close to the experimental glass transition T_g , since it does not even predict thermally activated behavior. Worse, MCT predicts a transition at which the system freezes completely: not only a fraction of the density fluctuations get frozen but also self-diffusion gets arrested (Fuchs *et al.*, 1998). This is a theoretical artifact as it can be rigorously proven (Osada, 1998) that the self-diffusion coefficient cannot go continuously to zero at thermal equilibrium and finite temperature and pressure (this excludes the case of hard particles at close packing).

With all of these major failures, then, why should one continue to study and talk about MCT? We provide several reasons below.

It is now recognized that the MCT transition must be interpreted as an approximate theory of a crossover taking place in the dynamics. Actually, there are many other physical examples, such as the Kondo model (Hewson, 1997) or spinodal points (Debenedetti, 1996), where crossovers become transitions in approximate self-consistent theory. The fact that the transition is sharp in the theoretical treatment allowed the derivation of a variety of scaling laws which are as many predictions that can be tested in real materials, or, more prosaically, a simple formula that can be used to “fit the data.” Part of the success of MCT has been its ability to propose such clear-cut predictions (and fits) and graphical representations along which data could be analyzed.

Indeed, one finds in the literature scores of papers where an MCT analysis of data is performed. Since the transition is (at best) only “avoided,” its “crossover” nature offers quite a lot of flexibility for fitting, and judging the quality of the fits is often a difficult (and subjective) exercise, while “negative” results can always be attributed to “preasymptotic” corrections rather than deficiencies of the theory itself. This has led to many controversies in the literature which persist to this day.

A major achievement of MCT is the possibility to apply the same formalism to different materials and theoretical models, basically starting from the microscopic interactions between atoms and molecules. This is again a reason for the success of MCT: Each time a new model with a different kind of interactions or chemical composition is defined, MCT can be used to analyze its behavior and possibly predict new qualitative trends for the time dependence of correlation functions and their evolution, even in cases where several control parameters are relevant (e.g., mixtures, attractive versus repulsive interactions, complex fluids, etc.). Striking and successful results and predictions, later confirmed by simulations and experiments, have been obtained in several cases: For example, for the dynamical phase diagram of attractive colloids, for the behavior of the nonergodic parameter as a function of the wave vector for glassy liquids, for the treatment of molecules or particles with nonspherical shapes, see the reviews by Kob (2003), Das (2004), and Götze (2008). Thus, MCT is always a useful starting point when a new system with unknown behavior arises.

Although the MCT predictions are limited to a modest time window of 2–3 decades corresponding to the onset of glassy dynamics in molecular liquids, this time window is actually the most experimentally relevant in colloidal materials

(Cipelletti and Ramos, 2005), since typical microscopic time scales for colloidal particles are in the millisecond range (instead of the nanosecond range for atoms). Thus, MCT performs much better in soft matter systems, to the point that actually observing deviations from MCT predictions in an experiment can represent a challenge. Even for the canonical and well-studied system of colloidal hard spheres, it was only recently suggested experimentally that the MCT transition is avoided in the same manner as in molecular liquids (Brambilla *et al.*, 2009). Thus we believe MCT will continue to be a useful tool, given the current rapid development in the synthesis of new colloidal particles.

On the theoretical side, it is now clear that MCT has the status of a mean-field theory (Andreanov *et al.*, 2009). As such, one expects major changes once fluctuations are taken into account. As we pointed out already some kinds of fluctuations wipe out the sharp MCT transition and make it a crossover. Moreover, exactly as for critical phenomena, one expects critical fluctuations to change the value of the MCT exponents below an upper critical dimension that was determined to be equal to 8 (Biroli and Bouchaud, 2007; Franz *et al.*, 2010). The role of fluctuations on the MCT transition is a current topic of research.

As a conclusion, MCT has clear and well-understood limitations, and it will never be possible to test its predictions in a sharp way because it is not related to a true phase transition but, likely, just to a crossover. Still, its overall efficiency and flexibility and its ability to deliver actual predictions make it useful. For this reason it continues to be developed, applied, and generalized to study many different physical systems and situations, including aging systems and nonlinear rheology of glassy materials; see Sec. V.

5. Quantitative computations using replica

In Sec. IV.B.1, we presented the theoretical picture emerging from solving mean-field models (or geometries) of the glass transition, and we found the resulting scenario rich and encouraging: It generically supports the existence of a configurational entropy vanishing transition associated, at a higher temperature, with a dynamical transition, *à la* MCT, which corresponds to the appearance of incipient metastable states.

Still, to make a connection with experimental results at least two main issues need to be addressed. First, one has to transform this set of mean-field ideas into a working tool able to produce quantitative calculations for the case of supercooled liquids. Second, dynamics within a rugged landscape must be revisited in order to explain the crossover nature of the MCT transition, and the existence of a regime where dynamics is thermally activated and the viscosity increases in a super-Arrhenius manner which is incompatible with the algebraic divergence predicted by mode-coupling theory. In this section and the next, we briefly review these two lines of research.

First, we focus on the approaches that have been devised to obtain quantitative microscopic predictions. In fact, MCT can be seen already as such a tool, but it is limited to the regime above T_{MCT} . Below this temperature it cannot be applied anymore. At the time of this writing, a quantitative microscopic theory of the dynamics valid below T_{MCT} is still

lacking; see [Bhattacharya et al. \(2005\)](#) for a possible attempt. An alternative strategy is to leave dynamics for a while and turn to thermodynamics. The idea is to compute approximately the configurational entropy, the Kauzmann temperature, and the plateau value of dynamical correlation functions in the glass phase ([Monasson, 1995](#); [Franz et al., 1998](#); [Mézard and Parisi, 1999](#); [Parisi and Zamponi, 2005](#); [Mézard and Parisi, 2010](#)).

All the approaches developed to compute static properties of systems characterized with a rugged landscape make use of replica in one way or another ([Parisi, 2003](#)). Physically, the reason is that one aims at describing (or at least counting) metastable states which all have amorphous density profiles. This is similar to the spin glass case where the amorphous order is not revealed by looking at magnetization profiles, as discussed in [Sec. III.B.1](#). Inspired once more by the physics of disordered systems, the idea is again to let the system itself indicate what these states are and use distinct copies of the system to “recognize” the metastable states. In the absence of quenched disorder, however, it is not enough to replicate the system; one is also forced to physically “couple” the different copies of the system using an appropriate field.

It is useful to first implement this idea for two copies ([Monasson, 1995](#)), 1 and 2, of the system, characterized by density profiles $\rho_1(\mathbf{x})$ and $\rho_2(\mathbf{x})$. Using notations from [Sec. IV.B.1](#), we write the free-energy density of a single copy of the system as

$$f = -\frac{T}{V} \log \int \mathcal{D}\rho_1 e^{-\beta H[\rho_1]}, \quad (55)$$

where $H[\rho_1]$ is the microscopic Hamiltonian. We now use the second copy of the system to scan the locally stable configurations of the first one. To do so, we introduce a quadratic coupling of strength $g > 0$ between the two copies and compute the new free energy

$$f_2[\rho_1] = -\frac{T}{V} \log \left[\int \mathcal{D}\rho_2 e^{-\beta H[\rho_2] - g \int d^d x [\rho_1 - \rho_2]^2} \right]. \quad (56)$$

The free energy $f_2[\rho_1]$ will be small when ρ_1 is a configuration which corresponds to a metastable state. Therefore, sampling all configurations of ρ_1 weighted with $\exp(-\beta f_2[\rho_1])$ is a procedure to scan all metastable states, so that

$$f_{\text{meta}} = \lim_{g \rightarrow 0} \frac{1}{Z} \int \mathcal{D}\rho_1 f_2[\rho_1] e^{-\beta f_2[\rho_1]} \quad (57)$$

is the average free energy of all metastable states; here $Z = \int \mathcal{D}\rho_1 \exp(-\beta f_2[\rho_1])$ is a normalization. When it exists, the difference between the total free-energy density of the system f and the free-energy density of the minima f_{meta} is related to the number of metastable state available to the system; see also [Eq. \(38\)](#). As a consequence, this free-energy cost is in fact equal to $-T s_c$. The lesson to be learned from this example is that the introduction of identical copies of the system allows one to directly compute properties of the free-energy landscape ([Monasson, 1995](#); [Franz and Parisi, 1998](#)). It is important to remember, however, that the limit $g \rightarrow 0$ in [Eq. \(57\)](#) has a strong mean-field flavor, since genuine metastable states exist only in this limit; see [Parisi \(2003\)](#) for a more precise discussion.

Several quantitative approaches have been developed and are based, in one way or another, on procedures similar to the one outlined above; see [Monasson \(1995\)](#), [Franz et al. \(1998\)](#), [Mézard and Parisi \(1999\)](#), and [Parisi and Zamponi \(2005\)](#). In the scheme of [Monasson \(1995\)](#), one introduced m copies of the system constrained to be in the same free-energy minimum. Technically, this corresponds to take m copies of the density configuration ρ_1 . This generalizes the partition function in [Eq. \(38\)](#) to

$$\begin{aligned} Z_m &= \lim_{g \rightarrow 0} \frac{1}{Z} \int \mathcal{D}\rho_1 e^{-\beta m f_2[\rho_1]} \\ &= \int df \exp \left[-\frac{N f m}{T} - N s_c(f, T) \right], \end{aligned}$$

associated to the replicated free energy $\psi(m, T) = -T \log Z_m$. Note that m enters only the first term, as all systems are identical and are characterized by the same metastable states. Repeating the saddle-point calculation yields

$$f = \frac{\partial \psi(m, T)}{\partial m}, \quad s_c = \frac{m^2}{T} \frac{\partial (\psi(m, T)/m)}{\partial m}, \quad (58)$$

which shows that the configurational entropy s_c can be accessed by computing the thermodynamic properties of a system of m coupled replicas, provided, as is usual within replica calculations, that the number of copies of the system is analytically continued to noninteger values, as implicitly assumed in [Eq. \(58\)](#).

An achievement ([Mézard and Parisi, 1999](#)) is that not only the properties of the liquid state above T_K can be computed analytically from [Eq. \(58\)](#), but also the ones of the “ideal” glass below T_K . Recall from [Fig. 12](#) that the Kauzmann temperature is defined by $T_K = (\partial s_c / \partial f)^{-1}$ for the value of f corresponding to $s_c = 0$. For the replicated system, one gets $T_K^{(m)} = m (\partial s_c / \partial f)^{-1}$ and the location of the transition depends on m . For values of $m < 1$, one typically finds that $T_K^{(m)} < T_K$. This means that the properties of the replicated liquid with $m \neq 1$ are deeply connected to the ones of the nonreplicated glass with $m = 1$. Indeed, assuming that the transition has a nature similar to the one found in mean-field models, one can use the fact that the free energy is continuous at T_K and glass states below T_K have $s_c(T < T_K) = 0$ to obtain the free energy of the (nonreplicated) glass as

$$f_{\text{glass}}(T) = \psi(m^*(T), T) / m^*(T), \quad (59)$$

where $m^*(T < T_K) < 1$ is self-consistently defined by $T_K^{(m^*)} = T$ and $\psi(m, T)$ is the energy of the replicated liquid defined above.

To summarize, starting from the hypothesis in which the free-energy landscape of supercooled liquids resembles the picture gained from mean-field models and geometries, one introduces replicas as a useful mathematical tool to probe the thermodynamics of systems both above and below T_K . One ends up with an additional variational parameter $m^*(T)$ to describe the low-temperature phase, which is formally strictly equivalent to the additional parameter m entering the one-step replica symmetry scheme needed to solve mean-field models ([Monasson, 1995](#)). Note that in this approach, the nature of the broken symmetry is a starting hypothesis rather than a natural outcome of the calculations.

In practice, of course, some approximations must be made to compute the free energy of the replicated liquid at low temperature, which make heavy use of liquid state theory and which might well depend on the studied system. The main outcomes are the calculation of the location of the Kauzmann transition, the thermodynamic properties of the liquid (in particular, the configurational entropy), and the glass (ground state energy, specific heat, and structure). These microscopic computations have been developed for a variety of glass-forming liquids, such as monoatomic or mixtures of Lennard-Jones particles (Coluzzi *et al.*, 2000), soft spheres (Coluzzi *et al.*, 1999; Mézard and Parisi, 1999), hard spheres (Franz *et al.*, 1998; Parisi and Zamponi, 2005), sticky hard spheres (Velenich *et al.*, 2006), and silica (Coluzzi and Verrocchio, 2002). Perhaps the most impressive achievement is the detailed description of the large volume fraction behavior of hard spheres (Parisi and Zamponi, 2005, 2010): The glass transition was located, the equation of state and structure of the glass obtained up to the “glass close packing” density, which can be seen as a firm definition of the notion of random close packing (Bernal and Mason, 1960), whose location can then be predicted accurately in any spatial dimension (Parisi and Zamponi, 2006) or for binary mixtures (Biazzo *et al.*, 2009), with excellent agreement with experimental results and simulations.

Although this quantitative side of RFOT theory is a most desirable feature, assessing quantitatively the quality of the results is not easy as experiments and simulations typically fail to approach the Kauzmann transition. Even then, cases are known where a transition is predicted in a regime where none is expected (Coluzzi and Verrocchio, 2002; Thalmann, 2002), suggesting that the quality of the approximations used to obtain quantitative results plays an important role (Ikeda and Miyazaki, 2010). Thus, when accurate results are sought, the problem might well become technically quite involved (Parisi and Zamponi, 2010).

6. Scaling arguments beyond mean-field theory and point-to-set length scale

The quantitative calculations described in the previous section remain mean field in nature, because they compute the properties of the supercooled liquid state as if it were formed by a collection of states with infinite lifetime, as is the case in mean-field models. This is clearly incorrect: Two thermodynamically stable states cannot coexist and have different intensive free energy at finite temperature, otherwise the system would nucleate from the one with highest free energy to the one with lowest, showing that the highest is, in fact, not a stable state. Furthermore, an exponential number (in the system size) of stable states seems impossible: For large sizes there would not be enough boundary conditions to select one state from the other (Newman and Stein, 2002; Fisher, 2003).

Additionally these calculations cannot address the connection to dynamical properties, a crucial missing ingredient for a theory of the glass transition. Presently, there only exist phenomenological arguments (Kirkpatrick *et al.*, 1989; Xia and Wolynes, 2000; Bouchaud and Biroli, 2004), backed by microscopic computations (Dzero *et al.*, 2005; Franz, 2005; Franz, 2006; Franz and Montanari, 2007) that yield a possible

scenario for the dynamics, dubbed “mosaic state” by Kirkpatrick *et al.* (1989). Since this aspect of RFOT theory was reviewed recently (Lubchenko and Wolynes, 2007; Biroli and Bouchaud, 2009), we shall be brief. Schematically, the mosaic picture states that, in the regime $T_K < T < T_{\text{MCT}}$, the liquid is composed of domains of linear size ξ . Physically, the length scale ξ represents the length scale above which it does not make sense to talk about metastable states anymore.

The way to measure, or even to precisely define, the mosaic length scale ξ was not clear from the way it was initially introduced. Recently, the so-called “point-to-set” correlation length scale was defined both in the context of RFOT theory as a practical measure of the mosaic length scale (Bouchaud and Biroli, 2004), and in more general settings (Mézard and Montanari, 2006; Montanari and Semerjian, 2006b). The point-to-set length is a measure of the spatial extent over which the effect of equilibrium amorphous boundary conditions propagate.

To understand the origin of this length scale, we consider the following “experiment” where, starting from an equilibrium configuration of the system, we freeze the positions of all particles outside a cavity of radius R . We then let the system evolve in the presence of this constraint, which acts as a pinning field. The point-to-set length scale is defined as the minimal cavity radius such that the pinning field has no influence at the center of the cavity. As such, it is a measure of the many-body correlations between a point (the center of the cavity) and a set of points (the pinned boundary). It is also important to emphasize the similarity between this cavity procedure and the coupling between copies applied in Eq. (56). While the latter was homogeneous, the former is spatially inhomogeneous, and quantifies how far in space the coupling between states can propagate (Kurchan and Levine, 2009).

The constraint on the boundary of the cavity, in fact, acts as a “template” for the particles inside the cavity, whose effect can be evaluated as follows. By selecting a different state and deforming it only close to the boundary to satisfy the constraint, one would get a free-energy cost of the order of $Y R^\theta$ with $\theta \leq 2$. However, doing so, one would also gain entropy as the system could explore a multiplicity of different states, giving rise to a free-energy contribution $-T s_c R^3$. Entropy obviously gains on large length scales $R \gg 1$, while interface cost dominates at small R . Therefore, the crossover in the competition between these two terms takes place for a length scale $R = \xi$ obtained by equating the two terms,

$$\xi = \left(\frac{Y}{T s_c(T)} \right)^{1/(3-\theta)}. \quad (60)$$

In a real liquid, where there is no cavity, one can conjecture that there is a self-generated dynamical boundary condition acting on each patch of length scale ξ .

The dynamical counterpart to this argument is as follows. Dynamically, the configurational entropy on scales smaller than ξ is too small to stir the configurations efficiently and loses against the dynamically generated pinning field due to the environment. By contrast, ergodicity is restored at larger length scale. Hence, the relaxation time of the system is the relaxation time $\tau(\xi)$ of a finite size region of the system. It is only after this long, but plausible series of arguments that

barriers encountered during relaxation finally become finite and involve a finite number of particles, unlike in the original mean-field treatment of the landscape where barriers diverge with system size.

Now, assuming thermal activation over energy barriers which are supposed to grow with size as ξ^ψ , with $\psi \geq \theta$, one predicts finally, using Eq. (60), that (Bouchaud and Biroli, 2004)

$$\log\left(\frac{\tau_\alpha}{\tau_0}\right) = c \frac{Y}{k_B T} \left(\frac{Y}{T S_c(T)}\right)^{\psi/(3-\theta)}, \quad (61)$$

where c is a constant. This argument is rather generic and therefore not very predictive. Recent microscopic computations (Dzero *et al.*, 2005; Franz, 2005, 2006; Montanari and Semerjian, 2006a; Franz and Montanari, 2007) attempted the computation of the exponents θ and ψ , directly addressing analytically the problem of the cavity described above. Equations for the overlap profile between the initial template configuration and configurations thermalized in the presence of the pinning boundaries were obtained. These calculations confirmed the existence of a nontrivial crossover length scale above which the overlap inside the cavity vanishes, indicating that order does not propagate on length scales much larger than ξ .

The results are unfortunately not yet conclusive. Although part of the computations can be justified and controlled by using, for instance, Kac models (Franz, 2005, 2006), other parts involve uncontrolled replica symmetry breaking schemes. The calculations provided the estimate $\theta = 2$. Note that some other phenomenological arguments suggest the value of $\theta = 3/2$ (Kirkpatrick *et al.*, 1989). There are no detailed computations available for ψ , only the suggestion that $\psi = \theta$ (Kirkpatrick *et al.*, 1989).

Note that using the value $\theta = 3/2$ with $\theta = \psi$ simplifies Eq. (61) into a form that is well known experimentally and relates $\log \tau_\alpha$ directly to $1/S_c$, which is the celebrated Adam-Gibbs relation (Adam and Gibbs, 1965) between relaxation time and configurational entropy. As discussed in Sec. II.A, such a relation is in rather good quantitative agreement with many experimental results (Angell, 1997; Hodge, 1997; Johari, 2000). RFOT theory, therefore, reformulates and generalizes the mechanism suggested by the Adam-Gibbs relation (Xia and Wolynes, 2000). Furthermore, using the fact that the configurational entropy vanishes linearly at T_K , Eq. (61) becomes similar to the VFT divergence of Eq. (2), with the identification between two important temperatures,

$$T_0 = T_K, \quad (62)$$

which embodies the deep connection between thermodynamics and dynamics characterizing RFOT theory. The above equality between two temperatures that are commonly used in the description of experimental data constitutes a central achievement of RFOT theory, since it accounts for the empirical relation found between the kinetics and the thermodynamics of supercooled liquids. It should be kept in mind, however, that experiments have not established its validity beyond any doubts, as discussed in detail in Sec. II.A.

Wolynes and co-workers obtained several other results using phenomenological arguments based on RFOT. Two remarkable ones are the relation between fragility and

specific heat jump at the glass transition and stretching exponent β of time-dependent correlation functions, and the speeding up of the dynamics close to a free surface [recently observed by Ashtekar *et al.* (2010)]. These predictions and several others are discussed in detail by Lubchenko and Wolynes (2007).

7. Current status of RFOT theory

We described RFOT theory as a ‘‘patchwork’’ (not to say mosaic) of apparently distinct theoretical approaches to the glass problem: Adam-Gibbs theory, mode-coupling theory, mean-field spin glass theory and replica approaches, and the mosaic state scaling picture. As such, RFOT theory is clearly an impressive theoretical piece of work, which gives a consistent overall scenario for the glass transition and nonequilibrium phenomena related to the glassy state, based on peculiar features of the free-energy landscape as well as tools to perform microscopic calculations.

Coming from high temperatures, dynamics primarily slows down because there appear incipient metastable states, in a restricted temperature window described in full microscopic detail by mode-coupling theory. Further decreasing the temperature, the dynamics becomes dominated by the thermally activated barrier to be crossed from one metastable state to another, in a way consistent with the deep relation between dynamical correlation length and time scale discussed in Sec. III. In this regime, the thermodynamic behavior can also be described at the thermodynamic level using replica calculations which predict the existence of a finite-temperature thermodynamic transition toward a genuine ideal glass state. A description of the dynamics near the transition exists, but contains several steps that heavily rely on empirical scaling concepts.

There are several weaknesses in this construction. First, although we attempted here to give a unified view, the theory is still pretty much made of distinct pieces that do not necessarily smoothly fit together. For instance, the details of the crossover between MCT and activated regimes are not well understood. In early works, attempts were made to include ‘‘hopping effects’’ in mode-coupling theory, deriving expressions for the memory kernels which transform the sharp MCT transition into a crossover (Das and Mazenko, 1986; Götze and Sjögren, 1987). However, the status of these ‘‘extended’’ MCT is debated (Andreanov *et al.*, 2006; Cates and Ramaswamy, 2006). Moreover, there are also strong indications that thermal activation is, in fact, already at play in the temperature regime usually described by MCT (Berthier and Garrahan, 2003b; Denny *et al.*, 2003; Doliwa and Heuer, 2003; Heuer, 2008). Finally, recent works attempted to include nonperturbative processes in the MCT description (Bhattacharya *et al.*, 2005; Mayer *et al.*, 2006), but no treatment generically applicable to liquids is yet available.

Second, when applied to three-dimensional liquids, RFOT theory relies on several, sometimes distinct, types of approximations. For finite-dimensional systems, a complete and solid version of RFOT theory remains to be worked out. This is especially true for the mosaic part of RFOT theory which yields dynamic predictions, namely, a Vogel-Fulcher divergence of the relaxation time. This implies that opponents

can criticize RFOT theory because it contains too many uncontrolled assumptions, while supporters can always hide a weak point as resulting from some approximation rather than from the approach itself. We do not see how this issue can be resolved, as data themselves do not allow clear-cut conclusions. Although the ultimate consequences of the theory are sometimes in good agreement with experiments, as Eq. (62), one should not conclude too fast that RFOT theory is correct. In this context, a pertinent line of investigation, allowed by numerical simulations, is to more directly test the microscopic mechanisms underpinning the derivation of the mosaic picture (Jack and Garrahan, 2005; Cavagna *et al.*, 2007). In particular, recent works have shown that the static point-to-set correlation length scale described in Eq. (60) does increase upon supercooling (Biroli *et al.*, 2008). Furthermore, first measurements of the exponent θ and ψ of the mosaic theory have been obtained with the somewhat surprising results $\theta \simeq 2 > \psi \simeq 1$ (Cammarota *et al.*, 2009, 2009). Presently, direct tests of the mosaic picture are quite involved (even conceptually), and hence are rare and not yet conclusive. This line of research appears, nevertheless, promising to establish, disprove, or further develop the mosaic picture; see Cavagna (2009) for more details.

The fact that these approximations become exact in several mean-field settings (fully connected models, Bethe lattices) suggests that RFOT theory might have a status similar to the Curie-Weiss theory for the ferromagnetic systems which contain correct elements of the real theory. Current research can thus be seen as an attempt to understand and describe better non-mean-field effects. Going beyond mean-field theory is not only technically but also conceptually difficult. For instance, Stillinger claimed that the configurational entropy vanishes only at zero temperature, thus suggesting that no entropy crisis can take place (Stillinger, 1988). This was related to his identification of metastable states with energy minima, which is now recognized to be an incorrect approximation, even in mean-field models (Biroli and Monasson, 2000), where the well-defined metastable states are, in general, made of a large number of energy minima, in the spirit of the “metabasins,” sometimes described in numerical works as a large assembly of inherent structures (Heuer, 2008). The same criticism applies to recent work that similarly claimed having demonstrated the absence of a glass transition in bidimensional binary mixtures (Donev *et al.*, 2007). However, a correct definition of metastable states beyond mean-field theory is still lacking; see Biroli and Kurchan (2001) for a discussion and a first attempt. Thus, going beyond mean-field theory is clearly a difficult, but quite exciting and important task, from which new results can be expected in the future.

A further source of concern for RFOT theory is the fact that quite often the mean-field models from which it largely originates seem to behave quite differently when studied in finite dimensions (Alvarez *et al.*, 1996; Brangian *et al.*, 2002; Moore and Drossel, 2002; Moore, 2006; Moore and Yeo, 2006). In fact, there does not yet exist a theoretical model in finite dimension, for which the RFOT theory scenario can be shown to apply; see Sarlat *et al.* (2009), Castellana *et al.* (2010), and Liers *et al.* (2010) for recent efforts. From a theoretical perspective, such a discovery

would be a highly decisive step, even if the model were abstract and not obviously connected to experimental systems.

Thus, there is hope that in the next few years, joint theoretical and experimental efforts will drive RFOT theory into a corner, where its status can be made precise. At the time of writing, one can state that RFOT theory is still imperfect, but the broadness of its scope and predictions, the number of distinct approaches that systematically give back at least some piece of it, and the generality of the concepts it uses makes one believe that it contains at least some useful seeds to construct a “final” theory of the glass transition, if such a thing exists.

C. Kinetically constrained models and dynamic facilitation

1. The physical picture

Another approach to the glass transition problem is based on the concept of dynamical facilitation; see (Chandler and Garrahan (2010) for a review. In short, “facilitation” captures the physical idea that since viscous liquids are almost solid, mobility is so sparse at any given time that any local relaxation event is likely to trigger, or “facilitate” the relaxation of nearby molecules after a time which is short compared to the macroscopic relaxation time but large compared to the microscopic one, so that mobility can propagate throughout the sample. Thus, the focus is less on molecules than on their mobility (Fredrickson and Andersen, 1984).

There is no doubt that at least some degree of facilitation is present in nearly jammed materials, but the theoretical approach described in this section goes well beyond this simple observation and posits that the entire dynamics of the system is mainly due to facilitation effects. This means that typically a mobile region of the sample can become unjammed and thus mobile only if it is adjacent to a region which is already unjammed (Garrahan and Chandler, 2003). This is equivalent to postulating that, except for rare events, mobility in a viscous liquid cannot spontaneously arise in an immobile region in space, nor can it spontaneously decay. This is obviously a strong assumption.

This constraint is conjectured to become effective roughly below T_{MCT} and to dominate the dynamical evolution close to T_g (Garrahan and Chandler, 2003). This is far from a trivial assumption since it implicitly uses the fact that there exists a temperature below which the material is nearly jammed, so that a description in terms of sparse mobility is valid. Thus, this approach cannot self-consistently capture the microscopic origin of the dynamical slowing down in supercooled liquids. Instead, it can possibly become an effective and useful description of structural relaxation occurring near the glass transition (Palmer *et al.*, 1984).

At present, it is still unclear whether this main assumption of mobility conservation is correct, only approximate, or whether it plays the central role suggested by the facilitation approach. An important point is the fact that a large number of theoretical models have been defined based solely on the idea of kinetic constraints. They are called “kinetically constrained models” (KCMs), and they all display a phenomenology which is strikingly consistent to the one described in Sec. II.A for molecular glass formers (Ritort and

Sollich, 2003). In the last decade or so, several KCMs have been defined and studied in detail. In turn, this large body of theoretical work produced new results and predictions and has thus also triggered more research on competing theories.

2. Kinetically constrained models

Over the last 25 years, KCMs have been central to the development of the facilitation approach to the glass transition.

The first example we present is the Kob-Andersen model (Kob and Andersen, 1993). Interestingly, this model is quite similar to the lattice glass models described in Sec. IV.B. The model is again an attempt to capture the physics of a hard-sphere system and the fact that dynamics becomes slow at high density because the environment of each particle is crowded. The Kob-Andersen model is a lattice gas, with occupation number n_i on each site i of a regular lattice. There is no interaction apart from the hard-core constraint, and the Hamiltonian is thus trivial:

$$H[\{n_i\}] = 0, \quad n_i = 0, 1. \quad (63)$$

Geometric frustration is introduced at the level of the kinetic rules that are defined as constrained local moves. Namely, a particle can jump to a nearest neighbor site only if (i) that site is empty, to satisfy the hard-core constraint; (ii) the sites occupied before and after the move have fewer than m neighbors, with m being an adjustable parameter. Kob and Andersen studied the case $m = 4$ for a cubic lattice in $d = 3$ ($m = 6$ corresponds to the unconstrained lattice gas), and the model displays glassy dynamics at large density (Kob and Andersen, 1993). Such kinetically constrained lattice gases have been studied in various spatial dimensions, for different values of m , for different constraints, or even different lattice geometries (Ritort and Sollich, 2003). They can be thought of as models capturing the idea of a cage effect in a strict sense, since a particle with a dense neighbor shell cannot diffuse. Dynamic facilitation is thus a direct consequence of steric effects in this model (Chaudhuri *et al.*, 2008).

The crucial difference with lattice glass models is that here all configurations are allowed by the Hamiltonian, but their kinetics depends on geometry, while in lattice glass models kinetic rules ignore the geometry but not all configurations are allowed (Biroli and Mézard, 2001). This is actually a major difference: KCMs assume that geometrical constraints act at the level of kinetic rules with no thermodynamic counterpart and no reference to the interactions which are responsible for them.

In this lattice gas picture, the connection with glass formers is not obvious because density, rather than temperature, controls the dynamics. Thermal models with similar features can, in fact, be defined by focusing on holes rather than particles. This points toward a model with a small concentration of mobile regions, which move by creation and annihilation. This is actually reminiscent of Glarum “defects” theory where the relaxation proceeds via simple diffusion of a low concentration of independent defects (Glarum, 1960). Using the conjugated ideas of kinetic constraints, facilitation, and rare defects, Fredrickson and Andersen (1984) defined and studied a family of kinetic Ising models for the glass transition. This last article is a seminal paper that opened a whole

new research avenue, making possible the study of phenomena associated with the glass transition via simple kinetic models. The Fredrickson-Andersen models consist of an assembly of noninteracting defects or spins,

$$H[\{n_i\}] = J \sum_{i=1}^N n_i, \quad n_i = 0, 1, \quad (64)$$

where J is an energy scale for creation of mobility, and $n_i = 1$ represent the mobility state at site i , whose averaged concentration becomes exponentially small at low temperature $\langle n_i \rangle \approx \exp(-J/T)$. As for the Kob-Andersen lattice gas, the nontrivial ingredient lies in the chosen rates for the transition between states. The kinetic rules stipulate that a transition at site i can happen with a usual Glauber rate, but only if site i is surrounded by at least k defects ($k = 0$ corresponds to the unconstrained limit).

As for kinetically constrained lattice gases, these models have been studied in different spatial dimensions, on different lattices, and using a number of distinct definitions of the kinetic rules, yielding a large number of possible glassy behaviors (Ritort and Sollich, 2003; Léonard *et al.*, 2007). The similarity between those spin-facilitated models and the kinetically constrained lattice gases is striking. Altogether, they now form a large family of models generically called KCMs.

These models can be divided into several classes. “Noncooperative” models, such as the Fredrickson-Andersen model for $k = 1$ (the least constrained model) display Arrhenius dynamic slowing down and are thus reminiscent of strong glass formers. They are well described by simple diffusion of point mobility defects. “Cooperative” models display a super-Arrhenius dependence of the structural relaxation time. This is the case for the Fredrickson-Andersen model with a stronger kinetic constraint, $k > 1$. Another example is the “East” model where the kinetic constraint with $k = 1$ has a directional character: Only excited sites to the left in each space dimension can facilitate the dynamics (Jäckle and Eisinger, 1991; Berthier and Garrahan, 2005), which can be rationalized on the basis that displacements in liquids have a vectorial character that could extend to facilitation (Garrahan and Chandler, 2003). For an overwhelming majority of KCMs, relaxation times diverge only in the limit of zero temperature, as even one single defect can diffuse and relax the entire system (at least in the simplest models), and the defect concentration vanishes only at $T = 0$. However, KCMs can also be defined with kinetic rules and geometries for which the existence of a finite-temperature glass transition can be established (Toninelli *et al.*, 2006).

We remark that the facilitation approach, and, in particular, KCMs, encode in a new and more microscopic way the older, but well-known, concept of free volume. Free-volume models are among the most widely used models to analyze experimental data, especially in polymeric systems. They have been reviewed before (Cohen and Grest, 1982; Debenedetti, 1996). Here, the main idea is that dynamic slowing down occurs because the “free volume to move” available to each particle v_f vanishes at some temperature T_0 as $v_f \approx \alpha(T - T_0)$, a relation which connects volume to temperature. Statistical arguments then relate relaxation time scales to free volume assuming that movement is possible if locally there is

“enough” free volume available, more than a typical value v_0 . A VFT divergence is then predicted:

$$\frac{\tau_\alpha}{\tau_0} \sim \exp\left(\gamma \frac{v_0}{v_f}\right) \sim \exp\left(\frac{\gamma v_0/\alpha}{[T - T_0]^\mu}\right), \quad (65)$$

where γ is a numerical factor and $\mu = 1$. Predictions such as Eq. (65) are used to justify the wide use of free-volume approaches, despite the many (justified) criticisms that have been raised. The physics at work is obviously strongly reminiscent of the above description of the Kob-Andersen kinetically constrained lattice gas. In fact, the analogy is even semiquantitative in some cases, since cooperative KCMs with a finite-temperature glass transition have been shown rigorously to be characterized by divergence of the relaxation time as in Eq. (65), albeit with a value of μ different from 1 (Toninelli and Biroli, 2008).

As with free-volume approaches, it is not exactly clear what is meant by “mobility defects” within KCMs in terms of the original interacting system they seek to describe, nor how kinetic constraint can truly emerge from the unconstrained dynamics of a many-body system. Good news on this front is that at least a proof of principle that kinetic rules can emerge has been obtained (Garrahan, 2002). Several examples are available but here we mention only the simple case of the bidimensional plaquette model defined by a Hamiltonian of a p -spin type, but in two dimensions on a square lattice of linear size L ,

$$H = -J \sum_{i=1}^{L-1} \sum_{j=1}^{L-1} S_{i,j} S_{i+1,j} S_{i,j+1} S_{i+1,j+1}, \quad (66)$$

where $S_{i,j} = \pm 1$ is an Ising variable lying at node (i, j) of the lattice. Contrary to KCMs, the Hamiltonian in Eq. (66) contains genuine interactions, which are no less (or no more) physical than p -spin models discussed in Sec. IV.B to which it actually strongly resembles. Interestingly the dynamics of this system is (trivially) mapped onto that of a KCM by analyzing its behavior in terms of plaquette variables $p_{i,j} \equiv S_{i,j} S_{i+1,j} S_{i,j+1} S_{i+1,j+1}$ such that the Hamiltonian becomes a noninteracting one $H = -J \sum_{i,j} p_{i,j}$ as in Eq. (64). More interestingly, the analogy also applies to the dynamics (Garrahan, 2002). The fundamental moves are spin flips, but when a single spin is flipped the states of the four plaquettes surrounding that spin change. Considering the different types of moves, one quickly realizes that excited plaquettes $p_{i,j} = +1$ act as sources of mobility, since the energetic barriers to spin flips are smaller in those regions. This observation allows one to identify the excited plaquettes as defects, by analogy with KCMs. Similarly to KCMs, also, spatially heterogeneous dynamics, diverging length scales accompanying diverging time scales and scaling behavior sufficiently close to $T = 0$ (see below) can be established by further analysis (Jack *et al.*, 2005), providing a simple, but concrete example, of how an interacting many-body system might effectively behave as a model with kinetic constraints. These types of plaquette models, and other similar spin models, were originally introduced (Sethna *et al.*, 1991; Lipowski *et al.*, 2000) to show how ultraslow glassy dynamics can emerge because of growing free-energy barriers.

3. Diffusing defects, excitation lines, and space-time bubbles

Research on the facilitation approach to glassy dynamics has mainly consisted of the analysis of the physical behavior of KCMs. Motivation for this work largely stems from the observation that KCMs behave, at the phenomenological level, much as real glass formers, as noted long ago for both thermal models (Fredrickson and Andersen, 1984, 1985; Fredrickson, 1986; Fredrickson and Brawer, 1986) and constrained lattice gases (Kob and Andersen, 1993; Jäckle and Krönig, 1994; Kurchan *et al.*, 1997). Actually, theoretical research on dynamical heterogeneity was partly sparked by the numerical observations that KCMs display strong spatial fluctuations of the local relaxation rate (Butler and Harrowell, 1991a, 1991b; Harrowell, 1993). Therefore, KCMs provide a simplified context to understand glassy phenomena in detail or at least to study one of their possible explanations.

In the following we shall not review all the different models and their physical behavior, as this was done thoroughly by Ritort and Sollich (2003). Neither shall we review in detail the dynamic facilitation approach as a theory of the glass transition, as this is the object of another recent review (Chandler and Garrahan, 2010). Instead, we present a simple physical picture, common to all KCMs, which is helpful in grasping the main physical behavior of KCMs and, therefore, the main predictions and limitations of the facilitation approach.

A common feature of all KCMs is that their relaxation can be accurately described in terms of the motion of sparse defects. In the simplest cases such as the noncooperative Fredrickson-Andersen model, these defects diffuse, but they might also undergo subdiffusive motion in some cases, such as in the directional East model. In cooperative models, such as the Kob-Andersen lattice gas or the Fredrickson-Andersen model with $k > 1$, defects do not coincide with mobile sites, but can be formed by extended clusters moving in a cooperative manner.

Since local relaxation at a given site occurs when it is visited by one such defect, explaining structural relaxation is equivalent to explaining the defect dynamics. To make the discussion more concrete, we explain how this defect description emerges for the simple case of the noncooperative Fredrickson-Andersen model with $k = 1$. In that case, a spin n_i can flip only if it has at least one spin $n_j = 1$ among its nearest neighbors. At low temperature, defects diffuse in an activated manner. Typically an isolated defect facilitates the excitation of one of the neighboring sites with rate $\exp(-J/T)$, and moves there with probability $1/2$. Schematically, one gets

$$0100 \rightarrow 0110 \rightarrow 0010 \rightarrow \dots \quad (67)$$

Overall, defects perform random walks with a diffusion coefficient $D \sim \exp(-J/T)$. Defects can also annihilate when they meet and be created from an existing defect. A representation of this diffusion, branching, and annihilation process is shown in Fig. 16 for the one-dimensional case. In particular, the central feature of the facilitation approach, namely, that a defect cannot be created out of a completely immobile region, is obvious from this figure, in particular, at low temperature where defects are sparse.

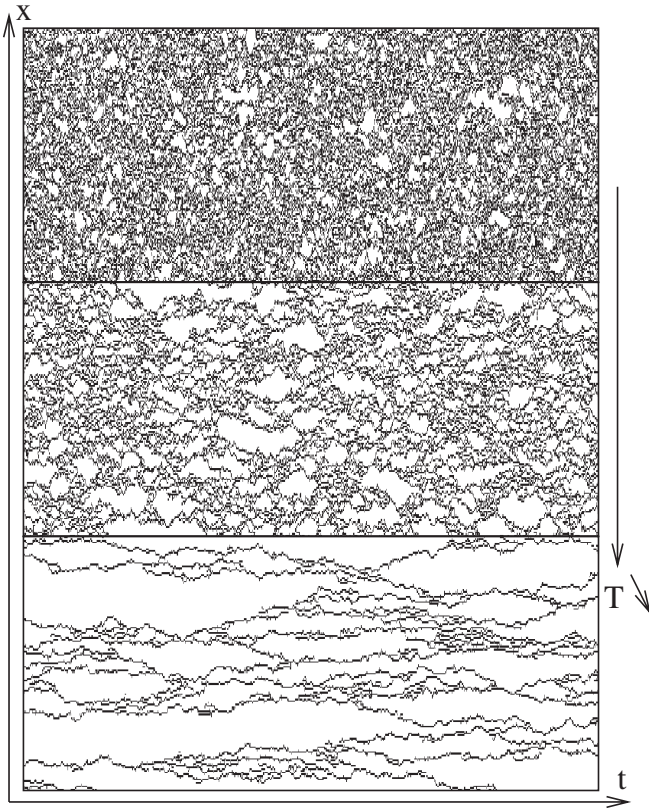


FIG. 16. Space-time representation of the dynamics of mobility defects in the noncooperative Fredrickson-Andersen model with $k = 1$ in $d = 1$. Dynamic facilitation, imposed by the kinetic constraints, implies the existence of excitation lines which can branch and coalesce. The physics changes from a homogeneous description at high temperatures to a strongly spatially and temporally heterogeneous dynamics at low temperatures when mobility is sparse. From Berthier and Garrahan, 2003b.

An approximate but good description of KCMs consists of focusing on sparse, possibly extended, defects of density ρ_d , which diffuse anomalously with an exponent z and a generalized diffusion coefficient D which is temperature (or density) dependent (Toninelli *et al.*, 2005). The relaxation time of the system can then be easily obtained by computing the time over which a finite fraction of the system, say $1/2$, has been visited by at least one defect. The number of distinct sites visited by a given defect after a time t is by definition equal to $(Dt)^{d_F/z}$, where d_F is the fractal dimension of the walk (or the space dimensionality d when $d_F > d$). For a random walk in $d = 3$, one has $d_F = z = 2$, and therefore the number of sites visited per defect is simply equal to Dt . The relaxation time τ_α is then given by the equation $\rho_d(D\tau_\alpha)^{d_F/z} \simeq 1/2$. Both the defect density ρ_d and the diffusion coefficient vanish when decreasing the temperature with expressions that are model dependent. The relaxation times thus generically scale as

$$\tau_\alpha \propto \frac{1}{D} \rho_d^{z/d_F}. \quad (68)$$

In the case of the noncooperative Fredrickson-Andersen model discussed before ($k = 1$), one gets $\tau_\alpha \propto e^{2J/T}$ for $d > 1$ and $\tau_\alpha \propto e^{3J/T}$ in $d = 1$, i.e., an Arrhenius dependence

in all dimensions, similar to the one describing the viscosity of strong glass formers.

As expected, stronger temperature dependencies are obtained when kinetic constraints become more and more severe. For the directional East model, for instance, the energy barrier to relax a domain of the form $10 \cdots 01$ containing ℓ unexcited sites increases with ℓ since the leftmost defect must, in principle, facilitate all sites to its right. The minimal energy barrier needed for this process to occur scales as $E(\ell) \sim \log(\ell)$ and corresponds to a “hierarchical” path (Sollich and Evans, 1999). Since the typical distance between defects at equilibrium is $\ell_{\text{eq}} \sim \exp(J/T)$, one finds that $\log \tau_\alpha \sim E(\ell_{\text{eq}})/T \sim 1/T^2$, which is reminiscent of the Bässler law in Eq. (3). Even more fragile behavior is obtained for cooperative Fredrickson-Andersen models and Kob-Andersen lattice gases. For instance, for the well-studied Fredrickson-Andersen model in $d = 2$ with $k = 2$ which is the original model studied by Fredrickson and Andersen (1984), the relaxation time increases as $\tau_\alpha \sim \exp[\exp(c/T)]$, with c a numerical constant (Ritort and Sollich, 2003; Toninelli *et al.*, 2004). It is interesting to note that both dependencies found for the East and $k = d = 2$ Fredrickson-Andersen fragile models seem to describe the viscosity data obtained in real molecular liquids quite well (Hecksher *et al.*, 2008; Elmatad *et al.*, 2009). Actually, it has been argued that in order to apply the East model results to real liquids, one should use a scaling $\ell_{\text{eq}} \sim \exp(J/T - J/T_{\text{on}})$. This leads to a modified version of the Bässler law, which has been discussed and tested by Elmatad *et al.* (2009), 2010).

The space-time representation of the defect diffusion dynamics in Fig. 16 can be understood as an alternative, illustrative way to represent the dynamical behavior of the system (Garrahan and Chandler, 2002; Chandler and Garrahan, 2010). To the extent that dynamics is facilitated, mobility cannot disappear except if it is close to another mobile region. Furthermore, the defect dynamics implies that mobile regions organize along “excitation lines,” when represented in a space-time phase diagram. Hence, in a system with facilitated dynamics space-time is structured with strings of excitations that are directed in time, can coalesce or branch but never die, nor appear spontaneously. In between these lines lie large inactive regions, also called “bubbles.” The larger the spatial extension of the bubbles, the longer it takes an excitation line to relax the corresponding domain, and the slower is the structural relaxation. Thus, all dynamical properties can, in fact, be understood characterizing the space-time structure of bubbles and excitations lines. This is fully equivalent to the defect dynamics laid out above.

To summarize, KCMs can be thought of as defect models, where defects can be nontrivial, extended objects possibly with nontrivial subdiffusive or cooperative dynamics. When temperature decreases both the density of defects becomes small and their dynamics slows down dramatically, implying that the overall relaxation slows down in an activated, possibly super-Arrhenius manner. Additionally, space-time representations, as shown in Fig. 16, suggest the appearance when temperature decreases of large immobility domains with broadly distributed spatial and temporal extensions. When temperature decreases, these fluctuations are amplified and the corresponding time scales and length scales increase rapidly and diverge (for most KCMs) in the limit of zero

temperature (or unit density for lattice gases), which can thus be considered as a dynamic critical point (Whitelam *et al.*, 2004), as we now discuss.

4. Main predictions and results

Within the facilitation approach and, hence, KCMs, thermodynamic properties are trivial, and the interesting physics is in the dynamics. As a consequence, nontrivial predictions and results concern the dynamical behavior, and, more precisely, dynamic heterogeneity, as was realized soon after their introduction (Harrowell, 1993; Franz *et al.*, 2002; Garrahan and Chandler, 2002). Remarkably, virtually all the aspects related to dynamic heterogeneity mentioned in Sec. III can be investigated and qualitatively or quantitatively rationalized in the language of KCMs.

Detailed numerical and analytical studies have indeed shown that in these systems, nonexponential relaxation patterns stem from a spatial, heterogeneous distribution of time scales, directly connected to a distribution of dynamic length scales (Garrahan and Chandler, 2002; Ritort and Sollich, 2003; Toninelli *et al.*, 2004; Whitelam *et al.*, 2005; Pan *et al.*, 2005; Jack *et al.*, 2006).

A decoupling phenomenon between the structural relaxation time and the self-diffusion coefficient naturally appears in KCMs and can be shown to be a direct, quantifiable, consequence of the dynamic heterogeneity (Jung *et al.*, 2004). In fact, two distinct time scales emerge in the facilitation and KCMs description which both characterize the dynamics. One is the persistence time t_p , which corresponds to the typical time a tracer particle has to wait to start moving, given an arbitrary start time for observation. The second time scale is the exchange time t_x , which is the typical time between elementary moves. The average values of t_p and $a^2/\langle t_x \rangle$ are, respectively, estimates of the relaxation time τ_α and the self-diffusion coefficient D , with a the typical size of particle jumps. As a consequence one finds $D\tau_\alpha \simeq \langle t_p \rangle / \langle t_x \rangle$. In some KCMs, this ratio increases substantially when decreasing the temperature; thus these models exhibit a substantial decoupling phenomenon.

This is due to the fact that bubbles in space-time typically persist for the time scale of structural relaxation, while particles diffuse faster by “surfing” on the excitation lines that surround these bubbles. Another way to understand the decoupling is to express $\langle t_p \rangle$ and $\langle t_x \rangle$ as distinct moments of the distribution of waiting time between jumps performed by a tracer particle, which do not coincide when the distribution broadens with decreasing temperatures (Tarjus and Kivelson, 1995; Hedges *et al.*, 2007; Heuer, 2008).

The above description of self-diffusion in fluctuating mobility fields such as shown in Fig. 16 has several nontrivial consequences such as, for instance, a strongly non-Fickian relation between time scales and length scales at distances smaller than a crossover length scale which grows when temperature decreases and decoupling increases (Berthier *et al.*, 2005), as observed in numerical simulations of supercooled liquids (Berthier, 2004).

Another useful aspect of KCMs is that multipoint susceptibilities and multipoint spatial correlation functions such as the ones defined in Eqs. (22) and (20) can be studied in greater detail than in molecular systems, to the point that

scaling relations between time scales, length scales, and dynamic susceptibilities can be established (Franz *et al.*, 2002; Whitelam *et al.*, 2004; Pan *et al.*, 2005; Toninelli *et al.*, 2005; Chandler *et al.*, 2006; Berthier *et al.*, 2007b).

The type of scaling behavior with the temperature or the density depends on the details of the model at hand, in particular, whether it has or does not have a transition. However, a unified qualitative description is still possible in terms of the defect motion description given in the previous section (Toninelli *et al.*, 2005). On small time scales compared to τ_α , all sites visited by the same defect are dynamically correlated. As a consequence, the dynamical correlation length $\xi_4(t)$ increases as $\xi_4(t) \sim (Dt)^{1/z}$ and the corresponding four-point susceptibility $\chi_4(t) \simeq \rho_d (Dt)^{2d_F/z}$, which is the square of the volume of the regions visited by the same defect times the defect density. When t is comparable to the relaxation time τ_α , one finds $\chi_4(\tau_\alpha) \simeq 1/\rho_d$ which, as expected, increases when decreasing the temperature and increasing the density. On longer time scales, $\chi_4(\gg \tau_\alpha)$ decreases with t , because a site can now be visited by more than one defect, and dynamical correlations are progressively erased. As a direct example of this behavior, we show in Fig. 17 the time and temperature evolution of $\chi_4(t)$ for the noncooperative ($k = 1$) Fredrickson-Andersen model in three dimensions (Whitelam *et al.*, 2005), where the above scaling relations hold (Toninelli *et al.*, 2005).

In summary, relaxation time scales and dynamic length scales are found to diverge with well-defined critical laws (Whitelam *et al.*, 2004; Jack *et al.*, 2006), which, however, are model dependent. The discovery of such “dynamic criticality” has proven useful, since it actually triggered several works aimed at computing similar laws within competing theories. It also implies the possibility that some universal behavior might truly emerge in the physics of supercooled liquids, precisely of the type observed numerically in Fig. 10, and experimentally in Fig. 11.

As suggested by the space-time representations shown in Fig. 16, dynamical heterogeneity studies are mostly

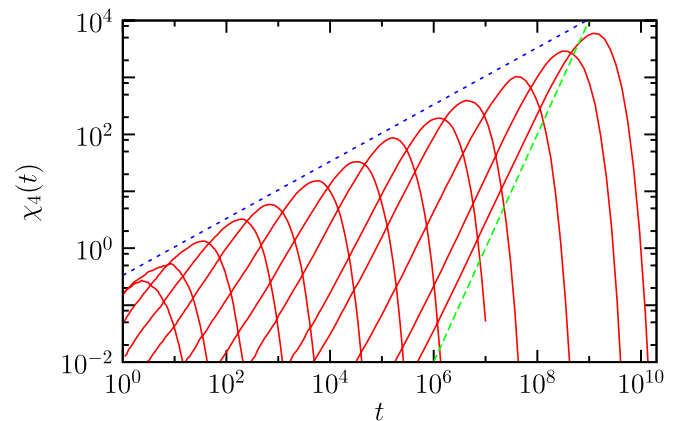


FIG. 17 (color online). Time evolution of $\chi_4(t)$ for different temperatures for the noncooperative ($k = 1$) Fredrickson-Andersen model in three dimensions. Temperature decreases from left to right. The peak height increases at low T as $\chi_4(\tau_\alpha) \sim 1/\rho_d \sim \exp(J/T)$, while the relaxation time scales as $\tau_\alpha \sim \exp(2J/T)$, such that $\chi_4(\tau_\alpha) \sim \tau_\alpha^{1/2}$, as shown with a dotted line, while the approach to the peak is diffusive $\chi_4(t) \sim t^2$ (dashed line).

concerned with distributions of dynamical quantities, most often through their variance; recall the definition of χ_4 in Eq. (22). However, there is useful information also in the overall shape of the distributions. It seems reasonable that regions where the correlation function is large possess rather stable structure at the molecular level, while regions where it is small correspond to relatively unstable local structure. To identify such trajectories over an observation time t_{obs} , it is useful to define a measure of dynamical activity, for example (Hedges *et al.*, 2009),

$$K(N, t_{\text{obs}}) = \sum_{i=1}^N \sum_{j=1}^{t_{\text{obs}}/\Delta t} |\mathbf{r}_i(t_j) - \mathbf{r}_i(t_j - \Delta t)|^2, \quad (69)$$

where $\mathbf{r}_i(t)$ is the position of particle i at time t and the $t_j = j\Delta t$ are equally spaced times. For large N and t_{obs} , the distribution of K becomes sharply peaked about its average $\langle K \rangle$. In general, for large N and t_{obs} , one expects the distribution of K to have the form

$$P(K) \simeq \exp[-Nt_{\text{obs}}f(K/Nt_{\text{obs}})], \quad (70)$$

where the function $f(k)$ resembles a free-energy density.

In some KCMs (Merolle *et al.*, 2005), the distribution $P(K)$ has a characteristic shape, skewed toward small activity, with an apparently exponential tail. Further, on estimating $f(k)$ from this plot, there is a range of K over which $f(k)$ is nonconvex [that is, $f''(K) < 0$]. Within such a framework, nonconvexity of $f(K)$ has a direct interpretation as a “dynamical phase transition” in the system (Garrahan *et al.*, 2009). The existence of these phase transitions has been proven in simple models (Garrahan *et al.*, 2009), and numerical results for Lennard-Jones model liquids are also consistent with the existence of such a transition (Hedges *et al.*, 2009), which also exists in mean-field models where RFOT theory of Sec. IV.B applies (Jack and Garrahan, 2010). This leads to the hypothesis in which the nature of the dynamically heterogeneous fluid state could be generically interpreted in terms of coexistence between an active liquid and inactive ideal glass states, which seems to suggest intriguing connections to the mean-field picture based on the existence of numerous metastable states.

5. Current status of the facilitation approach

We conveyed the idea that despite the large number of distinct KCMs capturing the idea of dynamic facilitation, these models are characterized by a common physics, based on the propagation of some rare defects. Quantitatively, however, different models behave quite differently. The variety of physical outcomes obtained from the variety of models and kinetic rules has proven useful, as it has widened the spectrum of all the possible behaviors that real material could display. Thus, in the recent effort aimed at devising tools to quantify and understand dynamic heterogeneity in glass formers, as described in Sec. III, KCMs have played a leading role.

As far as building a unique theory for the glass transition is concerned, this variety is also a source of worry since it is difficult to obtain a unified description: Many models do not have a glass transition at finite temperature, but some do. Some models seem to describe strong glass formers, while others are better for fragile materials. Quantitative results

about the behavior of high-order correlation functions or decoupling phenomena quite strongly depend on the chosen model; the value of an upper critical dimension qualifying the strength of fluctuations is also different from one model to another. At the moment, it is not clear whether or not one of these models should be preferred to the others, since there exists no systematic coarse-graining procedure to represent a molecular model with continuous degrees of freedom in terms of a lattice model with no interactions and kinetic constraints (Vogel and Glotzer, 2004; Downton and Kennett, 2007). Thus, the choice of a “reference” model to fit real data is an ambiguous issue, which deserves more work.

It is interesting that the theoretical status of the dynamic facilitation approach is almost opposite to that of the RFOT theory, since there are several well-defined finite-dimensional theoretical models capturing the idea of dynamic facilitation which can be thoroughly understood, but none of them can be derived from (even approximate) microscopic calculations. By contrast, RFOT theory is supported by several microscopic approaches, but theory is not confirmed within the framework of finite-dimensional models. This comparison raises the following question: Is it possible to obtain more microscopic theoretical insights from the dynamic facilitation approach beyond qualitative or scaling considerations? This absence of a microscopic derivation or at least of some empirical procedure to back these ideas makes the approach prone to criticism.

The idea that all thermodynamic aspects are unimportant implies that the facilitation approach has little to say about the thermodynamic behavior of glass formers close to T_g . A possible coincidence between VFT and Kauzmann temperatures T_0 and T_K is not expected (except if they are both zero), nor can the dynamics be deeply connected to thermodynamics, as in Adam-Gibbs relations. Some view this as a major flaw (Biroli *et al.*, 2005), while within the KCM approach, one is forced to disregard the significance of thermodynamics (Chandler and Garrahan, 2005, 2010). This is certainly the point where KCMs and RFOT theory differ most evidently. Even though the dynamics of KCMs shares similarities with systems characterized with a complex energy landscape (Berthier and Garrahan, 2003a; Whitlam and Garrahan, 2004) and KCMs even show a MCT-like transition on Bethe lattices (Toninelli *et al.*, 2004; Sellitto *et al.*, 2005), their thermodynamical behaviors are widely different from RFOT theory, as was recently highlighted by Jack and Garrahan (2005). It will be interesting to follow how the facilitation approach will handle the recent surge of interest in the definition and measurements of *static* point-to-set correlations, which are nonexistent in KCMs in the defect formulation.

A second central assumption made in KCMs is that mobility can neither be spontaneously created nor destroyed unless adjacent regions are mobile, or, at least, that events violating this constraint are rare and become rarer when approaching the glass transition (Garrahan and Chandler, 2003; Elmatad *et al.*, 2010). Without these assumptions, KCMs become trivial models where death and birth rates for mobility ultimately control the dynamics, and the features described in previous sections become irrelevant. The fact that some degree of facilitation is present in the dynamics is reasonable and partially proven by numerical simulations

(Vogel and Glotzer, 2004; Downton and Kennett, 2007; Candelier *et al.*, 2010; Chandler and Garrahan, 2010). However, the facilitation assumption goes much farther and states that almost nothing else is possible and that rare events, violating the kinetic constraints, become rarer approaching T_g , so that the mobility is effectively nearly conserved. There are at present no data supporting this assumption. A recent experimental analysis of a granular system close to its glass transition actually suggests the opposite behavior, i.e., that mobility becomes less conserved and facilitation plays a decreasing role when the transition is approached (Candelier *et al.*, 2009). Certainly, this is an important issue to be addressed in the future in order to validate or disprove this theoretical approach to the glass transition. It would be interesting, in particular, to repeat the analysis of Candelier *et al.* (2009) in a model of supercooled liquid.

D. Geometric frustration, avoided criticality, and Coulomb frustrated theories

1. Physical picture and simple models

In all of the above models, “real space” was present in the sense that special attention was paid to different length scales characterizing the physics of the models that were discussed. However, apart from the “packing models” with hard-core interactions, no or little attention was paid to the geometric structure of local arrangements in molecular liquids close to a glass transition. This is generally justified using concepts such as “universality” or “simplicity,” meaning that one studies complex phenomena using simple models, a typical statistical mechanics perspective. However, important questions remain: What is the liquid structure within mosaic states? What distinguishes the local structure of different states? What is the geometric origin of the defects invoked in KCMs? Are they similar to defects (disclinations, dislocations, vacancies, etc.) found in crystalline materials?

There exists a line of research which attempts to provide answers to these questions (Tarjus *et al.*, 2005). It makes heavy use of the concept of geometric frustration. Broadly speaking, frustration refers to the impossibility of simultaneously minimizing all the interaction terms in the energy function of the system (Toulouse, 1977). Frustration might arise from quenched disorder (as in the spin glass models described above), but liquids have no quenched randomness. In that case, frustration has a purely *geometric* origin. It is attributed to a competition between a short-range tendency to spatially extend a locally preferred order and global constraints that prevent the periodic tiling of space with this local structure.

This can be illustrated by considering once more the packing problem of spheres in three dimensions (Sadoc and Mosseri, 1999). In that case, the locally preferred cluster of spheres is an icosahedron. However, the fivefold rotational symmetry characteristic of icosahedral order is not compatible with translational symmetry, and formation of a periodic icosahedral crystal is impossible (Frank, 1952). By contrast, disks on a two-dimensional plane are arranged locally as a regular hexagon, with one atom at the center and six neighbors at the vertices. If periodically repeated, this structure can

then form a triangular lattice that can fill space with no influence of geometric frustration.

The geometric frustration that affects spheres in three-dimensional Euclidean space can be relieved in curved space (Nelson, 2002). This corresponds, for instance, to studying particles on a sphere, or on the hyperbolic plane (a surface of constant negative curvature). Indeed by changing the metrics and topology of the underlying space it may become possible for the local order to extend over larger length scales. One can fruitfully exploit this idea in two ways. The first possibility is to start from a curved space carefully chosen such that geometric frustration is entirely absent for the considered system. The structure of the system minimizing the energy can then be determined and serves as a useful reference state. Changing the space curvature to go back to the physical Euclidean space then generates topological defects that disturb the initially perfect order. Detailed analysis along those lines showed, in particular, that a sphere packing possesses, in Euclidian space, topological defects (mainly disclination lines), as the result of forcing the ideal icosahedral ordering into a flat space. Thus, the relevant topological defects in that case are one-dimensional objects forming a disordered network, presumably having a complex dynamics. Nelson and co-workers developed a solid theoretical framework based on this picture to suggest that the slowing down of supercooled liquids is due to the slow wandering of these topological defects (Nelson, 2002), but their treatment remains so complex that few quantitative, explicit results have been obtained, in particular, concerning the dynamical behavior of the frustrated systems (Nelson, 1983).

The picture of sphere packing disrupted by geometric frustration is appealing and provides handles to attack the problem of glass formation from an atomistic perspective. Furthermore, the idea of uniform frustration can be incorporated into simple models allowing for a more abstract approach in terms of simple statistical mechanics ideas and scaling type of approaches (Tarjus *et al.*, 2005). To build such models, one must be able to identify, and then capture the physics of geometric frustration. Using the concept of an ideal long-range ordering in a system of size L in a curved space, which is then strained back in the three-dimensional Euclidian space, Kivelson *et al.* (1995) suggested that the corresponding free energy should scale as

$$F(L, T) = \sigma(T)L^2 - \phi(T)L^3 + s(T)L^5. \quad (71)$$

In this equation, the first two terms express the tendency of growing local preferred order and they represent, respectively, the energy cost of having an interface between two phases and a bulk free-energy gain inside the domain. It is assumed that without the last term long-range order sets in at $T = T^*$. Geometric frustration is encoded in the third term which represents the strain free energy resulting from the frustration. This last term is responsible for the fact that the transition is avoided. The remarkable feature of Eq. (71) is the superextensive scaling of the energy cost due to frustration which opposes the growth of local order; in dimension d it would scale as L^{2+d} . As a consequence, when L is large, the last term becomes dominant and thus prevents the extension of order to the entire space. Thus, the system is broken up in a patchwork of locally ordered domains separated by domains

made of topological defects, hence the name of frustration-limited domains (FLD). Furthermore, minimizing the free energy per unit volume F/L^3 , one finds that the characteristic linear size L^* of the patches scales as $(\sigma/s)^{1/3}$. Since σ increases below T^* , one finds that the characteristic size of the patchwork increases below T^* too.

Turning to the dynamics, Kivelson *et al.* further argued that dynamics of the system involves restructuring of these domains in a thermally activated manner, using arguments similar to the ones used within the mosaic picture of RFOT theory. The typical energy barrier is given by a high-temperature constant plus a second term $\sigma(L^*)^2$, increasing below T^* , which means that the assumption $\psi = 2$ is made from the beginning; see Eq. (61). Using more refined but still heuristic arguments, Kivelson *et al.* argued that L^* grows as $(1 - T/T^*)^\nu/K^{1/2}$, where K is an adimensional parameter measuring the strength of frustration, and ν is the exponent governing the growth of the correlation length of the unfrustrated transition ($K = 0$). The corresponding prediction for the energy barrier is

$$\Delta(T < T^*) = \Delta_{>} + \frac{AT^*}{K} \left(1 - \frac{T}{T^*}\right)^{4\nu}, \quad (72)$$

where $\Delta_{>}$ is the high-temperature value of the barrier and A is a positive constant. Furthermore, it has also been argued that barrier fluctuations lead to typical glassy features such as a broad distribution of relaxation times or spatially heterogeneous dynamics, which can thus be discussed in a phenomenological manner (Tarjus and Kivelson, 1995). We refer the reader to Viot *et al.* (2000) for more details on these aspects. An important prediction obtained from scaling considerations is the variation of the glass fragility with frustration: In this approach, larger frustration means smaller domain sizes, and therefore less collective relaxation, yielding smaller fragility.

A complementary route consists of the analysis of relatively simple, finite-dimensional statistical models that supposedly retain the basic physical elements of Eq. (71). We consider first an interacting spin model, where the magnetization is meant to represent the “preferred local order,” nearest neighbor ferromagnetic interactions the tendency to local ordering, and longer-ranged antiferromagnetic interactions the opposite effect of the frustration. The following Hamiltonian possesses, in three dimensions, these minimal ingredients:

$$H = - \sum_{\langle i,j \rangle} \mathbf{S}_i \cdot \mathbf{S}_j + Q \sum_{i \neq j} \frac{\mathbf{S}_i \cdot \mathbf{S}_j}{|\mathbf{x}_i - \mathbf{x}_j|}, \quad (73)$$

where the spin \mathbf{S}_i occupies the site i at position \mathbf{x}_i . It can be shown that the long-range Coulombic interaction plays a role analogous to the superextensive free energy in Eq. (71). Of course, such Coulomb frustrated spin models can be for Ising or multicomponent spins, for hard or soft spins, or generalized to different spatial dimensions (Tarjus *et al.*, 2005). For theoretical studies it is convenient to study field-theoretical versions of the Hamiltonian (73):

$$H = \frac{1}{2} \int d^d x \left[r_0 \phi(\mathbf{x})^2 + [\nabla \phi(\mathbf{x})]^2 + \frac{u}{2} \phi(\mathbf{x})^4 \right] + \frac{Q}{8\pi} \int d^d x \int d^d x' \frac{\phi(\mathbf{x}) \phi(\mathbf{x}')}{|\mathbf{x} - \mathbf{x}'|}, \quad (74)$$

where the ferromagnetic and Coulombic terms are easily recognized, and the magnetization $\phi(\mathbf{x})$ is now a field.

It is interesting to note that the competition of interactions acting at different length scales, in fact, describes a larger body of problems, including the physics of diblock copolymers, magnetic multilayer compounds, Rayleigh-Bénard convection, doped Mott insulators, etc. A well-studied, related field theory is given by

$$H = \int d^d x \left[\frac{1}{2} \phi(\mathbf{x}) [r_0 + k_0^{-2} (\nabla^2 + k_0^2)^2] \phi(\mathbf{x}) + \frac{u}{4} \phi(\mathbf{x})^4 \right]. \quad (75)$$

Although this field theory was mainly considered from the point of view of diblock copolymers (Leibler, 1980) and Rayleigh-Bénard convection (Swift and Hohenberg, 1977), it was explicitly considered in the context of the glass problem by Geissler and Reichman (2003), Schmalian *et al.* (2003), and Geissler and Reichman (2004). Dimensional analysis shows that, in that case, the strength of frustration is related to k_0 through $k_0 \sim Q^{1/4}$.

This family of statistical models yields a rich physical behavior, with a complex phase diagram and dynamical behavior. In the absence of frustration $Q = 0$, they generally undergo a second-order phase transition from a paramagnetic to a ferromagnetic phase, which should be viewed, in this context, as the analog of the ordering transition occurring in the curved space relieving the geometric frustration of the sphere packing. That transition occurs at some finite temperature $T_c(Q = 0) = T^*$. The presence of frustration $Q > 0$ generally has dramatic effects whose details depend, however, on the studied model (Chayes *et al.*, 1996; Nussinov *et al.*, 1999). The transition can be entirely suppressed $T_c(Q > 0) = 0$ or severely depressed as soon as $Q > 0$ yielding a genuine discontinuity when $Q \rightarrow 0$. By decreasing T at small but finite Q , the system gets close to, but narrowly avoids the critical point at T^* . This situation occurs, for instance, in the $O(N \rightarrow \infty)$ and spherical versions of the model. In the more canonical Ising case, the situation is different since the second-order transition occurring for $Q = 0$ becomes first order at finite Q , but there is no discontinuity of the transition temperature as $Q \rightarrow 0$ (Brazovskii, 1975). At finite Q , the ordered phase is a spatially modulated phase (stripes in $d = 2$, lamellae in $d = 3$, etc.). Interestingly, the limit of stability of the paramagnetic phase (the spinodal) is lowered down to $T = 0$, and it is thus (in principle) possible to supercool the first-order transition and study the disordered phase down to low temperatures.

In all cases, therefore, there exists a temperature regime below the avoided critical point $T < T^*$, where the system is disordered and the dynamics is potentially affected by the presence of the frustration. Detailed Monte Carlo studies show that, for a given frustration strength Q , the dynamics slows down considerably when T decreases below T^* (Grousson *et al.*, 2001, 2002; Tarjus *et al.*, 2005). Grousson *et al.* quantified dynamics using spin-spin autocorrelation functions $C(t) = \langle \mathbf{S}_i(t) \cdot \mathbf{S}_i(0) \rangle$ in a variety of models (Ising, 5-state spins, and XY models) in three dimensions. They showed that the time decay of $C(t)$ gets nonexponential at low T and extracts a relaxation time scale that shows

activated, super-Arrhenius behavior. Remarkably, they also found that the fragility decreases when frustration increases, in agreement with the scaling approach of Kivelson *et al.* (1995), and simulations of Lennard-Jones models on the hyperbolic plane (Sausset *et al.*, 2008), suggesting that Coulomb frustrated spin models do indeed capture an essential part of the physical behavior of molecular glass formers.

This view was contradicted in more recent work (Geissler and Reichman, 2004), where numerical simulations of the Langevin dynamics of the field theory of Eq. (75) were reported. The numerical analysis yields results for spin auto-correlation functions $C(t)$ in agreement with those of Grousson *et al.* However, Geissler and Reichman also measured the time decay of fluctuations of the Fourier components of the field $C_{\mathbf{k}}(t) = \langle \phi(\mathbf{k}, t) \phi(-\mathbf{k}, 0) \rangle$ and found exponential decay for all Fourier modes $C_{\mathbf{k}}(t) \sim \exp[-t/\tau(k)]$. Therefore, they interpreted the stretched exponential relaxation reported by Grousson *et al.* as being the result of a trivial superposition effect $C(t) \propto \int d^d k C_{\mathbf{k}}(t)$. Even more striking was their finding that the relaxation times $\tau(k)$ were accurately predicted by a simple dynamical Hartree approximation mirroring the classic static treatment of the field theory (75) in Brazovskii (1975). This finding implies that the dynamical slowing down detected numerically results from the strong temperature dependence of static correlations which will eventually yield the system to undergo a first-order transition toward a modulated phase. This scenario bears little resemblance with the physics of supercooled liquids, where dynamics is not obviously driven by simple static correlations, as we emphasized several times in this paper.

2. Current status of the frustration-limited domains theory

We believe that the generic idea of geometric frustration is an appealing one, because it directly addresses the physics in terms of the real space at the molecular level. Moreover, it seems to yield quite naturally the idea that the system organizes itself, at low temperature and finite frustration level into some mosaic of domains corresponding to some local order whose size increases, but does not diverge, when T decreases. Tarjus, Kivelson, and co-workers clearly demonstrate that such an organization of supercooled liquids into mesoscopic domains allows one to understand most of the fundamental phenomena occurring in glass formers (Tarjus *et al.*, 2005). Our use of the word mosaic, as in RFOT theory, is not accidental. It was demonstrated in several works (Schmalian and Wolynes, 2000; Westfahl, Jr. *et al.*, 2001; Nussinov, 2004) that, when treated as systems with one step of replica symmetry breaking as discussed in Sec. IV.B.6, Coulomb frustrated systems such as in Eq. (74) undergo a Kauzmann transition similar to the one found in mean-field spin glasses. This is remarkable and suggests that the two theories may not be so different as they appear at first sight. The presence of structured domains also connects to ideas, such as cooperativity, dynamic heterogeneity, and spatial fluctuations, that directly explain, at least qualitatively, non-exponential relaxation, decoupling phenomena, or super-Arrhenius increase of the viscosity. The variation of fragility with the strength of the geometric frustration is perhaps the

most striking and original prediction stemming from this approach.

As for the RFOT mosaic picture, direct confirmations of this scenario from molecular simulations are difficult to obtain. Two independent routes have been followed recently. On the one hand, there have been studies focusing on the role of locally preferred structures. The identification of the locally preferred structure is, in general, quite difficult (Mossa and Tarjus, 2006), except when it can be linked to formation of local icosahedral order. Coslovich and Pastore (2007) found by numerical simulations of several models of glass-forming liquids that the increase of icosahedral order upon supercooling is more rapid and more pronounced for liquids characterized by a higher fragility. This success of the theory is tempered by recent simulations (Tanaka *et al.*, 2010) that suggest instead using different model systems, including three-dimensional polydisperse hard spheres, that the increasing local order is the hexagonal bond orientational order (characteristic of the crystal state) and not the icosahedral one. In yet another recent paper (Pedersen *et al.*, 2010), local order is again linked with slow structural relaxation but the interplay between local order and frustrated crystallization appears much more complicated than originally surmised in the frustration-limited domain approach. Thus, we are still far from understanding whether the basic content of this approach is wrong, correct, or too simplistic to describe supercooled liquids, and more work is needed to resolve this issue.

The other route that has been followed consisted of analyzing a situation similar to the one FLD advocates to happen for glass formers, such as a two-dimensional monoatomic Lennard-Jones system on the hyperbolic plane (Sausset and Tarjus, 2007, 2008; Sausset *et al.*, 2008). The hyperbolic plane is a two-dimensional surface of constant *negative* curvature, and its relevance was suggested earlier by Nelson and co-workers (Rubinstein and Nelson, 1983), but these numerical studies are technically not straightforward (Sausset and Tarjus, 2007). In the hyperbolic plane, the hexagonal crystal order is frustrated. In this setting the crystal order represents *mutatis mutandis* the locally preferred glass order that is conjectured to be frustrated for three-dimensional glass formers. This provides a concrete example of a particle model characterized by an avoided phase transition. Furthermore, by changing the curvature of the space one can test the predictions on the fragility dependence on frustration, which is related to the curvature of the plane. Sausset *et al.* confirmed numerically that by curving space, they can prevent crystal ordering, as expected, and that the low-temperature dynamical behavior of the liquid they obtain is sluggish and has a behavior similar to glass formers: Time-correlation functions decay in a two-step manner with a final decay which is not exponential, the dynamics is spatially heterogeneous, and decoupling occurs (Sausset and Tarjus, 2008). Interestingly, they also found that the fragility of the glass formers they obtained decreases when frustration grows (Sausset *et al.*, 2008). The physical explanation is that increasing the frustration also increases the density of topological defects, so that the putative collective behavior responsible for super-Arrhenius relaxation at small frustration becomes shorter ranged when frustration increases.

In conclusion, this approach to the glass transition is based on an appealing real space description. As others, it is compatible with several experimental results, and it has passed nontrivial benchmark tests. A possible criticism, which we also formulated in the case of the facilitation approach, is that no quantitative or microscopic results beyond scaling have been obtained, and it is not even clear how they could actually be derived. In fact, approximate analytical approaches to FLD, that could have provided quantitative predictions, have found back results consistent with RFOT theory. In order to further test the FLD approach, it would be interesting to have more detailed, quantitative, testable predictions regarding the behavior of thermodynamic (e.g., specific heat) and dynamic (e.g., four-point dynamic susceptibility) observables from this perspective; see [Sausset and Tarjus \(2010\)](#) for recent work in this direction.

V. OFF-EQUILIBRIUM DYNAMICS: AGING AND RHEOLOGY

A. Why aging? Phenomenology and simple models

We have dedicated most of the above discussion to physics taking place when approaching the glass transition at thermal equilibrium. We discussed a rich phenomenology and serious challenges for both our numerical and analytical capabilities to account for these phenomena. Most people, however, focus on the properties of glasses, i.e., on temperatures below the glass transition, so deep in the glass phase that the material seems to be frozen forever in an arrested amorphous state, endowed with enough mechanical stability for a glass to retain, say, the liquid it contains. One could think that in this state of matter the dynamical evolution is arrested. Is it true? The answer is clearly “no.” There is still life (and physics) below the glass transition. We recall that for molecular glasses, T_g is defined as the temperature below which equilibrium relaxation is too slow to occur within a given experimental time scale. Much below T_g , therefore, the equilibrium relaxation time scale is so astronomically large that thermal equilibrium is out of reach. One enters, therefore, the realm of off-equilibrium dynamics. A full physical understanding of the nonequilibrium glassy state remains a central challenge ([Young, 1998](#); [Barrat et al., 2003](#)).

An immediate consequence of studying materials in a time window smaller than equilibrium relaxation time scales is that the system can, in principle, remember its complete history, a most unwanted experimental situation since all details of the experimental protocol may then matter. The simplest protocol to study aging phenomena in the glass phase is quite brutal ([Struik, 1978](#)): Take a system equilibrated above the glass transition and suddenly quench it to a low temperature. The system then slowly attempts to reach thermal equilibrium, even though it has no hope to ever get there. Aging means that the system never forgets the time t_w spent in the low-temperature phase, its “age,” and that any measurement started at time t_w might have an outcome that explicitly depends on the value of t_w , unlike the situation at thermal equilibrium.

This implies, in particular, that any physical property of the glass becomes an age-dependent quantity in an aging protocol and more generally dependent on how the glass was prepared.

One can easily imagine using this property to tune mechanical or optical characteristics of a material by simply changing the way it is prepared, such as how fast it is cooled to the glassy state. A striking experimental realization of this idea was recently provided for organic glasses prepared in two different ways ([Swallen et al., 2007](#)). Ediger and collaborators compared the properties of glasses prepared in a canonical way (slow cooling of bulk samples) to the ones of samples grown using slow vapor deposition at about 50 K below the glass transition. They found that the latter samples are much more “stable,” in the sense that they behave as canonically prepared samples with a large effective aging time (40 years for some samples).

Coming back to the simplest situation of a sudden quench to low temperature, it is found that one-time physical observables such as density or energy evolve slowly with the age of the sample. In polymer glasses, for instance, the volume of the sample slowly decreases with t_w ([Struik, 1978](#)). Power laws with small exponents $v(t_w) \sim v_\infty + (t_0/t_w)^\alpha$ or even logarithmic relaxations $v(t_w) \sim v_0 - v_1 \log(t_w/t_0)$ are frequently reported. In some cases, the time evolution of these observables is so slow that aging behavior is not obviously revealed by their study and the system might superficially appear to have reached equilibrium.

In order to show that the system never equilibrates, two-time quantities, such as density-density or dipole-dipole correlation functions, are much more useful. A typical example is presented in [Fig. 18](#) where the self-part of the intermediate function in [Eq. \(6\)](#) is shown for a Lennard-Jones molecular liquid at low temperature. Immediately after the quench, the system exhibits a relatively fast relaxation: Particles still move substantially. However, when the age of the system increases, dynamics slows down and relaxation becomes much slower. The relaxation then separates into two well-defined “time sectors.” For short-time differences $t - t_w \ll t_w$, which corresponds to short-time dynamics of the amorphous structure, correlation functions at different t_w superpose. However, for large time differences $t - t_w \gg t_w$,

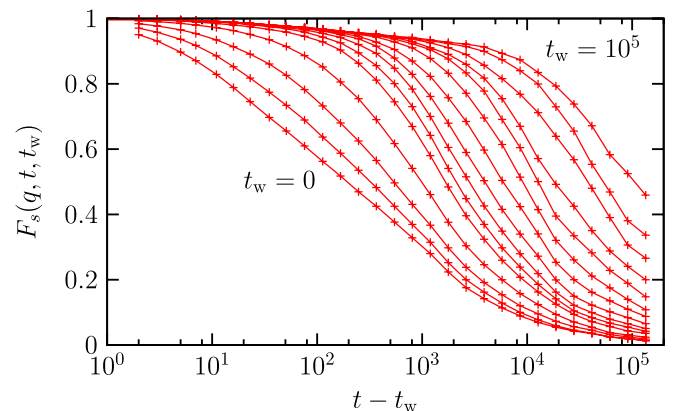


FIG. 18 (color online). Aging dynamics in a Monte Carlo study of a Lennard-Jones glass-forming liquid at low temperature. The system is quenched at time $t_w = 0$ to a low temperature which is then kept constant. Two-time self-intermediate scattering functions are then measured for 20 logarithmically spaced waiting times t_w from $t_w = 0$ to $t_w = 10^5$ (from left to right). The relaxation becomes slower when t_w increases: The system “ages.”

different curves relax at different rates, implying that structural relaxation becomes slower when the system gets older. Eventually, when t_w becomes large, the relaxation becomes too slow to be followed in the considered time window and the system seems frozen on that particular time scale. For practical purposes, it has now become a glass.

A striking feature conveyed by these data is that an aging system not only remains out of equilibrium forever, but its typical decorrelation or relaxation time³ is, in fact, directly set by its own age t_w , which also separates short-time, equilibrated dynamics from long-time, aging relaxation. Therefore, although the system itself has no intrinsic characteristic time scales for relaxation, it remains able to relax during an aging experiment in a finite time which is set by the experimental protocol. More quantitatively, it is found in the simplest cases that two-time correlators $C(t, t_w)$, or equivalently response functions, can be decomposed in the following way:

$$C(t, t_w) \approx C_{\text{eq}}(t - t_w) + C_{\text{aging}}(t/t_w), \quad (76)$$

in which case the relaxation time $\tau_\alpha(t_w)$ is directly proportional to t_w . This “time-aging time” superposition principle is reminiscent of the more standard “time-temperature” superposition principle often found at thermal equilibrium. It is found in many (but not all) polymeric liquids that τ_α grows sublinearly with t_w ,

$$\tau_\alpha(t_w) \sim t_w^\mu, \quad (77)$$

where μ is the so-called aging exponent (Struik, 1978), which usually takes value in the range $\mu \in [\frac{1}{2}, 1]$ (μ is equal to 0.8 in Fig. 18). The simple description (76) has been challenged by dielectric experiments of the aging of molecular liquids (Leheny and Nagel, 1998; Lunkenheimer *et al.*, 2005; Richert, 2010). These studies revealed that the aging part of the correlation function cannot be rescaled just by changing the relaxation time, i.e., the time-aging superposition is not always satisfied. One has to stress, however, that in experiments one can access only the behavior at frequency much higher than the inverse of the decorrelation time. This is due to the fact that the quench can be only performed at finite speed, of the order of 1 K/min, in order to avoid temperature gradients in the sample. As a consequence, when the final temperature is reached, the decorrelation time has already grown so much that it is out of the experimental window. Thus, it is not really known whether the violation of the time-aging time superposition principle affects only the high frequency tails of the dielectric susceptibility or whether Eq. (76) is incorrect even for t of the order of the decorrelation time for many glassy liquids.

Since the complete history of a sample in the glass phase matters, there is no reason to restrain experimental protocols to the simple aging experiment mentioned above. Indeed, experimentalists investigated scores of more elaborated protocols that revealed an incredibly rich, and sometimes quite unexpected, physics (Young, 1998), an old tradition in the field of polymer glasses (Kovacs, 1963; Struik, 1978). In particular,

³This is sometimes called the relaxation time. It does not mean that the system relaxes to equilibrium after this time but just that its structure changes substantially, i.e., decorrelates, over this time scale.

striking “memory” and “rejuvenation” effects are observed during temperature cycling experiments (Réfrégier *et al.*, 1987) (one can also imagine applying an electric field or a mechanical constraint, be they constant in time or sinusoidal, etc.). These two effects were first observed in spin glasses, but the protocol was then repeated in many different materials, from polymers (Bellon *et al.*, 2000; Fukao and Sakamoto, 2005; Montes *et al.*, 2006) and organic liquids (Leheny and Nagel, 1998; Yardimci and Leheny, 2003) to disordered ferroelectrics (Doussineau *et al.*, 1999).

In addition to being elegant and intriguing, such protocols are relevant because they probe more deeply the dynamics of aging materials, allowing one to ask more precise questions beyond the simplistic observation that this material displays aging. Moreover, the observation of similar effects in many different glassy materials implies that these effects are probably quite generic to systems with slow dynamics. Interesting also are the subtle differences possibly observed from one material to another. A large body of experimental, numerical, and theoretical papers have been devoted to this type of experiments; see Berthier *et al.* (2003) for an extensive review on this topic.

A popular interpretation of the aging phenomenon was obtained by considering trap models (Bouchaud, 1992; Monthus and Bouchaud, 1996). In this picture, reminiscent of the Goldstein view of the glass transition mentioned above (Goldstein, 1969), the system is described as a single particle evolving in a complex energy landscape with a broad distribution of trap depths. Thus, this is a paradigmatic mean-field approach. In particular, it is not easy to be specific about what the “traps” of the “rugged landscape” represent in physical terms, although much effort was recently dedicated to establish connections between landscape and real space pictures (Berthier and Garrahan, 2003a; Bertin, 2005; Heuer, 2008).

The simplest version of the trap model makes no reference to a spatial organization of the traps and, therefore, does not take into account possible interactions between traps (Monthus and Bouchaud, 1996). The dynamics of the model is written in terms of an evolution equation for $P(E, t)$, the probability that the system is in a trap of depth E at time t , and it is assumed that dynamics is thermally activated:

$$\frac{\partial P(E, t)}{\partial t} = -\Gamma_0 e^{-\beta E} P(E, t) + \Gamma(t) \rho(E), \quad (78)$$

where $\Gamma(t) = \Gamma_0 \int dE e^{-\beta E} P(E, t)$ is the average hopping rate at time t , with Γ_0 being an attempt frequency. The complexity of the glassy material is now hidden into the probability distribution of the trap depth $\rho(E)$. In Bouchaud’s trap model, an exponential distribution of trap depth is assumed,

$$\rho(E) = \frac{1}{k_B T_0} \exp\left(-\frac{E}{k_B T_0}\right), \quad (79)$$

but the Gaussian trap model was also often considered in the context of the equilibrium dynamics of supercooled liquids (Bässler, 1987; Dyre, 1995; Monthus and Bouchaud, 1996; Heuer, 2008). In the perspective of aging studies, the exponential trap distribution is more relevant because it induces a broader distribution of trapping times τ ,

$$\varphi(\tau) \sim \frac{\Gamma_0}{(\Gamma_0 \tau)^{1+T/T_0}}. \quad (80)$$

Remarkably, the first moment of this distribution diverges at low temperatures $T < T_0$ so that the system undergoes a true glass transition with a relaxation time scale which diverges at T_0 . In contrast, the Gaussian distribution does not lead to ergodicity breaking (i.e., aging is interrupted at long times) and it is thus mostly used in equilibrium studies, where it seems to account well for properties of the potential energy landscape accessed in computer simulations (Heuer, 2008).

When the system is suddenly quenched below T_0 , aging behavior arises because the system visits traps that are increasingly deep when t_w increases, corresponding to more and more stable states. Therefore, it takes more and more time for the system to escape, and the dynamics slows down with time, in a manner reminiscent of Fig. 18. More quantitatively, one can compute two-time correlation functions, such as the persistence function $C(t, t_w) = \int dEP(E, t_w) \times \exp[-(\Gamma_0 e^{-\beta E} t)]$, which represents the probability the system has not changed trap between times t_w and $t + t_w$:

$$C(t, t_w) = \frac{\sin(\pi x)}{\pi} \int_{t/(t+t_w)}^1 (1-x)^{T/T_0-1} x^{-T/T_0} dx = \mathcal{C}(t/t_w), \quad (81)$$

which represents, therefore, an explicit example where the aging exponent defined in Eq. (77) can be computed exactly, $\mu = 1$, and correlation functions are scaling functions of the rescaled time t/t_w , as in Eq. (76).

In Eq. (81), the correlation function is computed as an ensemble average. Important physical insights are also provided by trap models beyond averages at the level of the fluctuations, since the existence of waiting time distributions with long tails indeed implies that time series are typically highly intermittent, and that run-to-run fluctuations are also large, suggesting that it is interesting to consider also statistical distributions of the fluctuations. For instance, one can easily imagine that van Hove functions in aging systems described by trap models are far from Gaussian (Barkai and Cheng, 2003), and that nonergodic effects can be quite strong in systems described by Eq. (80); see He *et al.* (2008) for an example and Margolin and Barkai (2006) for a more formal approach.

B. Mean-field aging and effective temperatures

Theoretical studies of mean-field glassy models have provided important insights into the aging dynamics of both structural and spin glasses (Cugliandolo and Kurchan, 1993, 1994). We already encountered these models in Sec. IV.B.1. They provided a simple setting to study glassy models with a rugged free-energy landscape. As a consequence it is natural to analyze their aging dynamics and use the corresponding results as a mean-field guide line for real systems.

In Sec. IV.B.1, we described several alternative theoretical paths leading to essentially similar results for the equilibrium properties of glasses, which could all be described as “mean field.” Because aging studies now directly deal with states that are nonstationary, protocol dependent, and far from

equilibrium, not all of the mean-field equilibrium approaches are easily extended to low-temperature aging studies. We expect, for instance, that mode-coupling theory should be able to treat such time-dependent phenomena, but this seems to be technically quite involved (Latz, 2000), and a complete extension of MCT to the aging regime remains an open problem. For completeness, we mention a recent work, where the phenomenological RFOT mosaic scaling arguments were used to also describe nonequilibrium relaxation below the glass transition (Lubchenko and Wolynes, 2004). This framework makes contact with the older theoretical approach of Nayaranaswamy, Moynihan, and Tool (Tool, 1946; Narayanaswamy, 1971; Moynihan *et al.*, 1976), but it also predicts important deviations from their findings.

Even by focusing on fully connected disordered models, often described as “simple” models, we note that it took several years to derive a proper asymptotic solution of the long-time dynamics for a series of mean-field spin glasses (Cugliandolo, 2003). These results then triggered an enormous activity (Crisanti and Ritort, 2003) encompassing theoretical, numerical, and also experimental work trying to further understand these results, and to check in more realistic systems whether they have some reasonable range of applicability beyond mean field. This large activity, by itself, easily demonstrates the broad interest of these results.

Mathematically, understanding the aging dynamics of mean-field glass models means solving a closed set of dynamical equations. For concreteness, consider the following spin glass Hamiltonian (Nieuwenhuizen, 1995):

$$H = - \sum_{p=2}^{\infty} \sum_{j_1 < \dots < j_p} J_{j_1 \dots j_p} s_{i_1} \dots s_{i_p}, \quad (82)$$

where $s_i (i = 1, \dots, N)$ are spin variables interacting through coupling constants which are random Gaussian variables of zero mean and variance $p! J_p^2 / (2N^{p-1})$. This model is a straightforward generalization of the p -spin model of Eq. (40). We consider soft spin variables, which are real variables satisfying the spherical constraint $\sum_i s_i^2 = N$. Because of the mean-field nature of the Hamiltonian (82), a closed set of dynamical equations involving two-time correlation and response functions can be derived (Cugliandolo, 2003). Defining

$$C(t, t_w) = \frac{1}{N} \sum_{i=1}^N \overline{\langle s_i(t) s_i(t_w) \rangle}, \quad (83)$$

$$R(t, t_w) = \frac{1}{N} \sum_{i=1}^N \left. \frac{\partial \overline{\langle s_i(t) \rangle}}{\partial h_i(t_w)} \right|_{h_i=0},$$

where h_i is a magnetic field that couples to spin s_i , and

$$g(x) = \frac{1}{2} \sum_{p=2}^{\infty} J_p^2 x^p, \quad (84)$$

one gets the time evolution of the two-time dynamic functions following a quench from a completely disordered state at $t_w = 0$:

$$\begin{aligned}
\frac{\partial C(t, t_w)}{\partial t} &= -\mu(t)C(t, t_w) + 2TR(t, t_w) \\
&\quad + \int_0^{t_w} dt' D(C(t, t'))R(t_w, t') \\
&\quad + \int_0^t dt' \Sigma(t, t'')C(t'', t_w), \\
\frac{\partial R(t, t_w)}{\partial t} &= -\mu(t)R(t, t_w) + \delta(t - t_w) \\
&\quad + \int_{t_w}^t dt' \Sigma(t, t')R(t', t_w), \\
\mu(t) &= T + \int_0^t dt' [D(C(t, t'))R(t, t') + \Sigma(t, t')C(t, t')],
\end{aligned} \tag{85}$$

where the kernels are defined as

$$\begin{aligned}
D(t, t_w) &= g'[C(t, t_w)], \\
\Sigma(t, t_w) &= g''[C(t, t_w)]R(t, t_w).
\end{aligned} \tag{86}$$

The unique feature that makes the dynamics of mean-field spin glass models soluble is that the dynamical equations (85) are closed and only involve two-point functions. This great simplification stems from the fully connected nature of the Hamiltonian (82), and allows one to formulate an exact asymptotic solution for the dynamics of mean-field models (Cugliandolo and Kurchan, 1993).

A comparison with Eq. (42) immediately reveals why the aging regime is much harder to treat analytically, since one has to face two difficulties. First, two-time correlation functions now depend on both their arguments $C(t, t_w) \neq C(t - t_w)$. Second, the equations of motion (85) in the aging regime not only involve time correlations, but also time-dependent response functions. At thermal equilibrium response and correlations are not independent, since the fluctuation-dissipation theorem (FDT) relates both quantities,

$$R(t, t_w) = \frac{1}{T} \frac{\partial C(t, t_w)}{\partial t_w}. \tag{87}$$

Indeed, imposing both FDT and time translational invariance in Eqs. (85) yields the much simpler Eq. (49) for the p -spin model.

The solution to Eqs. (85) has been reviewed in great detail before (Cugliandolo, 2003), so we only briefly describe the most striking physical outcomes. As mentioned in Sec. IV.B.1, in these mean-field models, thermal equilibrium is never reached when the quench is performed below a critical temperature T_c , below which the relaxation time is infinite. It can be shown that aging proceeds forever by downhill motion in an increasingly flat free-energy landscape (Kurchan and Laloux, 1996), with subtle differences between spin glass and structural glass models. In both cases, however, time translational invariance is broken, and two-time correlation and response functions explicitly depend on both their time arguments. When $g(x)$ contains a single term with $p > 2$, as, for instance, in the spherical p -spin model, it can be shown that two-time correlation functions take the form (Cugliandolo, 2003; Andrianov and Lefèvre, 2006)

$$C(t, t_w) \approx C_{\text{eq}}(t - t_w) + \mathcal{C}\left(\frac{h(t)}{h(t_w)}\right), \tag{88}$$

$$h(t) = \exp(t^{1-\mu(T)}),$$

where $\mu(T)$ is an exponent that cannot be computed analytically. Numerical solutions show that $0 < \mu(T) < 1$ and $\mu(T \rightarrow 0) \rightarrow 1$. The scaling form (88) is appealing since it is similar to the empirical form in Eq. (76) and provides an explicit example, where the use of the aging exponent μ defined in Eq. (77) and introduced by Struik (1978) is analytically justified. From a broader perspective, it is interesting to note that the exact dynamic solution of the equations of motion for time correlators (Kim and Latz, 2001) displays a behavior in strikingly good agreement with the numerical results reported for structural glasses, e.g., in Fig. 18.

Note that a more complex time dependence for $C(t, t')$ can be obtained for some mean-field glassy systems. These generally display a phenomenology reminiscent of spin glasses and not structural glasses (the transition is continuous, the spin glass susceptibility diverges, etc.). This is, for example, the case of the “ $p = 2 + 4$ model” for which $g(x)$ takes a more complex form. In these cases the scaling form with a single function $h(t)$ in Eq. (88) does not hold anymore, but has to be generalized to include a continuous hierarchy of such functions. Physically, this implies that the relaxation of correlation functions in the aging regime is associated with an infinite number of aging time scales, which all diverge with the age of the system.

The temporal behavior of time-correlation functions already shows that mean-field spin glass models display a rich aging phenomenology. In aging systems, however, there is no reason to expect the FDT in Eq. (87) to hold and both correlation and response functions carry, at least in principle, distinct physical information. Again, the asymptotic solution obtained for mean-field models quantitatively establishes that the FDT does not apply in the aging regime. The solution also shows that a generalized form of the FDT holds at large waiting times (Cugliandolo and Kurchan, 1993). This generalized form of the FDT reads

$$R(t, t_w) = \frac{X(t, t_w)}{T} \frac{\partial C(t, t_w)}{\partial t_w}, \tag{89}$$

which defines $X(t, t_w)$, the so-called fluctuation-dissipation ratio (FDR). At equilibrium, correlation and response functions are time translational invariant and equilibrium FDT imposes that $X(t, t_w) = 1$ at all times. A parametric fluctuation-dissipation (FD) plot of the step response or susceptibility,

$$\chi(t, t_w) = T \int_{t_w}^t dt' R(t, t'), \tag{90}$$

against

$$\Delta C(t, t_w) = C(t, t) - C(t, t_w), \tag{91}$$

is then a straight line with unit slope. These simplifications do not necessarily occur in a nonequilibrium system. But the definition of an FDR through Eq. (89) becomes significant for mean-field aging systems (Cugliandolo and Kurchan, 1993, 1994). In mean-field spin glass models the dependence of the

FDR on both time arguments is only through the correlation function,

$$X(t, t_w) \approx x(C(t, t_w)), \quad (92)$$

valid at large wait times, $t_w \rightarrow \infty$.

For mean-field structural glass models (such as the p -spin model with $p > 2$), time-correlation functions display a two-step relaxation process as in Eq. (88). Correspondingly, the simplification (92) is even more spectacular since the FDR is shown to be characterized by only two numbers instead of a function, namely, $X \sim 1$ at short-time differences (large values of the correlator) corresponding to a quasiequilibrium regime, with a crossover to a nontrivial number $X \sim X^\infty$ for large times (small values of the correlator). This implies that parametric FD plots are simply made of two straight lines with slope 1 and X^∞ , instead of the single straight line of slope 1 obtained at equilibrium. Formally, the infinite-time FDR X^∞ is defined as

$$X^\infty = \lim_{t \rightarrow \infty} \lim_{t_w \rightarrow \infty} X(t, t_w). \quad (93)$$

These theoretical predictions were tested with success in numerical simulations (Barrat and Kob, 1999; Di Leonardo *et al.*, 2000). In Fig. 19 we present more recent numerical data obtained in an aging silica glass (Berthier, 2007b), presented in the form of a parametric response-correlation plot. The measured correlation functions are the self-part of the intermediate scattering functions defined in Eq. (6), while the conjugated response functions quantify the response of particle displacements to a spatially modulated field conjugated to the density. Plots for silicon and oxygen atoms at different ages of the system are presented. They seem to smoothly converge toward a two-straight-line plot, as obtained in mean-field models for structural glasses (note, however, that this could be a preasymptotic, finite “ t_w ” effect). Note also that the value of T_{eff} is much larger than other relevant temperature scales, in particular, than T_{MCT} , while both quantities nearly coincide in mean-field models.

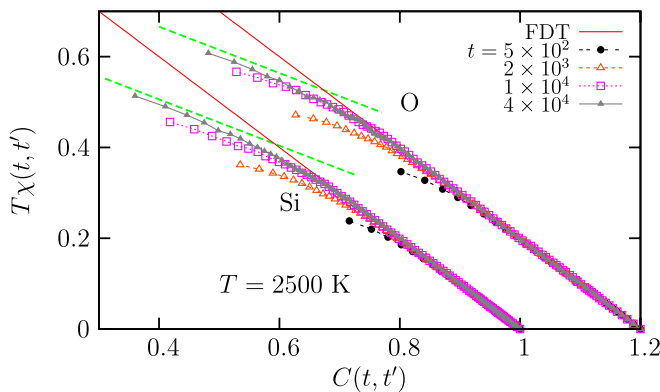


FIG. 19 (color online). Parametric correlation-response plots measured in the aging regime of a numerical model for a silica glass SiO_2 (Berthier, 2007b). The plots for both species smoothly converge toward a two-straight line plot of slope 1 at short times (large C values), and of slope $X^\infty \approx 0.51$ at large times (small values of C), yielding an effective temperature of about $T_{\text{eff}} = T/X^\infty \approx 4900$ K. Note that $T_{\text{eff}} > T_{\text{MCT}} \approx 3330 > T_g \approx 1450$ K.

The behavior of *spin glass* mean-field models, such as the $p = 2 + 4$ model, is again more involved. It is found that each time scale of the continuous hierarchy corresponds to a given value of the FDR. This means that the FDR has become a continuous function $X \sim x(C)$ in the aging regime, instead of the single number found for the p -spin model. For the spherical $p = 2 + 4$ model, for instance, one finds

$$x(C) = \frac{T}{2} \frac{g'''(C)}{[g''(C)]^{3/2}}, \quad (94)$$

for C values corresponding to the aging regime; $g(x)$ was defined in Eq. (84). Thus, the parametric FD plot is now made of a straight line of slope 1 for a large value of the correlation function (quasiequilibrium regime), followed by a continuous curve with slope < 1 for smaller values of the correlation that differs from the FDT even in the infinite-time limit, $t_w \rightarrow \infty$.

Since any kind of behavior is, in principle, allowed in nonequilibrium situations, getting such a simple, equilibrium-like structure for the FD relations is a remarkable result. This immediately led to the idea that aging systems might be characterized by an effective thermodynamic behavior and the idea of “effective equilibration” at different time scales (Cugliandolo *et al.*, 1997). In particular, generalized FD relations in Eq. (89) suggest the definition of an effective temperature, as

$$T_{\text{eff}} = \frac{T}{X(t, t_w)}, \quad (95)$$

such that mean-field structural glasses are characterized by a unique effective temperature $T_{\text{eff}} = T/X^\infty$ in their aging regime. It can be interpreted as the temperature at which slow modes are quasiequilibrated (Cugliandolo *et al.*, 1997; Franz and Virasoro, 2000). One finds, in general, that $0 < X^\infty < 1$, such that $T_{\text{eff}} > T$, as if the system had kept some memory of its high-temperature initial state. It was then proposed that FDRs, or equivalently effective temperatures, can be measured by focusing on any type of physical observables (Cugliandolo *et al.*, 1997). The FDR is then defined in terms of the two-time connected correlation function for generic physical observables $A(t)$ and $B(t)$,

$$C_{AB}(t, t_w) = \langle A(t)B(t_w) \rangle - \langle A(t) \rangle \langle B(t_w) \rangle, \quad (96)$$

with $t \geq t_w$, and the corresponding two-time (impulse) response function

$$R_{AB}(t, t_w) = \left. \frac{\delta \langle A(t) \rangle}{\delta h_B(t_w)} \right|_{h_B=0}. \quad (97)$$

Here h denotes the thermodynamically conjugate field to the observable A so that the perturbation to the Hamiltonian is $\delta H = -h_B \cdot B$. A practical measurement of the FDT is then performed by building a parametric FD plot of the integrated response function,

$$\chi_{AB} = T \int_{t_w}^t dt' R_{AB}(t, t'), \quad (98)$$

versus the correlation function $[C_{AB}(t, t) - C_{AB}(t, t_w)]$.

The name “temperature” for the quantity defined in Eq. (95) is not simply the result of a dimensional analysis but has a deeper, physically appealing meaning that is revealed by asking the following questions: How does one

measure temperatures in a many-body system whose relaxation involves well-separated time scales? What is a thermometer (and a temperature) in a far-from-equilibrium aging material? Answers are provided by [Cugliandolo *et al.* \(1997\)](#) and [Kurchan \(2005\)](#) both for mean-field models and for additional toy models with multiple relaxation time scales. The idea is to couple an additional degree of freedom, such as a harmonic oscillator $x(t)$, which plays the role of the thermometer operating at frequency ω , to an observable of interest $A(t)$ via a linear coupling $-\lambda x(t)A(t)$. Simple calculations show then that the thermometer reads the following temperature:

$$\frac{1}{2}k_B T_{\text{meas}}^2 \equiv \frac{1}{2}\omega^2 \langle x^2 \rangle = \frac{\omega C'_{AA}(\omega, t_w)}{2R''_{AA}(\omega, t_w)}, \quad (99)$$

where $C'_{AA}(\omega, t_w)$ is the real part of the Fourier transform of Eq. (96), and $R''_{AA}(\omega, t_w)$ is the imaginary part of the Fourier transform of Eq. (97), with $h = \lambda x$. Equation (99) indicates that the bath temperature is measured, $T_{\text{meas}} = T$, if frequency is high and the FDT is satisfied, while $T_{\text{meas}} = T_{\text{eff}} > T$ if frequency is slow enough to be tuned to that of the slow relaxation in the aging material. More generally, relaxation in mean-field glassy systems may occur in several, well-separated time sectors ([Cugliandolo and Kurchan, 1994](#)). It is then easy to imagine that each sector could be associated with its own effective temperature ([Kurchan, 2005](#)).

The direct link between the FDR in Eq. (89) and the effective temperature measured in Eq. (99) was numerically confirmed in computer simulations of glassy molecular liquids. [Berthier and Barrat \(2002a\)](#) used a tracer particle was used as a thermometer, its frequency being tuned by modifying its mass. It was verified that its kinetic energy was controlled by the temperature of the heat bath for light (high frequency) tracers, while it was related to the effective temperature of the slow degrees of freedom for heavy (low frequency) tracers. In the same spirit, a two-level system with adjustable frequency was studied by [Ilg and Barrat \(2007\)](#), and the activation rate changed from being proportional to $\exp(-E/T)$ to $\exp(-E/T_{\text{eff}})$ when decreasing the frequency. These two examples show that T_{eff} truly deserves the name of a temperature in a fundamental sense. We note that these modern concepts are related to, but make much more precise, older ideas of quasiequilibrium and fictive temperatures in aging glasses ([Tool, 1946](#); [Narayanaswamy, 1971](#); [Moynihan *et al.*, 1976](#)). Attempts were even made to develop a thermodynamic of the glass state, heavily relying on the idea of effective temperatures. This has become the subject of a book by [Leuzzi and Nieuwenhuizen \(2007\)](#).

The final piece of information extracted from the behavior of mean-field spin glass models is the existence of a connection between a nonequilibrium dynamic quantity, namely, the asymptotic FDR $x(C)$ defined in Eq. (92), and the thermodynamic behavior of the system in the low-temperature phase. It turns out that the thermodynamics of mean-field models for structural glasses is characterized by one-step replica symmetry breaking, while a full-step solution is needed to solve the thermodynamics of models for spin glasses ([Parisi, 2003](#)). Remarkably, the structure of the spin glass order parameter, the Parisi function $P_{\text{eq}}(q)$ describing the probability distribution of overlaps between equilibrium states, is directly related

to the structure of the function $x(C)$. For the $p = 2 + 4$ model, for instance, static calculations yield an explicit expression for P_{eq} ([Nieuwenhuizen, 1995](#)). Comparing with Eq. (94), it turns out that the following equality holds:

$$x(C) = \int_0^C dq P_{\text{eq}}(q). \quad (100)$$

The situation for mean-field structural glasses is more complicated, since Eq. (100) does not hold, but the integrated Parisi function [the right-hand side in (100)] has the same structure as the FDR (the left-hand side) ([Cugliandolo and Kurchan, 1993](#)). Therefore, the full-step or one-step replica symmetry breaking schemes needed to solve the static problem in these models have a direct dynamical counterpart, the FDR being a function or a number, respectively, in the aging regime. It was further argued that Eq. (100) might hold for finite-dimensional glassy systems as well ([Franz *et al.*, 1998](#)), raising the exciting possibility that the Parisi function might become experimentally accessible through aging experiments, which triggered a large research activity ([Crisanti and Ritort, 2003](#)). However, it is not easy to determine the conditions under which Eq. (100) might hold ([Parisi, 2003](#)). Moreover, aging studies are often performed far from any asymptotic regime, and little is known about how Eq. (100) is modified when the $t_w \rightarrow \infty$ limit cannot be taken ([Barrat and Berthier, 2001](#); [Castillo *et al.*, 2002](#)), making the thermodynamic interpretation of the outcome of aging measurements delicate.

Taken together, these results make the mean-field description of aging appealing, and they nicely complement the mode-coupling and RFOT description of the equilibrium glass transition described above. Moreover, they have set the agenda for a large body of numerical and experimental work, as reviewed by [Crisanti and Ritort \(2003\)](#). It should be clear, however, that these results are strictly valid in the mean-field limit in the sense discussed in Sec. IV.B.1. Nonequilibrium aging dynamics in mean-field spin glasses turns out to describe the slow descent of the system in an energy landscape which becomes more and more flat as the age increases ([Kurchan and Laloux, 1996](#)), with no access to the deeper metastable states that are supposed to play an important role in glasses near the experimental glass transition. This view is thus in striking contrast with the purely activated description given, for instance, by trap models. Additionally, it is important to understand the role of spatial fluctuations which are not naturally included in the mean-field description; see [Castillo *et al.* \(2002\)](#) and [Chamon *et al.* \(2004\)](#) for recent work in this direction. Thus, it is important to further test the mean-field concepts to understand how they apply to the three-dimensional world.

C. Beyond the mean field: Experiments, critical points, and kinetically constrained models

Despite success as shown in Fig. 19, the broader applicability of the mean-field scenario of aging dynamics remains unclear. While some experiments and simulations indeed seem to support the existence of well-behaved effective temperatures ([Grigera and Israeloff, 1999](#); [Abou and Gallet, 2004](#); [Wang *et al.*, 2006](#); [Oukris and Israeloff, 2010](#)), other

studies also reveal the limits of the mean-field scenario. Experiments have, for instance, reported anomalously large FDT violations associated with intermittent dynamics (Bellon *et al.*, 2001; Bellon and Ciliberto, 2002; Buisson, Bellon, and Ciliberto, 2003, Buisson, Ciliberto, and Garcimartin, 2003; Greinert *et al.*, 2006), while theoretical studies of model systems also found nonmonotonic or even negative response functions (Nicodemi, 1999; Viot *et al.*, 2003; Depken and Stinchcombe, 2005; Krzakala, 2005), and ill-defined or observable-dependent FDRs (Fielding and Sollich, 2002). Some experiments even reported an the absence of violations to the fluctuation-dissipation theorem (Jabbari-Farouji *et al.*, 2008; Jop *et al.*, 2009). In principle, these discrepancies with mean-field predictions are to be expected, since there are many systems of physical interest in which the dynamics are not of mean-field type, in particular, displaying activated processes. However, it is not possible to draw any consistent picture from the experiments at this stage. As a consequence it is not quite clear yet how and to what extent mean-field results are violated in real systems.

It is thus an important task to understand from the theoretical point of view when the mean-field concept of an FDR-related effective temperature remains viable. However, studying theoretically the interplay between relevant dynamic length scales and thermally activated dynamics in the non-equilibrium regime of disordered materials is clearly a challenging task. As a consequence, much work has been devoted to analyze simple effective models. Much attention has been focused on spin models.

A first class of systems that we discuss are coarsening systems. Although not directly related to the glass problem, they provide a simple, yet nontrivial, theoretical framework to study situations where both aging and spatial heterogeneity are present, and where time-correlation and response functions display interesting scaling behavior. The paradigmatic situation is that of an Ising ferromagnetic model (with a transition at T_c) suddenly quenched in the ferromagnetic phase at time $t_w = 0$. For $t_w > 0$ domains of positive and negative magnetizations appear and slowly coarsen with time. The appearance of domains that grow with time proves the presence of both aging and heterogeneity in this situation.

The case where the quench is performed down to $T < T_c$ is well understood. The only relevant length scale is the growing domain size $\ell(t_w)$, and the physical behavior can be understood by scaling theory (Bray, 1994). Correlation functions display aging, and scale invariance implies that $C(t, t_w) \sim f(\ell(t)/\ell(t_w))$. Response functions can be decomposed into two contributions (Barrat, 1998; Berthier *et al.*, 1999): One part stems from the bulk of the domains and behaves as the equilibrium response, and a second one from the domain walls and becomes vanishingly small in the long-time limit where $\ell(t_w) \rightarrow \infty$ and the density of domain walls vanishes. This implies that for coarsening systems in $d \geq 2$, one has $X^\infty = 0$, or equivalently an infinite effective temperature, $T_{\text{eff}} = \infty$. The case $d = 1$ is special because $T_c = 0$ and the response function remains dominated by the domain walls, which yields the nontrivial value $X^\infty = 1/2$ (Godrèche and Luck, 2000a; Lippiello and Zannetti, 2000).

Another special case has retained attention. When the quench is performed at $T = T_c$, there is no more distinction

between walls and domains and the above argument yielding $X^\infty = 0$ does not hold. Instead one studies the growth with time of critical fluctuations, with $\xi(t_w) \sim t_w^{1/z_c}$ the correlation length at time t_w , where z_c is the dynamic critical exponent. Both correlation and response functions become nontrivial at the critical point (Godrèche and Luck, 2000b). It proves useful in that case to consider the dynamics of the Fourier components of the magnetization fluctuations,

$$C_q(t, t_w) = \langle m_q(t)m_{-q}(t_w) \rangle, \quad (101)$$

and the conjugated response

$$R_q(t, t_w) = \left. \frac{\delta \langle m_q(t) \rangle}{\delta h_{-q}(t_w)} \right|_{h_{-q}=0}, \quad (102)$$

where $h_q(t)$ is the Fourier component of the magnetic field at time t . From Eq. (89) a wave-vector dependent FDR follows, $X_q(t, t_w)$, which has interesting properties that can be computed by a number of means, including dynamical renormalization techniques; see Calabrese and Gambassi (2005) for a review. One of the main outcomes of these studies is that the effective temperature for quenches at the critical point might in some cases depend on the observable (Calabrese and Gambassi, 2004) and on the initial condition (Calabrese *et al.*, 2006), thus weakening the interpretation of X_q in terms of effective temperature.

In dimension $d = 1$, it is possible to compute $X_q(t, t_w)$ exactly in the aging regime at $T = T_c = 0$. An interesting scaling form is found, and numerical simulations performed for $d > 1$ confirm its validity (Mayer *et al.*, 2003):

$$X_q(t, t_w) \approx \mathcal{X}[q\xi(t_w)], \quad (103)$$

where the scaling function $\mathcal{X}(x)$ is $\mathcal{X}(x \rightarrow \infty) \rightarrow 1$ at small length scale $q\xi \gg 1$, and $\mathcal{X}(x \rightarrow 0) \rightarrow X^\infty = 1/2$ (in $d = 1$) at large distance $q\xi \ll 1$; recall that $z_c = 2$ in that case.

In contrast to mean-field systems where geometry played no role, here the presence of a growing correlation length scale plays a crucial role in the off-equilibrium regime since $\xi(t_w)$ allows one to discriminate between fluctuations that satisfy the FDT at small length scale $X_q \sim 1$ and those at large length scale which are still far from equilibrium, $0 < X_q \sim X^\infty < 1$. These studies suggested therefore that generalized fluctuation-dissipation relations, in fact, have a strong length scale dependence, a result which is not predicted using mean-field approaches.

Another interesting result is that the FDT violation for global observables (i.e., those at $q = 0$) takes a particularly simple form, since the introduction of a single number is sufficient, the FDR at zero wave vector, $X_{q=0}(t, t_w) \equiv X^\infty = 1/2$ (in $d = 1$). This universal quantity takes nontrivial values in higher dimension (Godrèche and Luck, 2000b), e.g., $X^\infty \approx 0.34$ is measured in $d = 2$ (Mayer *et al.*, 2003). This shows that the study of global rather than local quantities makes the measurement of X^∞ much easier. Finally, having a nontrivial value of X^∞ for global observables suggests that the possibility to define an effective temperature remains valid, but it has become a more complicated object, related to global fluctuations on large length scale. The first experimental determination of the value of X^∞ near a critical point was reported only recently in a system of liquid crystals, where

the director is the relevant fluctuating observable (Joubaud *et al.*, 2009). An intriguing value $X^\infty \approx 0.31$ was reported, which has received, to our knowledge, no theoretical justification (Calabrese and Gambassi, 2005).

Kinetically constrained spin models represent a second class of non-mean-field systems whose off equilibrium has been thoroughly studied recently (Léonard *et al.*, 2007). This is quite a natural thing to do since these systems have local, finite ranged interactions, and they combine the interesting features of being defined in terms of (effective) microscopic degrees of freedom, having local dynamical rules, and displaying thermally activated and heterogeneous dynamics.

The case of the Fredrickson-Andersen model, described in Sec. IV, was studied in great detail (Léonard *et al.*, 2007), and we summarize the main results. Here, the relevant dynamic variables are the Fourier components of the mobility field, which also correspond in that case to the fluctuations of the energy density. Surprisingly, the structure of the generalized fluctuation-dissipation relation remains once more simple. In particular, in dimension $d > 2$, one finds a scaling form similar to Eq. (105), $X_q(t, t_w) = \mathcal{X}[q\xi(t_w)]$, with a well-defined limit at large distances $X_{q=0}(t, t_w) \equiv X^\infty$. The close analogy with critical Ising models stems from the fact that mobility defects in KCMs diffuse in a way similar to domain walls in coarsening Ising models. It is, in fact, by exploiting this analogy that analytic results are obtained in the aging regime of the Fredrickson-Andersen model (Mayer and Sollich, 2007).

There is, however, a major qualitative difference between the two families of model. The surprise lies in the sign of the asymptotic FDR, since calculations show that (Mayer *et al.*, 2006)

$$X^\infty = -3, \quad d > 2. \quad (104)$$

In dimension $d = 1$, one finds $X_{q=0}(t, t_w) = f(t/t_w)$ with

$$X_{q=0}(t \rightarrow \infty, t_w) = \frac{3\pi}{16 - 6\pi} \approx -3.307.$$

Numerical simulations in various spatial dimensions nicely confirm these calculations. In Fig. 20, we show such a comparison between simulations (symbols) and theory (lines) in the case of the $d = 3$ Fredrickson-Andersen model (Mayer *et al.*, 2006). Fourier components of the mobility field yield parametric FD plots that follow scaling with the variable $q\xi(t_w)$, as a direct result of the presence of a growing length scale for dynamic heterogeneity, with a simple diffusive behavior in that case, $\xi(t_w) \sim \sqrt{t_w}$. Again, generalized fluctuation-dissipation relations explicitly depend on the spatial length scale considered, unlike in mean-field studies. In Fig. 20, the limit $q = 0$ corresponding to global observables is also interesting since the plot is a pure straight line, as in equilibrium. Unlike equilibrium, however, the slope is not 1 but -3 . A negative slope in this plot means a negative FDR, and therefore suggests a negative effective temperature, $T_{\text{eff}} = -3T$, a nonintuitive result at first sight.

Negative response functions, in fact, directly follow from the thermally activated nature of the dynamics of these models (Mayer *et al.*, 2006). First, one should note that the global observable shown in Fig. 20 corresponds to fluctuations of the energy $e(t_w)$ whose conjugated field is tempera-

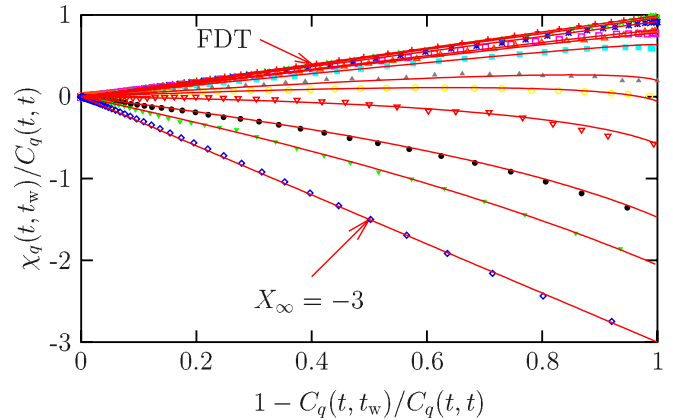


FIG. 20 (color online). Parametric response-correlation plots for the Fourier components of the mobility field in the $d = 3$ Fredrickson-Andersen model. Symbols are from simulations, lines from analytic calculations, and wave vectors decrease from top to bottom. The FDT is close to being satisfied at large q corresponding to local equilibrium. At larger distance deviations from the FDT are seen, with an asymptotic FDR which becomes negative. Finally, for energy fluctuations at $q = 0$ (bottom curve), the plot becomes a pure straight line of (negative) slope -3 , as a result of thermally activated dynamics.

ture. In the aging regime the system slowly drifts toward equilibrium. Microscopic moves result from thermally activated processes, corresponding to the local crossing of energy barriers. An infinitesimal change in temperature, $T \rightarrow T + \delta T$ with $\delta T > 0$, accelerates these barrier crossings and makes the relaxation dynamics faster. The energy response to a positive temperature pulse is therefore negative, $\delta e < 0$, which directly yields $\delta e/\delta T < 0$, and explains the negative sign of the FDR. This line of reasoning does not apply to mean-field glasses, where thermal activation plays no role. To our knowledge, negative effective temperatures in realistic aging materials have not yet been observed.

Finally, another scenario holds for local observables in some KCMs when kinetic constraints are stronger, such as the East model (Léonard *et al.*, 2007) or a bidimensional triangular plaquette model (Jack *et al.*, 2006). Here relaxation is governed by a hierarchy of energy barriers that endow the systems with specific dynamic properties. In the aging regime following a quench, in particular, the hierarchy yields an energy relaxation that arises in discrete steps which take place on different time scales, reminiscent of the time sectors encountered in mean-field spin glasses (but not in mean-field structural glass models). Surprisingly, it was found that to each of these discrete relaxations one can associate a well-defined (positive) value of the fluctuation-dissipation ratio, again reminiscent of the dynamics of mean-field spin glass models. Therefore, even in models that are far from the mean-field limit, the physical picture of a slow relaxation taking place on multiple time scales with each time scale characterized by an effective temperature seems to have some validity.

In conclusion, we described multiple non-mean-field situations where collective behavior (critical point in standard ferromagnets, dynamic criticality emerging in kinetically constrained models) produces nontrivial aging dynamics characterized by the emergence of universal fluctuation-dissipation properties. These results are instructive for

understanding how and to what extent mean-field results can change in finite-dimensional systems. However, it is not clear whether aging in structural glasses can be understood in terms of domain coarsening (domains between what?), nor that kinetically constrained models are faithful effective models of glasses. As a consequence, for theoretical models it is difficult to reach a consistent picture of effective temperature and aging valid for finite-dimensional structural glasses. However, these results suggest that, most certainly, nonequilibrium effective temperatures have a validity much beyond the realm of mean-field disordered spin models where they were first discovered (Kurchan, 2005).

D. Driven dynamics of glassy materials

We introduced aging phenomena with the argument that in a glass phase, the time scale to equilibrate becomes so long that the system always remembers its complete history. This is true in general, but one might wonder whether it is possible to invent a protocol where the material history can be erased, and the system rejuvenated (McKenna and Kovacs, 1984). This concept has been known for decades in the field of polymer glasses, where complex thermomechanical histories are often considered, for obvious practical reasons.

Let us consider an aging protocol, where a supercooled liquid is quenched to a low temperature at time $t_w = 0$, but is simultaneously forced by an external mechanical constraint. Experimentally, one often finds that a stationary state can be reached, which explicitly depends on the strength of the forcing: A system which is forced more strongly relaxes faster than a material which is less perturbed, a phenomenon called “shear thinning.” The material has, therefore, entered a driven steady state, where memory of its age is no longer present and dynamics has become stationary: Aging is stopped (Kurchan, 2001).

Many studies of these driven glassy states have been performed in recent years. Note that the drive is, in general, mechanical and, hence, these are relevant for the rheology of supercooled liquids and glasses, and the $T \ll T_g$ limit corresponds to studies of the plasticity of amorphous solids, which is a broad field in itself; see Falk and Langer (1998), Maloney and Lemaître (2006), Tanguy *et al.* (2006), Schall *et al.* (2007), and Bocquet *et al.* (2009) for a few modern perspectives in this direction. In the colloidal world, such studies are also relevant for the newly defined field of the rheology of soft glassy materials. These materials are (somewhat tautologically) defined as those for which the nonlinear rheological behavior is believed to result precisely from the competition between intrinsically slow relaxation processes of glassy origin and an external forcing (Sollich *et al.*, 1997). It is believed that the rheology of dense colloidal suspensions, foams, emulsions, pastes, or even biophysical systems are ruled by such a competition, quite a broad field of application indeed (Cates, 2003).

From the point of view of statistical mechanics modeling, the rheology of soft glassy materials can be naturally studied from the same angles as the equilibrium glass transition and aging phenomena. As such, trap models (Sollich *et al.*, 1997; Sollich, 1998; Fielding *et al.*, 2000), mean-field spin glasses (Cugliandolo *et al.*, 1997; Berthier *et al.*, 2000), and the

related mode-coupling theory approaches (Fuchs and Cates, 2002; Miyazaki and Reichman, 2002; Miyazaki *et al.*, 2004; Fuchs and Cates, 2005; Miyazaki *et al.*, 2006; Brader *et al.*, 2007; Fuchs and Cates, 2009) have been explicitly extended to include an external mechanical forcing. In all these cases, one generically finds that a driven steady state can be reached and aging is indeed expected to stop at a level that depends on the strength of the forcing. A most interesting aspect is that the broad relaxation spectra predicted to occur in glassy materials close to a glass transition directly translate into “anomalous” laws for both the linear rheological behavior [seen experimentally in the broad spectrum of elastic $G'(\omega)$ and loss $G''(\omega)$ moduli],⁴ and the nonlinear rheological behavior (such as a strong dependence of the steady state viscosity η upon an imposed shear rate $\dot{\gamma}$), while aging and rheology compete deep in the glass phase to produce interesting phenomena such as slow creep behavior. However, all these different theoretical approaches have their strengths and weaknesses, as we now briefly describe.

The trap model described in Sec. V.A was extended into the “soft glassy rheology” (SGR) model (Sollich *et al.*, 1997; Sollich, 1998). Its simplicity makes it a nice tool to investigate complex thermomechanical histories, where aging and mechanical forcing compete (Fielding *et al.*, 2000), leading to several interesting predicted behaviors. Thus, the model is often used by experimentalists to rationalize nontrivial rheological behaviors commonly encountered in complex materials; see, e.g., Rouyer *et al.* (2008).

The SGR model is a direct extension of the trap model, where each trap is characterized not only by its depth E , but additionally by a “strain” variable ℓ . The evolution equation now involves $P(E, \ell, t)$, which generalizes $P(E, t)$ to include the statistical fluctuations of the strain variable. Using notations similar to the ones used in Eq. (78), the dynamics of the SGR model is defined as

$$\begin{aligned} \frac{\partial P(E, \ell, t)}{\partial t} = & -\dot{\gamma} \frac{\partial P(E, \ell, t)}{\partial \ell} \\ & - \Gamma_0 e^{-\beta[E-(1/2)k\ell^2]} P(E, \ell, t) \\ & + \Gamma(t) \rho(E) \delta(\ell), \end{aligned} \quad (105)$$

where

$$\Gamma(t) = \Gamma_0 \int d\ell \int dE e^{-\beta[E-(1/2)k\ell^2]} P(E, \ell, t).$$

The first term represents the effect of the global shear rate $\dot{\gamma}$ in the absence of hopping between traps, namely, affine deformation of the traps. The second term describes the probability to leave the trap occupied at time t and takes into account in a linear manner the fact that shearing promotes hopping between traps by lowering the barrier heights, thereby defining an elastic constant k . Note that activated dynamics with an “effective temperature factor” $T_{\text{eff}} = 1/\beta$ is assumed, even though its meaning in the context of a driven colloidal system or emulsion is not clear (Cates, 2003). The last term now includes the new factor $\delta(\ell)$, implying that after a hop, the newly found trap is unstrained. Of course, for such a

⁴ $G(\omega)$ relates the stress to an imposed sinusoidal strain oscillating at frequency ω ; see Barnes *et al.* (1989).

mean-field description (a single particle hopping between traps), strain, shear rates, or shear stress are just names and are not intended to carry physical information about a real three-dimensional flow. As in the original trap model, an exponential form is adopted for the distribution of trap depths $\rho(E)$ (Sollich *et al.*, 1997). The global shear stress is defined by

$$\sigma(t) = k\langle\ell\rangle_p = k \int d\ell \int dE P(E, \ell, t) \ell, \quad (106)$$

so that knowledge of $P(E, \ell, t)$ from solving Eq. (105) allows one to predict any needed rheological quantity (Sollich, 1998). The success of the SGR model stems partly from the fact that depending on the value of the effective temperature, a broad variety of nontrivial, but experimentally realistic, rheological behavior can be predicted for both linear and nonlinear responses. The model can, therefore, easily be used to fit a set of experimental data by adjusting a few quantities, such as T_{eff} or Γ_0 ; see Fabry *et al.* (2001) for a biophysical example. Moreover, it is simple enough that extremely complex thermomechanical histories can be easily implemented and compared to experiments; see Viasnoff and Lequeux (2002) for an illustration. The weaknesses of the approach are the same as for the original trap model, as far as the interpretation of the traps in real space is concerned. Moreover, the lack of a spatial representation of the physics implies that the different traps are only coupled via the effective noise temperature, and the model cannot describe shear and kinetic heterogeneities. It would be interesting to develop spatial variations of the original SGR trap model to include mechanically realistic interactions between traps (Hébraud and Lequeux, 1998), as is also done in theoretical modeling of the elastoplastic response of amorphous solids (Picard *et al.*, 2005; Bocquet *et al.*, 2009).

Mean-field glass models can also be modified to include the physical effect of an external mechanical forcing in the dynamics (Horner, 1996; Cugliandolo *et al.*, 1997; Thalmann, 1998; Berthier *et al.*, 2000). Since these models contain fully connected Hamiltonians defined with no reference to geometry, the modeling of an external flow is necessarily crude. In the case of a sheared glassy material, it is argued that the main effect of the imposed shear flow in the equations of motion is to inject energy into the system (Kurchan, 2001). Taking again the example of the p -spin model in Eq. (40), one now considers the driven dynamics

$$\frac{\partial s_i(t)}{\partial t} = -\mu(t)s_i(t) - \frac{\partial H}{\partial s_i(t)} + f_i^{\text{drive}}(t) + \eta_i(t), \quad (107)$$

where $f_i^{\text{drive}}(t)$ stands for an external driving force. A natural choice in this context is to consider a driving force which has a functional form similar to the p -spin interaction but involves coupling constants which contain an asymmetric part, so that the resulting force cannot be derived from an energy function. The specific choice made by Berthier *et al.* (2000) is

$$f_i^{\text{drive}}(t) = \sigma(t) \sum_{j_1 < \dots < j_{k-1}, j_1, \dots, j_{k-1} \neq i} \tilde{J}_i^{j_1 \dots j_{k-1}} s_{j_1} \dots s_{j_{k-1}}, \quad (108)$$

with coupling constants that are random Gaussian variables of variance $k!/(2N^{k-1})$, which are symmetrical about permuta-

tions of (j_1, \dots, j_{k-1}) , but are uncorrelated about permutations of i with any element of (j_1, \dots, j_{k-1}) . With this particular choice of asymmetrical couplings and a constant amplitude of the driving force $\sigma(t) = \sigma$, a numerical solution of the two-time dynamical equations of the form similar to Eq. (85) shows that the dynamics becomes stationary for any $\sigma > 0$ (Cugliandolo *et al.*, 1997) and any temperature $T > 0$ (even for $T < T_c$). Therefore, in the stationary state following a quench at time $t_w = -\infty$ in the presence of a constant driving force, the dynamical equations become

$$\begin{aligned} \frac{dC(t)}{dt} &= -\mu C(t) + \int_0^t dt' \Sigma(t-t')C(t') \\ &\quad + \int_0^\infty dt' [\Sigma(t+t')C(t') + D(t+t')R(t')], \\ \frac{dR(t)}{dt} &= -\mu R(t) + \int_0^t dt' \Sigma(t-t')R(t'), \\ \mu &= T + \int_0^\infty dt' [D(t')R(t') + \Sigma(t')C(t')], \end{aligned} \quad (109)$$

with kernels given by

$$D(t) = \frac{p}{2} C(t)^{p-1} + \sigma^2 \frac{k}{2} C(t)^{k-1}, \quad (110)$$

$$\Sigma(t) = \frac{p(p-1)}{2} C(t)^{p-2} R(t). \quad (111)$$

Mathematically, the asymmetry in the coupling constants of the driving force shows up in the expressions of the kernels, since only $D(t)$ contains the driving term proportional to σ , with no counterpart in the expression for $\Sigma(t)$. It can be shown formally (Kurchan and Markov, 2003) that detailed balance imposes specific symmetries of the kernels D and Σ , which is indeed explicitly broken in Eqs. (109) by the term proportional to σ . As in the aging regime, Eq. (85), these equations involve both correlation and response functions, and are thus more difficult to solve than the equilibrium, high-temperature dynamics in Eq. (49). However, the solution proceeds much as in the aging regime (Berthier *et al.*, 2000).

The connection to rheological quantities was done using energetic considerations. Using a Green-Kubo type of arguments, the viscosity η was related to the relaxation time scale obtained from the time decay of $C(t)$ from Eq. (109), so that $\eta(T, \sigma) \sim \tau_\alpha$. The power dissipated by the driving force is then shown to be $\propto \sigma^2/\tau_\alpha \sim \sigma^2/\eta$, while it is $\propto \sigma\dot{\gamma} = \sigma^2/\eta$ for a sheared fluid. Thus, one identifies σ as the shear stress for the present system, and steady state constitutive rheological relations can readily be studied. As for the SGR model, the results showed that the interplay between the glass transition physics and external forcing induced strong shear-thinning behavior which depends quantitatively on the temperature, with experimentally relevant scaling laws for the viscosity across the (σ, T) plane (Berthier *et al.*, 2000). For $T \leq T_c$, for instance, a shear-thinning behavior is predicted at low shear rates,

$$\eta \sim \dot{\gamma}^{-\nu(T)}, \quad (112)$$

where $\nu(T)$ is a temperature-dependent exponent, with $\nu(T_c) \equiv \nu_c = 2/3$ and $\nu \rightarrow 1$ as $T \rightarrow 0$. This behavior is typical of a ‘‘power-law fluid’’ in the rheological literature

(Larson, 1999). The nontrivial shear-thinning exponent $\nu_c = -2/3$ at T_c reveals a complex interplay between thermal processes and mechanical forcing, while in the low- T limit the “natural” exponent $\nu = -1$ is recovered, as expected on dimensional grounds. Above T_c , the following scaling form is obtained:

$$\eta(\dot{\gamma}, T) \simeq \eta_0(T)[1 + \dot{\gamma}/\dot{\gamma}_0]^{-\nu_c}, \quad (113)$$

where $\eta_0(T)$ is the equilibrium value of the viscosity and $\dot{\gamma}_0$ is a constant. This form of scaling is well known and commonly found in the rheology literature (Larson, 1999), and these predictions compare rather well with computer simulations (Yamamoto and Onuki, 1998b; Barrat and Berthier, 2000; Berthier and Barrat, 2002b), and experiments (Crassous *et al.*, 2006; Besseling *et al.*, 2007).

As compared to the SGR model, the equations of motion (109) are mathematically more involved, even in the steady state, so that it is technically more difficult to solve for the response of the system to more complicated histories, although this is a technical rather than a fundamental limitation. A more fundamental difference, as already discussed in equilibrium and aging situations, is the absence, at the mean-field level, of thermally activated processes which would allow the system to visit the numerous deep metastable states that contribute to its configurational entropy between the mode-coupling and Kauzmann transitions.

Just as these activated processes explain why mode-coupling dynamic singularities are avoided in finite-dimensional systems, activated processes could, in principle, affect the rheological behavior of glassy materials. As discussed, including these processes in the context of mean-field glass theory is a challenging task. A phenomenological description in the framework of RFOT theory was recently proposed (Lubchenko, 2009), extending, in particular, the validity of Eq. (113) to lower temperatures. Note that distinct predictions were recently obtained by Biroli and Bouchaud (2009). Staying at the mean-field level, however, it can be argued (Berthier, 2003a) that thermal activation should allow the system to visit metastable states with lower free energy. In such a state, it can be shown that the system must be forced above a finite level of stress in order to flow. In rheological terms, this means that the presence of metastable states leads to materials with a static finite yield stress (although dynamically there is no finite yield stress). Recent calculations in the replica framework exposed in Sec. IV.B.6 have confirmed the existence of a finite shear modulus originating from the existence of metastable states (Yoshino and Mézard, 2010). In a realistic description, yet to be developed, one should describe within a single framework the effect of shear and thermal activation within a complex energy landscape.

Another difference with the SGR approach concerns the study of effective temperatures, which again mirrors the mean-field results obtained in aging situations (see Sec. V.B). Indeed, many of the results obtained in aging systems about deviations from fluctuation-dissipation relations can be shown to apply to the driven case as well. In particular, a fluctuation-dissipation ratio can still be defined from Eq. (94) leading to the notion of effective temperatures for driven systems. The solution of Eqs. (109) yields the time dependence of both correlation and response functions, from

which a parametric FD plot can be built. As for aging materials, it was predicted that these FD plots conserve an equilibrium shape, being piecewise linear, with each relaxation time scale being associated with its own value of the fluctuation-dissipation ratio and being interpreted in terms of an “effective equilibrium” for slow degrees of freedom. An interesting feature is that effective temperatures are predicted to occur even above the glass transition, provided the driving force is large enough that nonlinear rheological effects are observed. Thus, a deep connection between anomalous response functions and deviations from thermal equilibrium is established (Berthier *et al.*, 2000).

These predictions were confirmed in a number of numerical studies of sheared supercooled liquids (Barrat and Berthier, 2000; Berthier and Barrat, 2002a, 2002b; Ono *et al.*, 2002; Ilg and Barrat, 2007), and the main physical result, the existence of an effective temperature describing the relaxation of sheared glassy systems, now forms the basis of several recent phenomenological descriptions of the plastic deformation of amorphous solids (Haxton and Liu, 2007; Langer and Manning, 2007; Shi *et al.*, 2007; Bouchbinder, 2008). We are unaware of any experimental attempt to quantify violations of the fluctuation-dissipation theorem under stationary conditions created by a shear flow, although this should, in principle, be much easier than in nonstationary, aging situations where several experiments have already been performed.

We mentioned in Sec. V.B that mode-coupling theory had not been fully extended to deal with nonequilibrium aging situations. By contrast, in recent years, a large research activity was dedicated to the derivation of mode-coupling approximations to deal with the rheology of glassy liquids and colloidal suspensions. A first derivation is obtained starting from generalized fluctuating hydrodynamic equations, as in field-theoretic derivations of the equilibrium MCT (Das *et al.*, 1985). Among the several approximations involved, the standard mode-coupling decomposition of four-point static correlations as a product of two-point functions is performed, yielding closed dynamical equations for the time evolution of the intermediate scattering function under shear. For the case of a stationary simple shear flow with an imposed strain in the x direction $\gamma(t)$, one gets the following dynamical equations (Miyazaki and Reichman, 2002):

$$\begin{aligned} \frac{dF(\mathbf{q}, t)}{dt} &= -\frac{Dq(-t)^2}{S[q(-t)]}F(\mathbf{q}, t) \\ &\quad - \int_0^t dt' M(\mathbf{q}(-t), t-t') \frac{dF(\mathbf{q}, t')}{dt'}, \\ M(\mathbf{q}, t) &= \frac{\rho D}{2} \frac{q}{q(t)} \int d\mathbf{q}' V(\mathbf{q}, \mathbf{q}') V(\mathbf{q}(t), \mathbf{q}'(t)) F(\mathbf{q}(t) \\ &\quad - \mathbf{q}'(t), t) F(\mathbf{q}'(t), t), \end{aligned} \quad (114)$$

where $\mathbf{q}(t) = (q_x, q_y + \gamma(t)q_x, q_z)$ is a time-dependent wave vector, the vertex function has the standard mode-coupling expression as in Eq. (47), and $F(q, t) = \langle \rho_{\mathbf{q}(-t)}(t) \rho_{-\mathbf{q}}(0) \rangle$ is the intermediate scattering function modified to take into account the global advection by the shear flow. Formally, these equations are similar to the ones derived at equilibrium; see Eqs. (46) and (47). This implies that the physics captured

by this approximation stems from the advection, and thus the distortion, of density fluctuations along the x direction by the shear flow. Because of the mode-coupling mechanism in Eq. (114), relaxation of density fluctuations in the x direction triggers the relaxation of all the modes. In a parallel effort (Fuchs and Cates, 2002, 2005), similar MCT dynamic equations for glasses under shear flow were derived employing the technique of projection operators also used at thermal equilibrium to derive mode-coupling equations. Here also, a similar decoupling of four-point correlations into products of two-point quantities is performed, and in its latest version (Fuchs and Cates, 2009) the final dynamical equations are similar to the above expressions, Eqs. (114); see Fuchs and Cates (2009) for a detailed discussion of the technical differences between the two approaches.

The rheological behavior in steady shear flow above the mode-coupling transition resembles the description in Eq. (113), although the simple shear-thinning exponent $\nu = -1$ is found. In the glass (Fuchs and Cates, 2002), the system develops a finite yield stress, which jumps discontinuously from zero when the mode-coupling transition is crossed. Below T_c , the rheological behavior resembles that of a Bingham fluid (Larson, 1999). We note that although fully connected glass models and schematic mode-coupling models are fully equivalent at thermal equilibrium, both approaches seem to predict different behaviours out of equilibrium. It is not yet clear whether these differences are due to the set of approximations involved in the derivation of Eqs. (114), or to the peculiar form of the nonequilibrium drive (108) chosen for mean-field glass models, which may be unrealistic. Both approaches suffer from the same fundamental limitation that emerging critical or universal properties near the mode-coupling transition will be drastically modified in realistic numerical simulations or real experiments, as the mode-coupling singularity is not present in real materials, even in colloidal hard-sphere systems where the theory was often applied (Crassous *et al.*, 2006). This implies that all the problems and ambiguities due to the crossover nature of the dynamic transition encountered by MCT at thermal equilibrium (see Sec. IV.B.4) will again be present under shear, and the theory should fare with experimental data no better or no worse than at equilibrium.

Although initially developed to study stationary shear flows $\gamma(t) = \dot{\gamma}t$, MCT-based rheological equations have now been derived for arbitrary flows and shear histories (Brader *et al.*, 2007, 2008, 2009). The resulting equations are more complicated than Eqs. (114), involving, in particular, three-time memory functions in the general case. The case of oscillatory simple shear flows was also studied (Miyazaki *et al.*, 2006). The possibility to study time-dependent shear flows makes the MCT approach quite appealing, as it can thus compete with the flexibility offered by the SGR model described above, with the advantage that one is dealing with a microscopically realistic description of the liquid. However, it is possible to study the interplay of shear flow and aging in the SGR model (Fielding *et al.*, 2000), which is not yet feasible within MCT approaches.

As concrete applications of the theoretical framework, step strain protocols (Brader *et al.*, 2007) or sinusoidal shear flows of arbitrary amplitudes were studied (Miyazaki *et al.*, 2006).

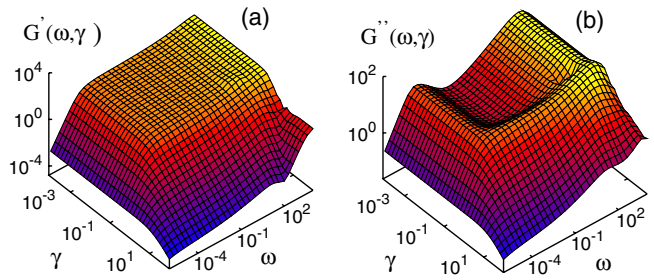


FIG. 21 (color online). Frequency and strain dependence of (a) the storage modulus and (b) the loss modulus for a hard-sphere suspension near the mode-coupling glass transition. The broad viscoelastic spectra emerging in fluids near the glass transition is affected in a nonlinear manner by a large external shear flow which accelerates the dynamics. From Miyazaki *et al.*, 2006.

In Fig. 21, we show the behavior obtained for the storage and loss moduli of a dense suspension of hard spheres close to the colloidal glass transition as a function of frequency (as in linear viscoelasticity) and strain amplitude (as in nonlinear steady shear flows). These results illustrate both the broad viscoelastic spectra emerging in fluids near the glass transition, and the strongly nonlinear competition between intrinsic slow dynamics and the external perturbation imposed by the shear flow which accelerates the dynamics.

The issue of a nonequilibrium extension to the fluctuation-dissipation theorem in shear flows was also discussed within MCT. A formal derivation of the Einstein relation between self-diffusion and mobility under shear flow is presented by Szamel (2004), while FDT violations are acknowledged (Miyazaki and Reichman, 2002), but do not play a role during the derivation of Eqs. (114) to arrive at dynamical equations involving correlation functions only, as opposed to coupled equations for response and correlations in Eqs. (109). Recently, an approximate expression for time-dependent susceptibilities was obtained (Krüger and Fuchs, 2010) and compared to the correlation obtained from the solution of Eqs. (114). In standard equilibrium MCT, the response function is obtained *a posteriori* using the FDT. Complementary approaches, such as field theory, are plagued by difficulties related to maintaining FDT in a self-consistent manner. As a consequence, the status of the approximation by Krüger and Fuchs (2010) is not entirely clear at this stage. Moreover, an important difference is found with mean-field results since a nearly constant value of the FDR, $X = 1/2$, is predicted (Krüger and Fuchs, 2010) in contrast to mean-field models where the FDR is generically dependent of the state point, with $X \sim T$ at low temperatures (Cugliandolo, 2003), as also found in numerical work (Di Leonardo *et al.*, 2000; Zamponi *et al.*, 2005; Berthier, 2007b). This suggests that still more work is needed to clarify the status (derivation and physical behavior) of nonequilibrium effective temperatures in glassy systems under shear.

E. Current status of nonequilibrium studies

Aging studies have a long history in the field of the glass transition (Struik, 1978), since glasses are all by definition

nonequilibrium aging materials. It is only since the 1990s, however, that a large body of work was performed to describe nonequilibrium glasses at a more fundamental level, using tools and concepts from statistical mechanics, as briefly reviewed. Despite much conceptual progress, it is not clear whether these theoretical advances have led to a better description of the physical properties of, say, polymer glasses under complex thermomechanical histories, and thus have had concrete experimental consequences (Angell *et al.*, 2000). It certainly remains true that a large number of experiments have been devised to analyze two-time response and correlations functions in a number of materials, in order to test theoretical predictions, although it appears that less studies of aging materials were performed in recent years.

We suggested that recent theoretical and experimental work to characterize and understand memory and rejuvenation effects in spin glasses could be fruitfully revisited in the field of structural glasses; see the experimental chapters in Young (1998). In particular, a clear link between memory effects and typical length scales over which the slow dynamics takes place was established in the context of spin glasses (Bouchaud *et al.*, 2001; Berthier and Bouchaud, 2002; Jönsson *et al.*, 2004). We discussed in previous sections that dynamic length scales also depend sensitively on temperature in structural glasses, as illustrated, for instance, in Fig. 11. Presently, it is not known how these ideas apply to aging of structural glasses and whether they yield memory effects similar to the ones observed in spin glasses. In the same vein, little work was performed to understand how the mosaic picture of RFOT theory (Lubchenko and Wolynes, 2004; Biroli and Bouchaud, 2009) or the frustration-limited domains discussed in Sec. IV.D would respond to complex thermal histories, nor has mode-coupling theory been fully developed to handle nonstationary dynamics far from equilibrium except in the context of mean-field glassy systems (Cugliandolo and Kurchan, 1999).

More work should also certainly be performed to characterize dynamic heterogeneities in nonequilibrium systems. Indeed, when experiments were devised to detect, for instance, two-time correlation functions in aging materials, it became immediately clear that slow dynamics in these far-from-thermal-equilibrium conditions was also characterized by intriguingly large dynamic fluctuations (Cipelletti and Ramos, 2005) showing up in the form of intermittent time signals (Bellon *et al.*, 2001; Buisson *et al.*, 2003; Duri and Cipelletti, 2006; Mamane *et al.*, 2009), large spatial correlations (Duri *et al.*, 2009), peculiar forms of relaxation functions (Cipelletti *et al.*, 2000; Bellour *et al.*, 2003; Bandyopadhyay *et al.*, 2004), or superdiffusive processes (Guo *et al.*, 2009; Mazoyer *et al.*, 2009). Although well documented experimentally and displaying some form of universality, these nontrivial dynamics received too little attention from the theoretical community; see, however, Bouchaud and Pitard (2001). It is, in particular, intriguing that these effects are apparently not observed in computer simulations where dynamic heterogeneity seems to proceed roughly as under equilibrium conditions (Parisi, 1999; Castillo and Parsaeian, 2007; Parsaeian and Castillo, 2008; El Masri *et al.*, 2010). In this context, an interesting develop-

ment is the extension of some of the concepts derived from mean-field spin glass models, in particular, the notion of time reparametrization invariance of the dynamical equations of motion, to finite-dimensional aging materials (Castillo *et al.*, 2002; Chamon *et al.*, 2004). In particular, this approach naturally explains the appearance of nontrivial mesoscopic dynamic fluctuations in aging materials and provides specific new tools to analyze a number of physical quantities, such as distributions of time-correlation functions (Chamon and Cugliandolo, 2007).

In contrast with aging studies, the rheology of soft glassy materials has been increasingly actively studied over the last decade, and has developed as a research field on its own that will certainly continue to expand in the coming years. Thus, we close this prospective section with just a few selected issues on the rheology of glasses that are currently the object of intense research. First, since all the above-mentioned theoretical modeling of glassy rheology is somehow mean field in nature, it is not clear how spatial heterogeneities or correlations can be described theoretically. Yet, experiments (Coussot *et al.*, 2002; Varnik *et al.*, 2003; Bécu *et al.*, 2006; Shi and Falk, 2006; Zink *et al.*, 2006; Ianni *et al.*, 2008) and simulations (Varnik *et al.*, 2003; Zink *et al.*, 2006; Shi and Falk, 2006) clearly reveal, for instance, that soft glassy materials commonly display the phenomenon of shear banding. Namely, when submitted to a macroscopic shear force, the system spontaneously “phase separates” between a flowing state supporting the shear and an immobile state with no flow. This observation means that at least two dynamical states exist for a given level of external forcing, so that the flow curve $\sigma(\dot{\gamma})$ is multivalued, but there is presently no agreement on the microscopic origins of this observation (Berthier, 2003a; Varnik *et al.*, 2003; Manning *et al.*, 2007; Fielding *et al.*, 2009; Besseling *et al.*, 2010). A second relevant question related to spatial aspects is the subject of dynamic heterogeneity. We have underlined in Sec. III the importance of spatial fluctuations of the dynamic at thermal equilibrium and have described in Sec. IV how different theories describe these fluctuations. Much less is known under shear, although numerical simulations revealed the existence of large scale heterogeneities under flow (Furukawa *et al.*, 2009) that are, in fact, strongly reminiscent of the plastic flow of low-temperature glasses (Falk and Langer, 1998; Tanguy *et al.*, 2006; Lemaître and Caroli, 2009). Further studies of these issues could also shed some light on the flow of soft glassy materials under confinement, a situation of interest due to the rapid development of microfluidic techniques and applications (Goyon *et al.*, 2008; Isa *et al.*, 2009).

VI. SOME GENERAL AND CONCLUDING REMARKS

We conclude this review with a few remarks on some key topics that are often debated in the literature and on which we present our point of view.

A. Growing length scale(s)

For a long time, the research on the glass transition has been focused on time scales more than length scales. The

reason is simple: The former are clearly increasing rapidly approaching T_g , whereas the latter remained elusive for a long time. Recently, this state of affairs has changed. First, the whole topic of dynamical heterogeneity made it clear that a complete theory of the glass transition has to be able to explain growing dynamical length scales. Furthermore, there are general theoretical and not just phenomenological reasons to believe that growing length scales play an important role. In fact, a system with a finite number, say N , of degrees of freedom is expected to have a relaxation time no larger than $\exp(KN)$, where K is independent of N and possibly dependent on temperature, but in a nonsingular way except at $T = 0$. A system, whose largest correlation length is ξ , can be viewed as a collection of independent subsystems of linear size ξ . The relaxation time τ is therefore equal to the one of a given subsystem and therefore cannot be larger than $\exp(K\xi^d)$. This implies that large relaxation times should be related to large numbers of spatially correlated degrees of freedom. This intuition was made rigorous by [Montanari and Semerjian \(2006a\)](#), where it was shown that indeed the point-to-set length defined in Sec. IV.B.6 has to grow at least as fast as $c(\log\tau_a)^{1/d}$, where d is the spatial dimension and c is a proportionality constant. Since c actually depends on temperature (as K in the previous expression), this inequality makes a growing length a necessity only if the relaxation time scale diverges at a finite temperature. If not, one should evaluate the constant and check whether the inequality indeed implies a length scale that indeed becomes “large” at low temperature. In any case, all these results, and many others, have been so influential in stressing the importance of possibly growing length scales that by now many, possibly too many, length scales have been defined and studied in the literature ([Berthier et al., 2011](#)). The more pressing open questions in this field concern the relation between the well-studied dynamical length scales (e.g., ξ_4), and the more recently devised static point-to-set length scales. Are these two types of spatial correlations related? Do structural correlations drive dynamical ones? What is their precise relation with the overall increase of the viscosity? Is there a unique way of defining static correlation length scales, and are point-to-set correlations equivalent to alternative, more geometric ways of defining static length scales ([Tarjus et al., 2005](#); [Coslovich and Pastore, 2007](#); [Kurchan and Levine, 2009](#); [Tanaka et al., 2010](#))? We believe that the intensive study of dynamical length scales in the past decade will be continued by a similar intensive search of static correlations in future work to disentangle all these issues.

B. Glass and jamming transitions

In Sec. II.B.1 we introduced the idea that many different materials undergo a fluid to amorphous solid transition reminiscent of the glass transition of molecular liquids, and indeed we included experimental or numerical results on colloids or granular materials without further discussion in the rest of the article. It is time to discuss more critically the assumption that all these materials “jam” in a similar way.

From a practical point of view, one should distinguish two distinct “solidity” transitions that can both be observed in the system of hard spheres, which we mentioned several times in

this review. At thermal equilibrium at temperature $k_B T$,⁵ hard spheres undergo in three dimensions a glass transition in the regime $\varphi_g \approx 0.57$ – 0.59 . Above this transition, the system appears as a solid, at least on experimental time scales. However, this system is compressible (it is a hard-sphere glass), its pressure is finite, and its equation of state $Z \equiv P(\varphi)/\rho k_B T = Z(\varphi)$ is a smooth function of φ across φ_g . At present, there is no indication that the physics of this first fluid-to-solid transition in the hard-sphere system at finite temperature, is any different from the glass transition observed, say, in a Lennard-Jones liquid. This means that all the concepts and theories reviewed in this paper are actually relevant to this situation. For instance, experimental evidence suggests that hard spheres undergo a change from MCT-like behavior to an activated regime when increasing φ ([Brambilla et al., 2009](#)), they display a similar spatially heterogeneous dynamics ([Weeks et al., 2000](#)), and display in analytical calculations a mode-coupling ([Barrat, et al., 1989](#)) and Kauzmann transitions ([Parisi and Zamponi, 2010](#)) completely analogous to model liquids. Interestingly, the same phenomenology is found in dense granular materials *driven*, for instance, by cyclic shear ([Marty and Dauchot, 2005](#)) or air flow ([Keys et al., 2007](#)). In these cases, a nonequilibrium steady state is reached thanks to the mechanical driving, which plays a role similar to Brownian forces in colloids. When increasing the density or decreasing the strength of the driving, these systems appear to display a “granular glass transition” with properties which are again similar to the ones observed for supercooled liquids, even at the most microscopic level ([Candelier et al., 2010](#)).

A second, distinct solidity transition occurs in hard spheres out of equilibrium. As discussed, it is not possible to compress hard spheres above a certain density and keep the system in equilibrium. This does not mean the system cannot be compressed anymore; it can, but in a nonequilibrium and protocol-dependent manner. This second solidity transition takes place when the system cannot be compressed anymore. This is mainly a geometrical problem and thermal energy plays no role in this transition. For a three-dimensional system, this occurs near random close packing $\varphi_{\text{rep}} = 0.63$ – 0.65 ([Bernal and Mason, 1960](#)). At this density, the compressibility vanishes, the reduced pressure $Z(\varphi)$ diverges, and the number of contacts per particle is exactly equal to the minimal number required for the system to behave mechanically as a solid ([Alexander, 1998](#)). This second transition is thus directly relevant to understand the static properties of granular materials. It is interesting also for systems made of large (athermal) particles such as foams and emulsions: Because the particles are soft, these systems can be compressed above φ_{rep} ([Liu and Nagel, 2001](#)). In these soft systems, the (osmotic) pressure in the solid phase is now proportional to the particle surface tension, and thus solidity is driven by the elasticity of the particles rather than temperature. From a dynamical point of view, much less is known about this second transition. Connections with the glass

⁵For hard spheres, the temperature simply sets the microscopic time scale. As long as the system is in equilibrium, the thermodynamic and dynamical properties at different temperatures are identical up to a trivial rescaling.

problem are still rather speculative but they are the focus of an intense research activity, triggered by the seminal contribution of Liu and Nagel (1998). For instance, dynamic heterogeneity at $T = 0$ near random close packing has been studied only recently (Lechenault *et al.*, 2008b; Sessoms *et al.*, 2009; Heussinger *et al.*, 2010), and important differences with the dynamics of viscous liquids were noted. Therefore, although glass and jamming transitions might be observed in the same system (say, hard spheres), they likely correspond to two distinct ways for the system to become a solid.

C. Metastability and the role of the crystal

We only briefly discussed the role of the crystalline state. As with many (but not all) researchers, we have assumed that the crystal does not play an important role for the glass transition phenomenon, apart from the fact that crystal nucleation has to be avoided by supercooling. (For all known glass formers, the melting temperature is larger than the experimental glass transition.) This may be questionable for several reasons. The first objection is that equilibrium thermodynamic theories of the glass transition are problematic because the true thermodynamic phase is indeed the crystal. This is not a real concern: Supercooled liquids are in a long-living metastable state. As long as the nucleation time is much larger than the structural relaxation time τ_α , they can be considered as *bona fide* equilibrium states, at least using Feynman's definition: "When all fast things have happened and all slow things have not, then the system is in equilibrium" (Feynman, 1972). A more serious concern is that the relaxation time of the supercooled liquid cannot really diverge at a finite temperature if the thermodynamically stable state is a crystal, because the nucleation time is necessarily finite at finite temperature if we assume a finite Gibbs free-energy difference between the crystal and the supercooled liquid.⁶ Thus, τ_α will inevitably hit the (finite) nucleation time before diverging. Below this temperature the supercooled liquid is no more a metastable state because it nucleates the crystal before actually being able to relax its structure. This, however, is also not necessarily a serious problem. First, not all theories are based on a divergence at finite temperature. Second, several theories explain the slowing down of the dynamics by the proximity to a phase transition but none of them needs the transition to actually take place to be proven correct. Thus, although important conceptually, the existence of the crystal does not imply that theories with no singularity should be preferred to describe the physically relevant temperature regime where nucleation is unimportant. A final, more physical, reason to take into account the crystal in explaining the glass transition would be that the slow dynamics in the supercooled state is due to the existence of some local order reminiscent of the crystal structure, as in frustration-limited domain approaches

⁶This is due to the fact that the maximum barrier to form the critical nucleus and also for its subsequent growth is necessarily finite; thus nuclei will form and expand even though these processes can be extremely slow. In practice, crystal nucleation can be much slower than what is expected; see Cavagna (2009).

(Tarjus *et al.*, 2005), and reemphasized in several recent numerical papers (Coslovich and Pastore, 2007; Pedersen *et al.*, 2010; Tanaka *et al.*, 2010).

D. The ideal glass transition

This is certainly a recurrent, probably utopian, but nevertheless fascinating, topic for discussion. Several theories explain the slowing down of the dynamics by the proximity to a phase transition. None of them requires that the transition actually take place. This holds either because the transition is avoided by construction as in the frustration-limited domain theory, or because it is not accessible experimentally as in dynamical facilitation theory or random first-order transition theory. What happens at lower temperatures, where no real system can be equilibrated, is, after all, just a matter of curiosity. It is interesting, however, just for a short while, to dwell on what an ideal glass transition could possibly be. It should correspond to a true divergence of the relaxation time and the viscosity at a finite temperature T_{ideal} . Because of the proof by Montanari and Semerjian (2006b) for lattice models, we now strongly suspect that static correlations, actually point-to-set correlations, would generally diverge at the transition.⁷ Thus, the transition corresponded to the development of some long-range order (likely amorphous order), since suitable boundary conditions fixed the density field in an amorphous configuration in the entire (infinite) sample.

It is also important to discuss what properties an ideal glass transition would not display. Actually, it is sometimes assumed that at an ideal glass transition, as discussed in the context of theories in Sec. IV, the dynamics would be completely arrested. This is not necessary and, actually, impossible if $T_{\text{ideal}} > 0$. For example, a probe particle will still be able to move at T_{ideal} and below. The situation would be similar to the crystalline state, where particles diffuse, although slowly, leaving the crystalline order intact. What would diverge at T_{ideal} is only the time to destroy the amorphous correlation in the density field. For example, at the ideal glass transition advocated in RFOT theory, the density field orders in one of the possible amorphous low-temperature configurations, so that the time to relax the structure becomes infinite, whereas, instead, the self-diffusion coefficient stays finite. Also, it is sometimes believed that the ideal glass transition is related to a fragmentation of the configuration space for *finite*-size systems, i.e., that below a certain temperature or above a certain density it is no more possible to go from any typical equilibrium configuration to another one. This is clearly not true, as it can be seen easily for soft particle models, and actually even for hard spheres. This can be harder to prove for some effective models (Eckmann and Procaccia, 2008). In any case, this is not what the ideal glass transition would be: Such dynamical arrests can take place only in effective theories whose domain of applicability must break down at some point (maybe not accessible in experiments).

⁷If the relaxation time scale diverges only at zero temperature but faster than Arrhenius, then the ideal glass transition would take place at $T = 0$. Again, on the basis of the bound of Montanari and Semerjian, we expect a diverging length in this case too.

Thus, the theoretical possibility of a finite-temperature ideal glass transition toward a genuine glass state exists and will no doubt continue to obsess many physicists in coming years.

E. Concluding remarks

The problem of the glass transition, already exciting in itself, has ramifications well beyond the physics of supercooled liquids. Glassy systems figure among the even larger class of “complex systems.” These are formed by a set of interacting degrees of freedom that show an emergent behavior: As a whole they exhibit properties not obvious from the properties of the individual parts. As a consequence the study of glass formers as statistical mechanics models characterized by frustrated interactions is a fertile ground to develop new concepts and techniques that will likely be applied to other physical, and more generally, scientific situations. The glass transition in supercooled liquids can, in fact, be considered as one of the simplest situations where frustration, geometry, ergodicity, and disorder compete to produce a glassy state. Hence, the concepts reviewed in this article should be directly applicable to scores of more complex systems, such as, for instance, physical gels, liquids in confined geometries, diffusion in crowded biological environments, dense granular media, self-assembly, or microfluidic flows of dense emulsions and colloidal suspensions. Thus, we certainly expect more progress to emerge in the future along these interdisciplinary routes.

ACKNOWLEDGMENTS

The views and analyses exposed in this paper are the results of interactions with a large number of researchers in this field. We thank, in particular, our collaborators on these subjects: We believe our joint work largely contributed in one way or another to this contribution. The image of colloids in Fig. 1 is taken from the home page of Professor C. Bechinger’s research group. Our work was supported by the ANR Grants CHEF, TSANET, and DYNHET. G. B. thanks A. A. for her patience without which this work and many others would not have been completed.

REFERENCES

Abate, A. R., and D. J. Durian, 2007, *Phys. Rev. E* **76**, 021306.
 Abou, B., and F. Gallet, 2004, *Phys. Rev. Lett.* **93**, 160603.
 Adam, G., and J. H. Gibbs, 1965, *J. Chem. Phys.* **43**, 139.
 Adhikari, A. N., N. A. Capurso, and D. Bingemann, 2007, *J. Chem. Phys.* **127**, 114508.
 Alder, B. J., and T. E. Wainwright, 1962, *Phys. Rev.* **127**, 359.
 Alexander, S., 1998, *Phys. Rep.* **296**, 65.
 Allen, M., and D. Tildesley, 1987, *Computer Simulation of Liquids* (Oxford University Press, Oxford).
 Alvarez, D., S. Franz, and F. Ritort, 1996, *Phys. Rev. B* **54**, 9756.
 Andersen, H. C., 2005, *Proc. Natl. Acad. Sci. U.S.A.* **102**, 6686.
 Andreanov, A., G. Biroli, and J.-P. Bouchaud, 2009, *Europhys. Lett.* **88**, 16001.
 Andreanov, A., G. Biroli, and A. Lefèvre, 2006, *J. Stat. Mech.*, P07008.
 Andreanov, A., and A. Lefèvre, 2006, *Europhys. Lett.* **76**, 919.

Angell, C. A., 1995, *Science* **267**, 1924.
 Angell, C. A., 1997, *J. Res. Natl. Inst. Stand. Technol.* **102**, 171 [<http://nvl.nist.gov/pub/nistpubs/jres/102/2/cnt102-2.htm>].
 Angell, C. A., and S. Borick, 2002, *J. Non-Cryst. Solids* **307–310**, 393.
 Angell, C. A., K. L. Ngai, G. B. McKenna, P. F. McMillan, and S. W. Martin, 2000, *J. Appl. Phys.* **88**, 3113.
 Appignanesi, G. A., J. A. Rodriguez Fris, R. A. Montani, and W. Kob, 2006, *Phys. Rev. Lett.* **96**, 057801.
 Ashcroft, N. W., and N. D. Mermin, 1976, *Solid State Physics* (Saunders College, Philadelphia).
 Ashtekar, S., G. Scott, J. Lyding, and M. Gruebele, 2010, *J. Phys. Chem. Lett.* **1**, 1941.
 Bandyopadhyay, R., D. Liang, H. Yardimci, D. A. Sessoms, M. A. Borthwick, S. G. J. Mochrie, J. L. Harden, and R. L. Leheny, 2004, *Phys. Rev. Lett.* **93**, 228302.
 Barkai, E., and Y. C. Cheng, 2003, *J. Chem. Phys.* **118**, 6167.
 Barnes, H. A., J. F. Hutton, and K. Walters, 1989, *An Introduction to Rheology* (Elsevier, Amsterdam).
 Barrat, A., 1998, *Phys. Rev. E* **57**, 3629.
 Barrat, A., and L. Berthier, 2001, *Phys. Rev. Lett.* **87**, 087204.
 Barrat, A., R. Burioni, and M. Mézard, 1996, *J. Phys. A* **29**, L81.
 Barrat, J.-L., and L. Berthier, 2000, *Phys. Rev. E* **63**, 012503.
 Barrat, J.-L., J. Dalibard, M. Feigelman, and J. Kurchan, 2003, Eds., *Slow Relaxations and Nonequilibrium Dynamics in Condensed Matter* (Springer, Berlin).
 Barrat, J.-L., W. Götze, and A. Latz, 1989, *J. Phys. Condens. Matter* **1**, 7163.
 Barrat, J.-L., and W. Kob, 1999, *Europhys. Lett.* **46**, 637.
 Barrat, J.-L., and A. Latz, 1990, *J. Phys. Condens. Matter* **2**, 4289.
 Bässler, H., 1987, *Phys. Rev. Lett.* **58**, 767.
 Bécu L., S. Manneville, and A. Colin, 2006, *Phys. Rev. Lett.* **96**, 138302.
 Bellon, L., and S. Ciliberto, 2002, *Physica (Amsterdam) D* **168–169**, 325.
 Bellon, L., S. Ciliberto, and C. Laroche, 2000, *Europhys. Lett.* **51**, 551.
 Bellon, L., S. Ciliberto, and C. Laroche, 2001, *Europhys. Lett.* **53**, 511.
 Bellour, M., A. Knaebel, J. L. Harden, and J. P. Munch, 2003, *Phys. Rev. E* **67**, 031405.
 Bengtzelius, U., 1986, *Phys. Rev. A* **34**, 5059.
 Bengtzelius, U., W. Götze, and A. Sjölander, 1984, *J. Phys. C* **17**, 5915.
 Bennemann, C., C. Donati, J. Baschnagel, and S. C. Glotzer, 1999, *Nature (London)* **399**, 246.
 Bernal, J. D., and J. Mason, 1960, *Nature (London)* **188**, 910.
 Berthier, L., 2003a, *J. Phys. Condens. Matter* **15**, S933.
 Berthier, L., 2003b, *Phys. Rev. Lett.* **91**, 055701.
 Berthier, L., 2004, *Phys. Rev. E* **69**, 020201(R).
 Berthier, L., 2007a, *Phys. Rev. E* **76**, 011507.
 Berthier, L., 2007b, *Phys. Rev. Lett.* **98**, 220601.
 Berthier, L., G. Biroli, J.-P. Bouchaud, L. Cipelletti, D. El Masri, D. L’Hôte, F. Ladieu, and M. Pierno, 2005, *Science* **310**, 1797.
 Berthier, L., G. Biroli, J.-P. Bouchaud, L. Cipelletti, and W. van Saarloos, 2011, Eds., *Dynamical Heterogeneities in Glasses, Colloids, and Granular Media* (Oxford University Press, Oxford).
 Berthier, L., G. Biroli, J.-P. Bouchaud, W. Kob, K. Miyazaki, and D. R. Reichman, 2007a, *J. Chem. Phys.* **126**, 184503.
 Berthier, L., G. Biroli, J.-P. Bouchaud, W. Kob, K. Miyazaki, and D. R. Reichman, 2007b, *J. Chem. Phys.* **126**, 184504.
 Berthier, L., D. Chandler, and J. P. Garrahan, 2005, *Europhys. Lett.* **69**, 320.

- Berthier, L., and J. P. Garrahan, 2003a, *J. Chem. Phys.* **119**, 4367.
- Berthier, L., and J. P. Garrahan, 2003b, *Phys. Rev. E* **68**, 041201.
- Berthier, L., and J. P. Garrahan, 2005, *J. Phys. Chem. B* **109**, 3578.
- Berthier, L., and J.-L. Barrat, 2002a, *Phys. Rev. Lett.* **89**, 095702.
- Berthier, L., and J.-L. Barrat, 2002b, *J. Chem. Phys.* **116**, 6228.
- Berthier, L., J.-L. Barrat, and J. Kurchan, 1999, *Eur. Phys. J. B* **11**, 635.
- Berthier, L., J.-L. Barrat, and J. Kurchan, 2000, *Phys. Rev. E* **61**, 5464.
- Berthier, L., J.-L. Barrat, and J. Kurchan, 2000, *Phys. Rev. E* **63**, 016105.
- Berthier, L., and J.-P. Bouchaud, 2002, *Phys. Rev. B* **66**, 054404.
- Berthier, L., and W. Kob, 2007, *J. Phys. Condens. Matter* **19**, 205130.
- Berthier, L., V. Viasnoff, O. White, V. Orlyanchik, and F. Krzakala, 2003, *Slow Relaxations and Nonequilibrium Dynamics in Condensed Matter* (Springer, Berlin).
- Bertin, E., 2005, *Europhys. Lett.* **71**, 452.
- Besseling, R., L. Isa, P. Ballesta, G. Petekidis, M. E. Cates, and W. C. K. Poon, 2010, [arXiv:1009.1579](https://arxiv.org/abs/1009.1579).
- Besseling, R., E. R. Weeks, A. B. Schofield, and W. C. K. Poon, 2007, *Phys. Rev. Lett.* **99**, 028301.
- Bhattacharya, S. M., B. Bagchi, and P. G. Wolynes, 2005, *Phys. Rev. E* **72**, 031509.
- Biazzo, I., F. Caltagirone, G. Parisi, and F. Zamponi, 2009, *Phys. Rev. Lett.* **102**, 195701.
- Binder, K., and W. Kob, 2005, *Glassy Materials and Disordered Solids* (World Scientific, Singapore).
- Binder, K., and A. P. Young, 1986, *Rev. Mod. Phys.* **58**, 801.
- Biroli, G., and J. P. Bouchaud, 2004, *Europhys. Lett.* **67**, 21.
- Biroli, G., and J.-P. Bouchaud, 2009, [arXiv:0912.2542](https://arxiv.org/abs/0912.2542).
- Biroli, G., and J.-P. Bouchaud, 2007, *J. Phys. Condens. Matter* **19**, 205101.
- Biroli, G., J.-P. Bouchaud, A. Cavagna, T. S. Grigera, and P. Verrocchio, 2008, *Nature Phys.* **4**, 771.
- Biroli, G., J.-P. Bouchaud, K. Miyazaki, and D. R. Reichman, 2006, *Phys. Rev. Lett.* **97**, 195701.
- Biroli, G., J.-P. Bouchaud, and G. Tarjus, 2005, *J. Chem. Phys.* **123**, 044510.
- Biroli, G., and J. Kurchan, 2001, *Phys. Rev. E* **64**, 016101.
- Biroli, G., and M. Mézard, 2001, *Phys. Rev. Lett.* **88**, 025501.
- Biroli, G., and R. Monasson, 2000, *Europhys. Lett.* **50**, 155.
- Blochowicz, T., C. Gainaru, P. Medick, C. Tschirwitz, and E. A. RöSSLer, 2006, *J. Chem. Phys.* **124**, 134503.
- Bocquet, L., A. Colin, and A. Ajdari, 2009, *Phys. Rev. Lett.* **103**, 036001.
- Bouchaud, J. P., 1992, *J. Phys. I (France)* **2**, 1705.
- Bouchaud, J.-P., and G. Biroli, 2004, *J. Chem. Phys.* **121**, 7347.
- Bouchaud, J.-P., and G. Biroli, 2005, *Phys. Rev. B* **72**, 064204.
- Bouchaud, J.-P., L. Cugliandolo, J. Kurchan, and M. Mézard, 1996, *Physica (Amsterdam)* **226A**, 243.
- Bouchaud, J.-P., V. Dupuis, J. Hammann, and E. Vincent, 2001, *Phys. Rev. B* **65**, 024439.
- Bouchaud, J.-P., and E. Pitard, 2001, *Eur. Phys. J. E* **6**, 231.
- Bouchbinder, E., 2008, *Phys. Rev. E* **77**, 051505.
- Brader, J. M., M. E. Cates, and M. Fuchs, 2008, *Phys. Rev. Lett.* **101**, 138301.
- Brader, J. M., T. Voigtmann, M. E. Cates, and M. Fuchs, 2007, *Phys. Rev. Lett.* **98**, 058301.
- Brader, J. M., T. Voigtmann, M. Fuchs, R. G. Larson, and M. E. Cates, 2009, *Proc. Natl. Acad. Sci. U.S.A.* **106**, 15 186.
- Brambilla, G., D. El Masri, M. Pierno, L. Berthier, L. Cipelletti, G. Petekidis, and A. B. Schofield, 2009, *Phys. Rev. Lett.* **102**, 085703.
- Brangian, C., W. Kob, and K. Binder, 2002, *Europhys. Lett.* **59**, 546.
- Bray, A. J., 1994, *Adv. Phys.* **43**, 357.
- Brazovskii, S. A., 1975, *Sov. Phys. JETP* **41**, 85.
- Buisson, L., L. Bellon, and S. Ciliberto, 2003, *J. Phys. Condens. Matter* **15**, S1163.
- Buisson, L., S. Ciliberto, and A. Garcimartin, 2003, *Europhys. Lett.* **63**, 603.
- Butler, S., and P. Harrowell, 1991a, *J. Chem. Phys.* **95**, 4454.
- Butler, S., and P. Harrowell, 1991b, *J. Chem. Phys.* **95**, 4466.
- Calabrese, P., and A. Gambassi, 2004, *J. Stat. Mech.*, P07013.
- Calabrese, P., and A. Gambassi, 2005, *J. Phys. A* **38**, R133.
- Calabrese, P., A. Gambassi, and F. Krzakala, 2006, *J. Stat. Mech.*, P0606016.
- Camarrota, C., A. Cavagna, G. Gradenigo, T. S. Grigera, and P. Verrocchio, 2009, *J. Stat. Mech.*, L12002.
- Camarrota, C., A. Cavagna, G. Gradenigo, T. S. Grigera, and P. Verrocchio, 2009, *J. Chem. Phys.* **131**, 194901.
- Candelier, R., O. Dauchot, and G. Biroli, 2009, [arXiv:0912.0472](https://arxiv.org/abs/0912.0472).
- Candelier, R., A. Widmer-Cooper, J. K. Kummerfeld, O. Dauchot, G. Biroli, P. Harrowell, and D. R. Reichman, 2010, *Phys. Rev. Lett.* **105**, 135702.
- Capaccioli, S., G. Ruocco, and F. Zamponi, 2008, *J. Phys. Chem. B* **112**, 10 652.
- Castellana, M., A. Decelle, S. Franz, M. Mézard, and G. Parisi, 2010, *Phys. Rev. Lett.* **104**, 127206.
- Castellani, T., and A. Cavagna, 2005, *J. Stat. Mech.*, P05012.
- Castillo, H. E., C. Chamon, L. F. Cugliandolo, and M. P. Kennett, 2002, *Phys. Rev. Lett.* **88**, 237201.
- Castillo, H. E., and A. Parsaeian, 2007, *Nature Phys.* **3**, 26.
- Cates, M. E., 2003, *Slow Relaxations and Nonequilibrium Dynamics in Condensed Matter* (Springer, Berlin).
- Cates, M. E., and S. Ramaswamy, 2006, *Phys. Rev. Lett.* **96**, 135701.
- Cavagna, A., 2009, *Phys. Rep.* **476**, 51.
- Cavagna, A., T. S. Grigera, and P. Verrocchio, 2007, *Phys. Rev. Lett.* **98**, 187801.
- Chaikin, P. M., and T. C. Lubensky, 2000, *Principles of Condensed Matter Physics* (Cambridge University Press, Cambridge).
- Chamon, C., P. Charbonneau, L. F. Cugliandolo, D. R. Reichman, and M. Sellitto, 2004, *J. Chem. Phys.* **121**, 10 120.
- Chamon, C., and L. F. Cugliandolo, 2007, *J. Stat. Mech.*, P07022.
- Chandler, D., 1987, *Introduction to Modern Statistical Mechanics* (Oxford University Press, Oxford).
- Chandler, D., and J. P. Garrahan, 2005, *J. Chem. Phys.* **123**, 044511.
- Chandler, D., and J. P. Garrahan, 2010, *Annu. Rev. Phys. Chem.* **61**, 191.
- Chandler, D., J. P. Garrahan, R. L. Jack, L. Maibaum, and A. C. Pan, 2006, *Phys. Rev. E* **74**, 051501.
- Chaudhuri, P., L. Berthier, and W. Kob, 2007, *Phys. Rev. Lett.* **99**, 060604.
- Chaudhuri, P., S. Karmakar, and C. Dasgupta, 2008, *Phys. Rev. Lett.* **100**, 125701.
- Chaudhuri, P., S. Sastry, and W. Kob, 2008, *Phys. Rev. Lett.* **101**, 190601.
- Chayes, L., V. J. Emery, S. A. Kivelson, Z. Nussinov, and G. Tarjus, 1996, *Physica (Amsterdam)* **225A**, 129.
- Chen, K., E. J. Saltzman, and K. S. Schweizer, 2010, *Annu. Rev. Condens. Matter Phys.* **1**, 277.
- Chen, S. H., Y. Zhang, M. Lagi, S. H. Chong, P. Baglioni, and F. Mallamace, 2009, *J. Phys. Condens. Matter* **21**, 504102.
- Cheng, Z., J. Zhu, P. M. Chaikin, S.-E. Phan, and W. B. Russel, 2002, *Phys. Rev. E* **65**, 041405.
- Cipelletti, L., S. Manley, R. C. Ball, and D. A. Weitz, 2000, *Phys. Rev. Lett.* **84**, 2275.

- Cipelletti, L., and L. Ramos, 2005, *J. Phys. Condens. Matter* **17**, R253.
- Cohen, M.H., and G.S. Grest, 1982, *Phys. Rev. B* **26**, 6313.
- Coluzzi, B., M. Mézard, G. Parisi, and P. Verrocchio, 1999, *J. Chem. Phys.* **111**, 9039.
- Coluzzi, B., G. Parisi, and P. Verrocchio, 2000, *Phys. Rev. Lett.* **84**, 306.
- Coluzzi, B., and P. Verrocchio, 2002, *J. Chem. Phys.* **116**, 3789.
- Coslovich, D., and G. Pastore, 2007, *J. Chem. Phys.* **127**, 124504.
- Coussot, P., Q.D. Nguyen, H.T. Huynh, and D. Bonn, 2002, *Phys. Rev. Lett.* **88**, 175501.
- Crassous, J.J., M. Siebenbürger, M. Ballauff, M. Drechsler, O. Henrich, and M. Fuchs, 2006, *J. Chem. Phys.* **125**, 204906.
- Crauste-Thibierge, C., C. Brun, F. Ladiou, D. L'Hôte, G. Biroli, and J.-P. Bouchaud, 2010, *Phys. Rev. Lett.* **104**, 165703.
- Crisanti, A., and F. Ritort, 2003, *J. Phys. A* **36**, R181.
- Cugliandolo, L.F., 2003, *Slow Relaxations and Nonequilibrium Dynamics in Condensed Matter* (Springer, Berlin).
- Cugliandolo, L.F., and J. Kurchan, 1993, *Phys. Rev. Lett.* **71**, 173.
- Cugliandolo, L.F., and J. Kurchan, 1994, *J. Phys. A* **27**, 5749.
- Cugliandolo, L.F., and J. Kurchan, 1999, *Phys. Rev. B* **60**, 922.
- Cugliandolo, L.F., J. Kurchan, P. Le Doussal, and L. Peliti, 1997, *Phys. Rev. Lett.* **78**, 350.
- Cugliandolo, L.F., J. Kurchan, and L. Peliti, 1997, *Phys. Rev. E* **55**, 3898.
- Dalle-Ferrier, C., S. Eibl, C. Pappas, and C. Alba-Simionesco, 2008, *J. Phys. Condens. Matter* **20**, 494240.
- Dalle-Ferrier, C., C. Thibierge, C. Alba-Simionesco, L. Berthier, G. Biroli, J.-P. Bouchaud, F. Ladiou, D. L'Hôte, and G. Tarjus, 2007, *Phys. Rev. E* **76**, 041510.
- D'Anna, G., and G. Gremaud, 2001, *Nature (London)* **413**, 407.
- Darst, R.K., D.R. Reichman, and G. Biroli, 2010, *J. Chem. Phys.* **132**, 044510.
- Das, S.P., 1990, *Phys. Rev. A* **42**, 6116.
- Das, S.P., 2004, *Rev. Mod. Phys.* **76**, 785.
- Das, S.P., and G.F. Mazenko, 1986, *Phys. Rev. A* **34**, 2265.
- Das, S.P., G.F. Mazenko, S. Ramaswamy, and J.J. Toner, 1985, *Phys. Rev. Lett.* **54**, 118.
- Dasgupta, C., A.V. Indrani, S. Ramaswamy, and M.K. Phani, 1991, *Europhys. Lett.* **15**, 307.
- Dasgupta, C., and O.T. Valls, 2000, *J. Phys. Condens. Matter* **12**, 6553.
- Dauchot, O., G. Marty, and G. Biroli, 2005, *Phys. Rev. Lett.* **95**, 265701.
- Debenedetti, P.G., 1996, *Metastable Liquids* (Princeton University Press, Princeton).
- Debenedetti, P.G. and F.H. Stillinger, 2001, *Nature (London)* **410**, 259.
- Denny, R. A., D. R. Reichman, and J.-P. Bouchaud, 2003, *Phys. Rev. Lett.* **90**, 025503.
- Depken, M., and R. Stinchcombe, 2005, *Phys. Rev. E* **71**, 065102.
- Di Leonardo, R., L. Angelani, G. Parisi, and G. Ruocco, 2000, *Phys. Rev. Lett.* **84**, 6054.
- Dixon, P.K., L. Wu, S.R. Nagel, B.D. Williams, and J.P. Carini, 1990, *Phys. Rev. Lett.* **65**, 1108.
- Doliwa, B., and A. Heuer, 2000, *Phys. Rev. E* **61**, 6898.
- Doliwa, B., and A. Heuer, 2003, *Phys. Rev. E* **67**, 030501.
- Donati, C., J. Douglas, W. Kob, S.J. Plimpton, P.H. Poole, and S.C. Glotzer, 1998, *Phys. Rev. Lett.* **80**, 2338.
- Donati, C., S.C. Glotzer, and P.H. Poole, 1999, *Phys. Rev. Lett.* **82**, 5064.
- Donev, A., F.H. Stillinger, and S. Torquato, 2007, *J. Chem. Phys.* **127**, 124509.
- Donth, E., 2001, *The Glass Transition* (Springer, Berlin).
- Doussineau, P., T. de Lacerda-Aroso, and A. Levelut, 1999, *Europhys. Lett.* **46**, 401.
- Downton, M. T., and M. P. Kennett, 2007, *Phys. Rev. E* **76**, 031502.
- Duri, A., and L. Cipelletti, 2006, *Europhys. Lett.* **76**, 972.
- Duri, A., D.A. Sessoms, V. Trappe, and L. Cipelletti, 2009, *Phys. Rev. Lett.* **102**, 085702.
- Dyre, J., 1995, *Phys. Rev. B* **51**, 12 276.
- Dyre, J., 2006, *Rev. Mod. Phys.* **78**, 953.
- Dzero, M., J. Schmalian, and P.G. Wolynes, 2005, *Phys. Rev. B* **72**, 100201.
- Eckmann, J.P., and I. Procaccia, 2008, *Phys. Rev. E* **78**, 011503.
- Ediger, M.D., 1998, *J. Non-Cryst. Solids* **235–237**, 10.
- Ediger, M.D., 2000, *Annu. Rev. Phys. Chem.* **51**, 99.
- Edwards, S.F., and P.W. Anderson, 1975, *J. Phys. F* **5**, 965.
- El Masri, D., L. Berthier, and L. Cipelletti, 2010, *Phys. Rev. E* **82**, 031503.
- Elmatad, Y.S., D. Chandler, and J.P. Garrahan, 2009, *J. Phys. Chem. B* **113**, 5563.
- Elmatad, Y.S., R.L. Jack, J.P. Garrahan, and D. Chandler, 2010, *arXiv:1003.3161*.
- Evans, D.J., and G. Morris, 2008, *Statistical Mechanics of Nonequilibrium Liquids* (Cambridge University Press, Cambridge).
- Fabry, B., G.N. Maksym, J.P. Butler, M. Glogauer, D. Navajas, and J.J. Fredberg, 2001, *Phys. Rev. Lett.* **87**, 148102.
- Falk, M.L., and J.S. Langer, 1998, *Phys. Rev. E* **57**, 7192.
- Fernandez, L.A., V. Martin-Mayor, and P. Verrocchio, 2006, *Phys. Rev. E* **73**, 020501.
- Feynman, R., 1972, *Statistical Mechanics: A Set of Lectures* (Addison-Wesley, Reading).
- Fielding, S., and P. Sollich, 2002, *Phys. Rev. Lett.* **88**, 050603.
- Fielding, S.M., M.E. Cates, and P. Sollich, 2009, *Soft Matter* **5**, 2378.
- Fielding, S.M., P. Sollich, and M.E. Cates, 2000, *J. Rheol.* **44**, 323.
- D. S. Fisher, 2003, *Slow Relaxations and Nonequilibrium Dynamics in Condensed Matter* (Springer, Berlin).
- Flenner, E., and G. Szamel, 2007, *J. Phys. Condens. Matter* **19**, 205125.
- Flenner, E., and G. Szamel, 2010, *Phys. Rev. Lett.* **105**, 217801.
- Foffi, G., W. Götze, F. Sciortino, P. Tartaglia, and T. Voigtmann, 2003, *Phys. Rev. Lett.* **91**, 085701.
- Frank, F.C., 1952, *Proc. R. Soc. London* **215**, 43.
- Franz, S., 2005, *J. Stat. Mech.*, P04001.
- Franz, S., 2006, *Europhys. Lett.* **73**, 492.
- Franz, S., M. Cardenas, and G. Parisi, 1998, *J. Phys. A* **31**, L163.
- Franz, S., C. Donati, G. Parisi, and S.C. Glotzer, 1999, *Philos. Mag. B* **79**, 1827.
- Franz, S., M. Mézard, G. Parisi, and L. Peliti, 1998, *Phys. Rev. Lett.* **81**, 1758.
- Franz, S., and A. Montanari, 2007, *J. Phys. A* **40**, F251.
- Franz, S., R. Mulet, and G. Parisi, 2002, *Phys. Rev. E* **65**, 021506.
- Franz, S., and G. Parisi, 1998, *Physica (Amsterdam)* **261A**, 317.
- Franz, S., and G. Parisi, 2000, *J. Phys. Condens. Matter* **12**, 6335.
- Franz, S., G. Parisi, F. Ricci-Tersenghi, and T. Rizzo, 2010, *arXiv:1001.1746*.
- Franz, S., and M.A. Virasoro, 2000, *J. Phys. A* **33**, 891.
- Fredrickson, G.H., 1986, *Ann. N.Y. Acad. Sci.* **484**, 185.
- Fredrickson, G.H., and H.C. Andersen, 1984, *Phys. Rev. Lett.* **53**, 1244.
- Fredrickson, G.H., and H.C. Andersen, 1985, *J. Chem. Phys.* **83**, 5822.
- Fredrickson, G.H., and S.A. Brawer, 1986, *J. Chem. Phys.* **84**, 3351.

- Fuchs, M., and M.E. Cates, 2002, *Phys. Rev. Lett.* **89**, 248304.
- Fuchs, M., and M.E. Cates, 2005, *J. Phys. Condens. Matter* **17**, S1681.
- Fuchs, M., and M.E. Cates, 2009, *J. Rheol.* **53**, 957.
- Fuchs, M., W. Götze, and M.R. Mayr, 1998, *Phys. Rev. E* **58**, 3384.
- Fukao, K., and A. Sakamoto, 2005, *Phys. Rev. E* **71**, 041803.
- Furukawa, A., K. Kim, S. Saito, and H. Tanaka, 2009, *Phys. Rev. Lett.* **102**, 016001.
- Gainaru, C., W. Hiller, and R. Boehmer, 2010, *Macromolecules* **43**, 1907.
- Garrahan, J.P., 2002, *J. Phys. Condens. Matter* **14**, 1571.
- Garrahan, J.P., and D. Chandler, 2002, *Phys. Rev. Lett.* **89**, 035704.
- Garrahan, J.P., and D. Chandler, 2003, *Proc. Natl. Acad. Sci. U.S.A.* **100**, 9710.
- Garrahan, J.P., R.L. Jack, V. Lecomte, E. Pitard, K. van Duijvendijk, and F. van Wijland, 2009, *J. Phys. A* **42**, 075007.
- Geissler, P.L., and D.R. Reichman, 2003, *cond-mat/0307176*.
- Geissler, P.L., and D.R. Reichman, 2004, *Phys. Rev. E* **69**, 021501.
- Glarum, S.H., 1960, *J. Chem. Phys.* **33**, 639.
- Gleim, T., W. Kob, and K. Binder, 1998, *Phys. Rev. Lett.* **81**, 4404.
- Glotzer, S.C., 2000, *J. Non-Cryst. Solids* **274**, 342.
- Godrèche, C., and J.-M. Luck, 2000a, *J. Phys. A* **33**, 1151.
- Godrèche, C., and J.-M. Luck, 2000b, *J. Phys. A* **33**, 9141.
- Goldstein, M., 1969, *J. Chem. Phys.* **51**, 3728.
- Götze, W., 1985, *Z. Phys. B* **60**, 195.
- Götze, W., 1999, *J. Phys. Condens. Matter* **11**, A1.
- Götze, W., 2008, *Complex Dynamics of Glass-Forming Liquids: A Mode-Coupling Theory* (Oxford University Press, Oxford).
- Götze, W., and L. Sjögren, 1987, *Z. Phys. B* **65**, 415.
- Goyon, J., A. Colin, G. Ovarlez, A. Ajdari, and L. Bocquet, 2008, *Nature (London)* **454**, 84.
- Greinert, N., T. Wood, and P. Bartlett, 2006, *Phys. Rev. Lett.* **97**, 265702.
- Grigera, T.S., and N.E. Israeloff, 1999, *Phys. Rev. Lett.* **83**, 5038.
- Gross, J., and M. Mézard, 1984, *Nucl. Phys.* **B240**, 431.
- Grousson, M., G. Tarjus, and P. Viot, 2001, *Phys. Rev. Lett.* **86**, 3455.
- Grousson, M., G. Tarjus, and P. Viot, 2002, *Phys. Rev. E* **65**, 065103.
- Guo, H. Y., G. Bourret, M. K. Corbierre, S. Rucareanu, R. B. Lenox, K. Laaziri, L. Piche, M. Sutton, J.L. Harden, and R.L. Leheny, 2009, *Phys. Rev. Lett.* **102**, 075702.
- Hansen, J.P., and I.R. McDonald, 2006, *Theory of Simple Liquids* (Academic, London).
- Hansen-Goos, H., and M. Weigt, 2005, *J. Stat. Mech.*, P04006.
- Harrowell, P., 1993, *Phys. Rev. E* **48**, 4359.
- Haxton, T.K., and A.J. Liu, 2007, *Phys. Rev. Lett.* **99**, 195701.
- He, Y., S. Burov, R. Metzler, and E. Barkai, 2008, *Phys. Rev. Lett.* **101**, 058101.
- Hébraud, P., and F. Lequeux, 1998, *Phys. Rev. Lett.* **81**, 2934.
- Hecksher, T., A.I. Nielsen, N.B. Olsen, and J. Dyre, 2008, *Nature Phys.* **4**, 737.
- Hedges, L.O., R.L. Jack, J.P. Garrahan, and D. Chandler, 2009, *Science* **323**, 1309.
- Hedges, L.O., L. Maibaum, D. Chandler, and J.P. Garrahan, 2007, *J. Chem. Phys.* **127**, 211101.
- Heuer, A., 2008, *J. Phys. Condens. Matter* **20**, 373101.
- Heussinger, C., L. Berthier, and J.-L. Barrat, 2010, *Europhys. Lett.* **90**, 20005.
- Hewson, A.C., 1997, *The Kondo Problem to Heavy Fermions* (Cambridge University Press, Cambridge).
- Hodge, I.M., 1997, *J. Res. Natl. Inst. Stand. Technol.* **102**, 195 [<http://nvl.nist.gov/pub/nistpubs/jres/102/2/cnt102-2.htm>].
- Horbach, J., and W. Kob, 2001, *Phys. Rev. E* **64**, 041503.
- Horner, H., 1996, *Z. Phys. B* **100**, 243.
- Ianni, F., R. Di Leonardo, S. Gentilini, and G. Ruocco, 2008, *Phys. Rev. E* **77**, 031406.
- Ikeda, A., and K. Miyazaki, 2010, *Phys. Rev. Lett.* **104**, 255704.
- Ilg, P., and J.-L. Barrat, 2007, *Europhys. Lett.* **79**, 26001.
- Isa, L., R. Besseling, A.N. Morozov, and W.C.K. Poon, 2009, *Phys. Rev. Lett.* **102**, 058302.
- Jabbari-Farouji, S., D. Mizuno, D. Derks, G.H. Wegdam, F.C. MacKintosh, C.F. Schmidt, and D. Bonn, 2008, *Europhys. Lett.* **84**, 20006.
- Jack, R.L., L. Berthier, and J.P. Garrahan, 2006, *J. Stat. Mech.*, P12005.
- Jack, R.L., L. Berthier, and J.P. Garrahan, 2005, *Phys. Rev. E* **72**, 016103.
- Jack, R.L., and J.P. Garrahan, 2005, *J. Chem. Phys.* **123**, 164508.
- Jack, R.L., and J.P. Garrahan, 2010, *Phys. Rev. E* **81**, 011111.
- Jack, R.L., P. Mayer, and P. Sollich, 2006, *J. Stat. Mech.*, P03006.
- Jäckle, J., and S. Eisinger, 1991, *Z. Phys. B* **84**, 115.
- Jäckle, J., and A. Krönig, 1994, *J. Phys. Condens. Matter* **6**, 7633.
- Jaeger, H.M., S.R. Nagel, and R.P. Behringer, 1996, *Rev. Mod. Phys.* **68**, 1259.
- Jakobsen, B., K. Niss, and N.B. Olsen, 2005, *J. Chem. Phys.* **123**, 234511.
- Johari, G.P., 2000, *J. Chem. Phys.* **112**, 8958.
- Johari, G.P., and M. Goldstein, 1970, *J. Chem. Phys.* **53**, 2372.
- Jönsson, P.E., R. Mathieu, P. Nordblad, H. Yoshino, H. Aruga Katori, and A. Ito, 2004, *Phys. Rev. B* **70**, 174402.
- Jop, P., J.R. Gomez-Solano, A. Petrosyan, and S. Ciliberto, 2009, *J. Stat. Mech.*, P04012.
- Joubaud, S., B. Percier, A. Petrosyan, and S. Ciliberto, 2009, *Phys. Rev. Lett.* **102**, 130601.
- Jung, Y., J.P. Garrahan, and D. Chandler, 2004, *Phys. Rev. E* **69**, 061205.
- Karmakara, S., C. Dasgupta, and S. Sastry, 2009, *Proc. Natl. Acad. Sci. U.S.A.* **106**, 3675.
- Kauzmann, A.W., 1948, *Chem. Rev.* **43**, 219.
- Kegel, W.K., and A. van Blaaderen, 2000, *Science* **287**, 290.
- Keys, A.S., A.R. Abate, S.C. Glotzer, and D.J. Durian, 2007, *Nature Phys.* **3**, 260.
- Kim, B., and K. Kawasaki, 2008, *J. Stat. Mech.*, P02004.
- Kim, B., and A. Latz, 2001, *Europhys. Lett.* **53**, 660.
- Kirkpatrick, T.R., and D. Thirumalai, 1987, *Phys. Rev. Lett.* **58**, 2091.
- Kirkpatrick, T.R., and D. Thirumalai, 1988, *Phys. Rev. A* **37**, 4439.
- Kirkpatrick, T.R., D. Thirumalai, and P.G. Wolynes, 1989, *Phys. Rev. A* **40**, 1045.
- Kirkpatrick, T.R., and P.G. Wolynes, 1987, *Phys. Rev. A* **35**, 3072.
- Kivelson, D., S.A. Kivelson, X.-L. Zhao, Z. Nussinov, and G. Tarjus, 1995, *Physica (Amsterdam)* **219A**, 27.
- Kob, W., 2003, in *Slow Relaxations and Nonequilibrium Dynamics in Condensed Matter*, edited by J.-L. Barrat, M.V. Feigelman, J. Kurchan, and J. Dalibard (Springer-Verlag, Berlin).
- Kob, W., and H.C. Andersen, 1993, *Phys. Rev. E* **48**, 4364.
- Kob, W., and H.C. Andersen, 1994, *Phys. Rev. Lett.* **73**, 1376.
- Kob, W., and H.C. Andersen, 1995a, *Phys. Rev. E* **51**, 4626.
- Kob, W., and H.C. Andersen, 1995b, *Phys. Rev. E* **52**, 4134.
- Kob, W., C. Donati, S.J. Plimpton, P.H. Poole, and S.C. Glotzer, 1997, *Phys. Rev. Lett.* **79**, 2827.
- Koppensteiner, J., W. Schranz, and M.A. Carpenter, 2010, *Phys. Rev. B* **81**, 024202.
- Kovacs, A.J., 1963, *Adv. Polym. Sci.* **3**, 394.
- Krüger, M., and M. Fuchs, 2010, *Phys. Rev. E* **81**, 011408.
- Krzakala, F., 2005, *Phys. Rev. Lett.* **94**, 077204.
- Krzakala, F., A. Montanari, F. Ricci-Tersenghi, G. Semerjian, and L. Zdeborová, 2007, *Proc. Natl. Acad. Sci. U.S.A.* **104**, 10318.

- Kurchan, J., 2001, *Jamming and Rheology* (Taylor and Francis, New York).
- Kurchan, J., 2005, *Nature (London)* **433**, 222.
- Kurchan, J., and L. Laloux, 1996, *J. Phys. A* **29**, 1929.
- Kurchan, J., and D. Levine, 2009, [arXiv:0904.4850](https://arxiv.org/abs/0904.4850).
- Kurchan, J., 2003, *Markov Processes and Related Fields* **9**, 243.
- Kurchan, J., L. Peliti, and M. Sellitto, 1997, *Europhys. Lett.* **39**, 365.
- Lacevic, N., F.W. Starr, T.B. Schroder, and S.C. Glotzer, 2003, *J. Chem. Phys.* **119**, 7372.
- Lacevic, N., F.W. Starr, T.B. Schroder, V.N. Novikov, and S.C. Glotzer, 2002, *Phys. Rev. E* **66**, 030101.
- Langer, J.S., and M.L. Manning, 2007, *Phys. Rev. E* **76**, 056107.
- Larson, R.G., 1999, *The Structure and Rheology of Complex Fluids* (Oxford University Press, New York).
- Latz, A., 2000, *J. Phys. Condens. Matter* **12**, 6353.
- Lebowitz, J.L., J.K. Percus, and L. Verlet, 1967, *Phys. Rev.* **153**, 250.
- Lechenault, F., O. Dauchot, G. Biroli, and J.P. Bouchaud, 2008a, *Europhys. Lett.* **83**, 46002.
- Lechenault, F., O. Dauchot, G. Biroli, and J.P. Bouchaud, 2008b, *Europhys. Lett.* **83**, 46003.
- Leheny, R.L., and S.R. Nagel, 1998, *Phys. Rev. B* **57**, 5154.
- Leibler, L., 1980, *Macromolecules* **13**, 1602.
- Lemaître, A., and C. Caroli, 2009, *Phys. Rev. Lett.* **103**, 065501.
- Léonard, S., P. Mayer, P. Sollich, L. Berthier, and J.P. Garrahan, 2007, *J. Stat. Mech.*, P07017.
- Leutheusser, E., 1984, *Phys. Rev. A* **29**, 2765.
- Leuzzi, L., and T.M. Nieuwenhuizen, 2007, *Thermodynamics of The Glassy State* (Taylor and Francis, New York).
- Liers, F., E. Marinari, U. Pagacz, F. Ricci-Tersenghi, and V. Schmitz, 2010, *J. Stat. Mech.*, L05003.
- Lipowski, A., D. Johnston, and D. Espriu, 2000, *Phys. Rev. E* **62**, 3404.
- Lippiello, E., and M. Zannetti, 2000, *Phys. Rev. E* **61**, 3369.
- Liu, A.J., and S.R. Nagel, 1998, *Nature (London)* **396**, 21.
- Liu, A.J. and S.R. Nagel, 2001, Eds., *Jamming and Rheology* (Taylor and Francis, New York).
- Lubchenko, V., 2009, *Proc. Natl. Acad. Sci. U.S.A.* **106**, 11 506.
- Lubchenko, V., and P.G. Wolynes, 2004, *J. Chem. Phys.* **121**, 2852.
- Lubchenko, V., and P.G. Wolynes, 2007, *Annu. Rev. Phys. Chem.* **58**, 235.
- Lunkenheimer, P., R. Wehn, U. Schneider, and A. Loidl, 2005, *Phys. Rev. Lett.* **95**, 055702.
- Maccarrone, S., *et al.*, 2010, *Soft Matter* **6**, 5514.
- Mackowiak, S. A., T.K. Herman, and L.J. Kaufman, 2009, *J. Chem. Phys.* **131**, 244513.
- Maggi, C., B. Jakobsen, and J.C. Dyre, 2010, [arXiv:1003.0341](https://arxiv.org/abs/1003.0341).
- Maloney, C.E., and A. Lemaître, 2006, *Phys. Rev. E* **74**, 016118.
- Mamane, A., C. Fretigny, F. Lequeux, and L. Talini, 2009, *Europhys. Lett.* **88**, 58002.
- Manning, M.L., J.S. Langer, and J.M. Carlson, 2007, *Phys. Rev. E* **76**, 056106.
- Mapes, M.K., S.F. Swallen, and M.D. Ediger, 2006, *J. Phys. Chem. B* **110**, 507.
- Margolin, G., and E. Barkai, 2006, *J. Stat. Phys.* **122**, 137.
- Martinez, L.-M., and C.A. Angell, 2001, *Nature (London)* **410**, 663.
- Marty, G., and O. Dauchot, 2005, *Phys. Rev. Lett.* **94**, 015701.
- Mayer, P., L. Berthier, J.P. Garrahan, and P. Sollich, 2003, *Phys. Rev. E* **68**, 016116.
- Mayer, P., H. Bissig, L. Berthier, L. Cipelletti, J.P. Garrahan, P. Sollich, and V. Trappe, 2004, *Phys. Rev. Lett.* **93**, 115701.
- Mayer, P., S. Léonard, L. Berthier, J.P. Garrahan, and P. Sollich, 2006, *Phys. Rev. Lett.* **96**, 030602.
- Mayer, P., K. Miyazaki, and D.R. Reichman, 2006, *Phys. Rev. Lett.* **97**, 095702.
- Mayer, P., and P. Sollich, 2007, *J. Phys. A* **40**, 5823.
- Mazoyer, S., L. Cipelletti, and L. Ramos, 2009, *Phys. Rev. E* **79**, 011501.
- McKenna, G.B., and A.J. Kovacs, 1984, *Polym. Eng. Sci.* **24**, 1138.
- Menon, N., and S.R. Nagel, 1995, *Phys. Rev. Lett.* **74**, 1230.
- Merolle, M., J.P. Garrahan, and D. Chandler, 2005, *Proc. Natl. Acad. Sci. U.S.A.* **102**, 10 837.
- Mézard, M., J.-P. Bouchaud, and J. Dalibard, 2007, Eds., *Complex Systems* (Springer, Berlin).
- Mézard M. and A. Montanari, 2006, *J. Stat. Phys.* **124**, 1317.
- Mézard M. and G. Parisi, 2010, [arXiv:0910.2838](https://arxiv.org/abs/0910.2838).
- Mézard M. and G. Parisi, 1999, *Phys. Rev. Lett.* **82**, 747.
- Mézard, M., G. Parisi, and M. Virasoro, 1988, *Spin Glass Theory and Beyond* (World Scientific, Singapore).
- Miyazaki, K., and D.R. Reichman, 2002, *Phys. Rev. E* **66**, 050501 (R).
- Miyazaki, K., and D.R. Reichman, 2005, *J. Phys. A* **38**, L343.
- Miyazaki, K., D.R. Reichman, and R. Yamamoto, 2004, *Phys. Rev. E* **70**, 011501.
- Miyazaki, K., H.M. Wyss, D.A. Weitz, and D.R. Reichman, 2006, *Europhys. Lett.* **75**, 915.
- Monasson, R., 1995, *Phys. Rev. Lett.* **75**, 2847.
- Montanari, A., and G. Semerjian, 2006a, *J. Stat. Phys.* **124**, 103.
- Montanari, A., and G. Semerjian, 2006b, *J. Stat. Phys.* **125**, 23.
- Montes, H., V. Viasnoff, S. Jurine, and F. Lequeux, 2006, *J. Stat. Mech.*, P03003.
- Monthus, C., and J.-P. Bouchaud, 1996, *J. Phys. A* **29**, 3847.
- Moore, M.A., 2006, *Phys. Rev. Lett.* **96**, 137202.
- Moore, M.A., and B. Drossel, 2002, *Phys. Rev. Lett.* **89**, 217202.
- Moore, M.A., and J. Yeo, 2006, *Phys. Rev. Lett.* **96**, 095701.
- Mossa, S., and G. Tarjus, 2006, *J. Non-Cryst. Solids* **352**, 4847.
- Moynihán, C.T., A.J. Eastal, M.A. Debolt, and J. Tucker, 1976, *J. Am. Ceram. Soc.* **59**, 12.
- Narayanaswamy, O.S., 1971, *J. Am. Ceram. Soc.* **54**, 491.
- Nauroth, M., and W. Kob, 1997, *Phys. Rev. E* **55**, 657.
- Nelson, D.R., 1983, *Phys. Rev. B* **28**, 5515.
- Nelson, D.R., 2002, *Defects and Geometry in Condensed Matter Physics* (Cambridge University Press, Cambridge).
- Newman, C.M., and D.S. Stein, 2002, *J. Stat. Phys.* **106**, 213.
- Nicodemi, M., 1999, *Phys. Rev. Lett.* **82**, 3734.
- Nieuwenhuizen, T.M., 1995, *Phys. Rev. Lett.* **74**, 4289.
- Nishino, T.H., and H. Hayakawa, 2008, *Phys. Rev. E* **78**, 061502.
- Nussinov, Z., 2004, *Phys. Rev. B* **69**, 014208.
- Nussinov, Z., J. Rudnick, S.A. Kivelson, and L.N. Chayes, 1999, *Phys. Rev. Lett.* **83**, 472.
- Ono, I.K., C.S. O'Hern, D.J. Durian, S.A. Langer, A.J. Liu, and S.R. Nagel, 2002, *Phys. Rev. Lett.* **89**, 095703.
- Osada, H., 1998, *Probab. Theory Relat. Fields* **112**, 53.
- Oukris, H., and N.E. Israeloff, 2010, *Nature Phys.* **6**, 135.
- Oxtoby, D.W., 1990, in *Liquids, Freezing and Glass Transition (Les Houches Session 51)*, edited by J.-P. Hansen, D. Levesque, and J. Zinn-Justin (Elsevier, New York).
- Palmer, R.G., D.L. Stein, E. Abrahams, and P.W. Anderson, 1984, *Phys. Rev. Lett.* **53**, 958.
- Pan, A.C., J.P. Garrahan, and D. Chandler, 2005, *Phys. Rev. E* **72**, 041106.
- Pardo, L.C., P. Lunkenheimer, and A. Loidl, 2007, *Phys. Rev. E* **76**, 030502(R).
- Parisi, G., 2003, in *Slow Relaxations and Nonequilibrium Dynamics in Condensed Matter* (Springer, Berlin).
- Parisi, G., 1980, *J. Phys. A* **13**, 1101.
- Parisi, G., 1999, *J. Phys. Chem. B* **103**, 4128.

- Parisi, G., and F. Zamponi, 2006, *J. Stat. Mech.*, P03017.
- Parisi, G., and F. Zamponi, 2005, *J. Chem. Phys.* **123**, 144501.
- Parisi, G., and F. Zamponi, 2010, *Rev. Mod. Phys.* **82**, 789.
- Parsaeian, A., and H. E. Castillo, 2008, *Phys. Rev. E* **78**, 060105.
- Pedersen, U. R., T. B. Schroder, J. C. Dyre, and P. Harrowell, 2010, *Phys. Rev. Lett.* **104**, 105701.
- Pica Ciamarra, M., M. Tarzia, A. de Candia, and A. Coniglio, 2003, *Phys. Rev. E* **67**, 057105.
- Picard, G., A. Ajdari, F. Lequeux, and L. Bocquet, 2005, *Phys. Rev. E* **71**, 010501(R).
- Pusey, P.N., and W. van Meegen, 1986, *Nature (London)* **320**, 340.
- Pusey, P.N., and W. van Meegen, 1987, *Phys. Rev. Lett.* **59**, 2083.
- Réfrégier, P., E. Vincent, J. Hammann, and M. Ocio, 1987, *J. Phys. (Paris)* **48**, 1533.
- Reichman, D. R., and P. Charbonneau, 2005, *J. Stat. Mech.*, P05013.
- Reinsberg, S. A., X. H. Qiu, M. Wilhelm, H. W. Spiess, and M. D. Ediger, 2001, *J. Chem. Phys.* **114**, 7299.
- Richert, R., 2002, *J. Phys. Condens. Matter* **14**, R703.
- Richert, R., 2010, *Phys. Rev. Lett.* **104**, 085702.
- Richert, R., and C. A. Angell, 1998, *J. Chem. Phys.* **108**, 9016.
- Ritort, F., and P. Sollich, 2003, *Adv. Phys.* **52**, 219.
- Rivoire, O., G. Biroli, O. C. Martin, and Mézard M., 2004, *Eur. Phys. J. B* **37**, 55.
- Roland, C. M., D. Fragiadakis, D. Coslovich, S. Capaccioli, and K. L. Ngai, 2010, *J. Chem. Phys.* **133**, 124507.
- Rouyer, F., S. Cohen-Addad, R. Höhler, P. Sollich, and S. M. Fielding, 2008, *Eur. Phys. J. E* **27**, 309.
- Rubinstein, M., and D. R. Nelson, 1983, *Phys. Rev. B* **28**, 6377.
- Sadoc, J. F., and R. Mosseri, 1999, *Geometrical Frustration* (Cambridge University Press, Cambridge).
- Santen, L., and W. Krauth, 2000, *Nature (London)* **405**, 550.
- Sarlat, T., A. Billoire, G. Biroli, and J.-P. Bouchaud, 2009, *J. Stat. Mech.*, P08014.
- Sausset, F., G. Biroli, and J. Kurchan, 2010, *J. Stat. Phys.* **140**, 718.
- Sausset, F., and G. Tarjus, 2007, *J. Phys. A* **40**, 12873.
- Sausset, F., and G. Tarjus, 2008, *Philos. Mag.* **88**, 4025.
- Sausset, F., and G. Tarjus, 2010, *Phys. Rev. Lett.* **104**, 065701.
- Sausset, F., G. Tarjus, and P. Viot, 2008, *Phys. Rev. Lett.* **101**, 155701.
- Schall, P., D. A. Weitz, and F. Spaepen, 2007, *Science* **318**, 1895.
- Schmalian, J., and P. G. Wolynes, 2000, *Phys. Rev. Lett.* **85**, 836.
- Schmalian, J., S. Wu, and P. G. Wolynes, 2003, *cond-mat/0305420*.
- Schmid, B., and R. Schilling, 2010, *Phys. Rev. E* **81**, 041502.
- Sciortino, F., 2005, *J. Stat. Mech.*, P05015.
- Sciortino, F., and W. Kob, 2001, *Phys. Rev. Lett.* **86**, 648.
- Sellitto, M., G. Biroli, and C. Toninelli, 2005, *Europhys. Lett.* **69**, 496.
- Sessoms, D. A., I. Bischofberger, L. Cipelletti, and V. Trappe, 2009, *Phil. Trans. R. Soc. A* **367**, 5013.
- Sethna, J. P., 2006, *Statistical Mechanics: Entropy, Order Parameters, and Complexity* (Oxford University Press, Oxford).
- Sethna, J. P., J. D. Shore, and M. Huang, 1991, *Phys. Rev. B* **44**, 4943.
- Shi, Y., M. B. Katz, H. Li, and M. L. Falk, 2007, *Phys. Rev. Lett.* **98**, 185505.
- Shi, Y. F., and M. L. Falk, 2006, *Phys. Rev. B* **73**, 214201.
- Sillescu, H., 1999, *J. Non-Cryst. Solids* **243**, 81.
- Singh, Y., J. P. Stoessel, and P. G. Wolynes, 1985, *Phys. Rev. Lett.* **54**, 1059.
- Sollich, P., 1998, *Phys. Rev. E* **58**, 738.
- Sollich, P., and M. R. Evans, 1999, *Phys. Rev. Lett.* **83**, 3238.
- Sollich, P., F. Lequeux, P. Hébraud, and M. E. Cates, 1997, *Phys. Rev. Lett.* **78**, 2020.
- Stein, R. S. L., and H. C. Andersen, 2008, *Phys. Rev. Lett.* **101**, 267802.
- Stevenson, J. D., J. Schmalian, and P. G. Wolynes, 2006, *Nature Phys.* **2**, 268.
- Stevenson, J. D., and P. G. Wolynes, 2006, *arXiv:cond-mat/0609677*.
- Stillinger, F. H., 1988, *J. Chem. Phys.* **88**, 7818.
- Stillinger, Frank H., and Jennifer A. Hodgdon, 1994, *Phys. Rev. E* **50**, 2064.
- Struik, L. C. E., 1978, *Physical Aging in Amorphous Polymers and Other Materials* (Elsevier, Amsterdam).
- Sugimoto, Y., P. Pou, M. Abe, P. Jelinek, R. Pérez, S. Morita, and O. Custance, 2007, *Nature (London)* **446**, 64.
- Swallen, S. F., K. L. Kearns, M. K. Mapes, Y. S. Kim, R. J. McMahon, M. D. Ediger, T. Wu, L. Yu, and S. Satija, 2007, *Science* **315**, 353.
- Swift, J., and P. C. Hohenberg, 1977, *Phys. Rev. A* **15**, 319.
- Szamel, G., 2004, *Phys. Rev. Lett.* **93**, 178301.
- Szamel, G., and E. Flenner, 2004, *Europhys. Lett.* **67**, 779.
- Szamel, G., and E. Flenner, 2006, *Phys. Rev. E* **74**, 021507.
- Tabor, D., 1991, *Gases, Liquids, and Solids (and Other States of Matter)* (Cambridge University Press, Cambridge).
- Tanaka, H., 2003, *Phys. Rev. Lett.* **90**, 055701.
- Tanaka, H., T. Kawasaki, H. Shintani, and K. Watanabe, 2010, *Nature Mater.* **9**, 324.
- Tanguy, A., F. Leonforte, and J.-L. Barrat, 2006, *Eur. Phys. J. E* **20**, 355.
- Tarjus, G., and D. Kivelson, 1995, *J. Chem. Phys.* **103**, 3071.
- Tarjus, G., S. A. Kivelson, Z. Nussinov, and P. Viot, 2005, *J. Phys. Condens. Matter* **17**, R1143.
- Tarzia, M., G. Biroli, and G. Tarjus (work in progress).
- Thalman, F., 1998, *Eur. Phys. J. B* **3**, 497.
- Thalman, F., 2002, *J. Chem. Phys.* **116**, 3378.
- Thouless, D. J., P. W. Anderson, and R. G. Palmer, 1977, *Philos. Mag.* **35**, 593.
- Toninelli, C., and G. Biroli, 2008, *J. Stat. Phys.* **130**, 83.
- Toninelli, C., G. Biroli, and D. S. Fisher, 2004, *Phys. Rev. Lett.* **92**, 185504.
- Toninelli, C., G. Biroli, and D. S. Fisher, 2006, *Phys. Rev. Lett.* **96**, 035702.
- Toninelli, C., M. Wyart, L. Berthier, G. Biroli, and J.-P. Bouchaud, 2005, *Phys. Rev. E* **71**, 041505.
- Tool, A. Q., 1946, *J. Am. Ceram. Soc.* **29**, 240.
- Toulouse, G., 1977, *Commun. Phys.* **2**, 115.
- Tracht, U., M. Wilhelm, A. Heuer, H. Feng, K. Schmidt-Rohr, and H. W. Spiess, 1998, *Phys. Rev. Lett.* **81**, 2727.
- Varnik, F., L. Bocquet, J.-L. Barrat, and L. Berthier, 2003, *Phys. Rev. Lett.* **90**, 095702.
- Velenich, A., A. Parola, and L. Reatto, 2006, *Phys. Rev. E* **74**, 021410.
- Viasnoff, V., and F. Lequeux, 2002, *Phys. Rev. Lett.* **89**, 065701.
- Vidal Russell, E., and N. E. Israeloff, 2000, *Nature (London)* **408**, 695.
- Viot, P., J. Talbot, and G. Tarjus, 2003, *Fractals* **11**, 185.
- Viot, P., G. Tarjus, and D. Kivelson, 2000, *J. Chem. Phys.* **112**, 10368.
- Vogel, M., and S. C. Glotzer, 2004, *Phys. Rev. E* **70**, 061504.
- Wang, P., C. M. Song, and H. A. Makse, 2006, *Nature Phys.* **2**, 526.
- Weeks, E., J. C. Crocker, A. C. Levitt, A. Schofield, and D. A. Weitz, 2000, *Science* **287**, 627.
- Weeks, E. R., J. C. Crocker, and D. A. Weitz, 2007, *J. Phys. Condens. Matter* **19**, 205131.
- Westfahl, Jr., H., J. Schmalian, and P. G. Wolynes, 2001, *Phys. Rev. B* **64**, 174203.

- Whitelam, S., L. Berthier, and J. P. Garrahan, 2004, *Phys. Rev. Lett.* **92**, 185705.
- Whitelam, S., L. Berthier, and J. P. Garrahan, 2005, *Phys. Rev. E* **71**, 026128.
- Whitelam, S., and J. P. Garrahan, 2004, *J. Phys. Chem. B* **108**, 6611.
- Wuttke, J., W. Petry, and S. Pouget, 1996, *J. Chem. Phys.* **105**, 5177.
- Wyart, M., 2010, *Phys. Rev. Lett.* **104**, 095901.
- Xia, X. Y., and P. G. Wolynes, 2000, *Proc. Natl. Acad. Sci. U.S.A.* **97**, 2990.
- Yamamoto, R., and A. Onuki, 1998a, *Phys. Rev. Lett.* **81**, 4915.
- Yamamoto, R., and A. Onuki, 1998b, *Phys. Rev. E* **58**, 3515.
- Yardimci, H., and R. L. Leheny, 2003, *Europhys. Lett.* **62**, 203.
- Yoshino, H., and M. Mézard, 2010, *Phys. Rev. Lett.* **105**, 015504.
- Young, A. P., 1998, Ed., *Spin Glasses and Random Fields* (World Scientific, Singapore).
- Zamponi, F., G. Ruocco, and L. Angelani, 2005, *Phys. Rev. E* **71**, 020101.
- Zanotto, E. D., 1998, *Am. J. Phys.* **66**, 392.
- Zdeborova, L., and F. Krzakala, 2011, *J. Chem. Phys.* **134**, 034512.
- Zink, M., K. Samwer, W. L. Johnson, and S. G. Mayr, 2006, *Phys. Rev. B* **73**, 172203.
- Zwanzig, R., 2001, *Non Equilibrium Statistical Mechanics* (Oxford University Press, Oxford).